



# ENERGY AND WATER

## Summary of Activities 2022

Geoscience BC Report 2023-02



# **GEOSCIENCE BC SUMMARY OF ACTIVITIES 2022: ENERGY AND WATER**

© 2023 by Geoscience BC.

All rights reserved. Electronic edition published 2023.

This publication is also available, free of charge, as colour digital files in Adobe Acrobat® PDF format from the Geoscience BC website: <http://www.geosciencebc.com/updates/summary-of-activities/>.

Every reasonable effort is made to ensure the accuracy of the information contained in this report, but Geoscience BC does not assume any liability for errors that may occur. Source references are included in the report and the user should verify critical information.

When using information from this publication in other publications or presentations, due acknowledgment should be given to Geoscience BC. The recommended reference is included on the title page of each paper. The complete volume should be referenced as follows:

Geoscience BC (2023): Geoscience BC Summary of Activities 2022: Energy and Water; Geoscience BC, Report 2023-02, 72 p.

Summary of Activities: Energy and Water (Geoscience BC)

Annual publication

ISSN 2562-2757 (Print)

ISSN 2562-2765 (Online)

Geoscience BC

1101–750 West Pender Street

Vancouver, British Columbia V6C 2T7

Canada

**Front cover photo and credit:** Surveying of high water levels at the Doig River hydrometric station, northeastern British Columbia. Photo by R. Rolick.

## Foreword

It has been another busy and exciting year at Geoscience BC. We launched a membership program early in 2022 and introduced ‘Project Concepts’, which are outlines of future research programs, in July. And throughout, we continued to support leading-edge geoscience research in British Columbia, highlights of which are presented in our annual *Summary of Activities* publication. Papers are published in two separate volumes: *Minerals*, and this volume, *Energy and Water*. Both volumes are available in print and online via [www.geosciencebc.com](http://www.geosciencebc.com).

### Summary of Activities 2022: Energy and Water

This *Summary of Activities 2022: Energy and Water* volume contains seven papers from ongoing Geoscience BC projects and 2022 Geoscience BC Scholarship recipients that are within Geoscience BC’s strategic focus areas of energy and water. The papers are divided into four sections, based on Geoscience BC’s strategic objectives of

- 1) Identifying New Natural Resource Opportunities,
- 2) Facilitating Responsible Natural Resource Development,
- 3) Enabling Clean Energy, and
- 4) Understanding Water.

The volume starts off with Pelletier et al. providing an update on a multiyear project to develop a database of brines containing lithium and other dissolved minerals and metals through a large-scale sampling program in northeastern British Columbia (BC). In the ‘Facilitating Responsible Natural Resource Development’ section, Geoscience BC Scholarship recipient Esmaeilzadeh and co-author Eaton investigate the effect of fault sealing on induced seismicity in northeastern BC.

The ‘Enabling Clean Energy’ section contains four papers on geological carbon capture and storage, and geothermal energy. First, Hughes summarizes the *Northeast BC Geological Carbon Capture and Storage Atlas*, which Geoscience BC published in early 2023. Next, Geoscience BC Scholarship recipient Nazemi and co-author Dashtgard present research on a 3-D reconstruction of the Georgia Basin and its potential to sequester carbon dioxide. Grasby et al. provide an update on fieldwork undertaken at Mount Cayley as part of ongoing research into the geothermal potential of the Garibaldi Volcanic Belt. This is followed by an examination by Scholarship recipient Hormozzade Ghalati and co-authors of the Mount Meager Volcanic Complex using 3-D inversion of audio-magnetotelluric data.

The volume concludes with a summary by Rolick et al. of the second year of a pilot collaborative water-monitoring program in northeastern BC.

### Geoscience BC Energy and Water Publications 2022

Geoscience BC published the following six Energy and Water geoscience reports in 2022:

- Ten technical papers in the **Geoscience BC Summary of Activities 2021: Energy and Water** volume (Geoscience BC Report 2022-02)
- **Amplification of Seismic Ground Motion in the Fort St. John – Dawson Creek Area, Northeastern British Columbia**, by P.A. Monahan, B.J. Hayes, M. Perra, Y. Mykula, J. Clarke, C. Gugins, C. Candy, D. Griffiths, O. Bayarsaikhan, O. Jones and U. Oki (Geoscience BC Report 2022-05)
- **Distribution, Origin, and Implications of Hydrogen Sulphide in Unconventional Reservoir Rocks in Western Canada with Insights into the Stratigraphic Zonation and Lateral Variability of Producing Hydrocarbon Liquids**, by R.M. Bustin, G. Chalmers, P.L. Silva and A. Bustin (Geoscience BC Report 2022-06)
- **A Comprehensive Investigation of Injection-Induced Earthquakes in Northeastern British Columbia, Canada**, by H. Kao (Geoscience BC Report 2022-10)
- **B.C. Montney Produced Water to Saleable Salt Technology Pilot Test**, by Saltworks Technologies Inc. (Geoscience BC Report 2022-11)
- **Garibaldi Geothermal Energy Project – Phase 2: Mount Cayley 2021 Field Report**, by S.E. Grasby, R.W. Barendregt, A. Borch, A. Calahorrano-DiPatre, Z. Chen, C. Hanneson, M. Harris, S.L. Quane, J.K. Russell, E.G. Slobodian, M.J. Unsworth, G. Williams-Jones and W. Yuan (Geoscience BC Report 2022-14)

All releases of Geoscience BC reports, maps and data are published on our website and announced through our website and e-mail updates. Most final reports and data can be viewed or accessed through our Earth Science Viewer at <https://gis.geosciencebc.com/esv/?viewer=esv>.

## Looking Forward: 2023 and Beyond

### Project Concepts

As Geoscience BC looks ahead to 2023 and beyond, we are working with partners and members to develop project concepts: proposed research relating to critical minerals and metals, geological carbon capture and storage, generating cleaner energy (including geothermal, hydrogen and low carbon intensity natural gas), and monitoring and mitigating greenhouse gas emissions. These are designed for a collaborative funding model with input and contributions from federal and provincial governments, industry, trusts and others. Geoscience BC is currently applying for research funding and reaching out to prospective project sponsors for all project concepts.

Some of the new project concepts take already successful Geoscience BC project ideas and apply them to a new part of the province. Building on the *Northeast BC Geological Capture and Storage Atlas*, conceptual projects in the Nechako and Georgia basins would compile existing geoscience data and assess the carbon sequestration potential in central and south-western BC. Geothermal energy remains a priority as well, with project concepts developed for both northwestern and southeastern BC. Finally, project concept ‘HazNet (Hazard Network) Pacific’ would involve a multiyear program to assess regional environmental hazards (e.g., earthquakes, air quality, etc.) using ultra-high density, strategically placed sensors, initially in the Lower Mainland of BC.

### Membership

Geoscience BC membership opportunities make it easy for a wide range of partners to learn about new project concepts, as well as support, provide input, network and stay up to date on Geoscience BC minerals, energy and water research. Corporate, Individual, Student and Associate memberships provide a variety of opportunities to suit industry, academia, communities, Indigenous groups and governments as we work toward shared goals. Geoscience BC launched the membership program early in 2022 and, as of mid-December 2022, has 140 members.

### Acknowledgments

Geoscience BC would like to thank all authors and reviewers of the *Summary of Activities* for their contributions to this volume. RnD Technical is also acknowledged for its work in editing and assembling both volumes.

Geoscience BC would like to thank all members, project sponsors and champions for their ongoing support of public geoscience. As well, Geoscience BC would like to express our appreciation for the leaders and volunteers in British Columbia’s mineral exploration, mining and energy sectors who support our organization through their guidance, and their use and recognition of the data and information that we collect and distribute.

Randy Hughes  
Manager, Energy and Water  
Geoscience BC  
[www.geosciencebc.com](http://www.geosciencebc.com)

## Contents

### Identifying New Natural Resource Opportunities

- E. Pelletier, C. Williams, D. Murfitt and T. Wilson:** Northeastern British Columbia lithium formation-water database project: 2022 field sampling program update . . . . . 1

### Facilitating Responsible Natural Resource Development

- Z. Esmailzadeh and D.W. Eaton:** Investigating fault-sealing effects on induced seismicity and pore-pressure distribution in northeastern British Columbia: observations and modelling . . . . . 11

### Enabling Clean Energy

- R. Hughes:** Northeast BC Geological Carbon Capture and Storage Atlas: a key step toward net zero emissions. . . . . 21

- M. Nazemi and S. Dashtgard:** Three-dimensional reconstruction of the Georgia Basin and potential for carbon dioxide sequestration in the Lower Mainland, southwestern British Columbia . . . . . 31

- S.E. Grasby, A. Borch, A. Calahorrano-Di Patre, Z. Chen, J. Craven, X. Liu, M. Muhammad, J.K. Russell, V. Tschirhart, M.J. Unsworth, G. Williams-Jones and W. Yuan:** Garibaldi Geothermal Volcanic Belt Assessment Project, southwestern British Columbia, phase 2: 2022 field report . . 47

- F. Hormozzade Ghalati, J.A. Craven, D. Motazedian and S.E. Grasby:** Investigation of geothermal systems in the Mount Meager Volcanic Complex, southwestern British Columbia, using 3-D inversion of audio-magnetotelluric data . . . . . 55

### Understanding Water

- R.L. Rolick, S.L. Lapp, E.G. Johnson, D.L. Cottrell, W.T. Van Dijk and B. Shepherd:** Pilot Collaborative Water Monitoring Program, northeastern British Columbia: year two update . . . . . 63



# Northeastern British Columbia Lithium Formation-Water Database Project (NTS 093P, 094A, B, G–J, O, P, Part of 093I): 2022 Field Sampling Program Update

E. Pelletier, Matrix Solutions Inc., Calgary, Alberta

C. Williams, Canadian Discovery Ltd., Calgary, Alberta, [cwilliams@canadiandiscovery.com](mailto:cwilliams@canadiandiscovery.com)

D. Murfitt, Matrix Solutions Inc., Calgary, Alberta

T. Wilson, Canadian Discovery Ltd., Calgary, Alberta

---

Pelletier, E., Williams, C., Murfitt, D. and Wilson, T. (2023): Northeastern British Columbia lithium formation-water database project (NTS 093P, 094A, B, G–J, O, P, part of 093I): 2022 field sampling program update; *in* Geoscience BC Summary of Activities 2022: Energy and Water, Geoscience BC, Report 2023-02, p. 1–10.

## Introduction and Background

In the fall of 2021, the northeastern British Columbia (BC) lithium formation-water database project was initiated to 1) collect, assess and characterize subsurface brines for dissolved metal concentrations, and 2) establish the potential for extracting critical minerals and metals from brine in northeastern BC (Wilson et al., 2022). This project was devised in response to the increasing demand for lithium and other critical minerals and metals, as identified by the Canadian government (Natural Resources Canada, 2021). These minerals and metals will help enable the country's transition to low carbon energy.

This project expands upon previous discoveries of elevated concentrations of dissolved metals (specifically lithium) in a number of geological formations in both Alberta and Saskatchewan and throughout the Western Canada Sedimentary Basin (Figure 1; Eccles and Jean, 2010; Eccles, 2011; Jensen, 2012, 2016; Jensen et al., 2017; Blondes, 2018; Lopez et al., 2020). Despite historical oil and gas industry sampling of formation water for routine water analyses, the publicly available datasets for the brine chemistries and associated lithium concentrations remain relatively limited. This is due to historical samples not being routinely analyzed for lithium and other metals. At present, Alberta has recorded over 1600 formation-water samples with lithium concentrations (Eccles, 2011; Lopez et al., 2020) and Saskatchewan over 200 (Jensen, 2012, 2016; Jensen et al., 2017) whereas northeastern BC, prior to this project, had only recorded five samples with lithium concentrations (Eccles, 2011). This data scarcity presents a significant challenge for operators looking to develop lithium resources in BC. Adding data is complicated by the fact that formation water can only be sampled from existing oil and gas infrastructure, that is, from wells that are in production

and can bring associated water to surface. This joint study, conducted by Canadian Discovery Ltd. and Matrix Solutions Inc. (Matrix) for Geoscience BC, strives to deliver an initial lithium and other dissolved minerals and metals brine database through a large-scale sampling program undertaken in northeastern BC. Supporting partners include the Northern Development Initiative Trust, the Geological Survey of Canada (GSC) and LithiumBank Resources Corp. This study aims to collect and analyze formation-water samples to create a statistically robust stratigraphic database of up to 500 samples from 380 oil and gas wells within active oil and gas fields in northeastern BC. Background information pertaining to lithium deposit types, enrichment mechanisms and direct lithium extraction technologies was published in Wilson et al. (2022). All of the final deliverables from this project will assist operators in making exploration, development and investment decisions and help to inform important policy decisions on permitting prospective critical mineral and metal resources and regulating their exploration and extraction within the province.

This paper provides an interim update on the progress of sampling underway in northeastern BC, as well as a brief description of ongoing activities and key challenges encountered as part of this effort.

## Project Design and Progress

This project represents a first of its kind in northeastern BC and was devised in a three-phase approach, which was slated to take place over approximately 24 months but the timeline has been extended to accommodate additional participation from key operators. The three project phases comprise:

- 1) co-ordination and scoping,
  - a) project co-ordination, logistics and safety standards,
  - b) prospective formation review and high-level scoping of wells to be sampled,

---

*This publication is also available, free of charge, as colour digital files in Adobe Acrobat® PDF format from the Geoscience BC website: <http://geosciencebc.com/updates/summary-of-activities/>.*

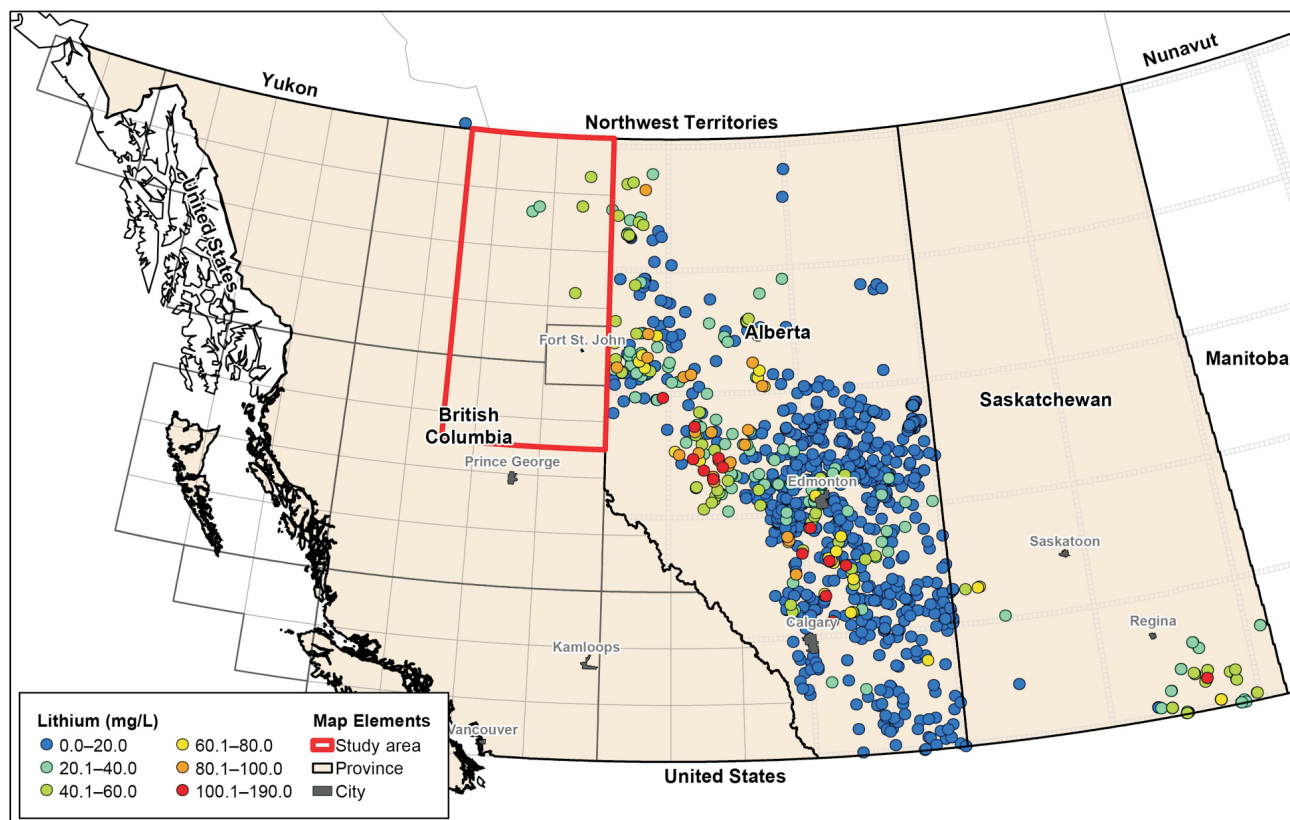


**Figure 1.** Concentration of lithium in formation waters throughout the Western Canada Sedimentary Basin (data from Eccles and Jean, 2010; Jensen, 2012, 2016; Jensen and Rostron, 2017).

- c) operator engagement, access negotiations and field logistics,
- 2) field sampling and data analysis,
  - a) field sampling program,
  - b) laboratory analysis,
  - c) data processing, quality assurance–quality control (QA-QC) and analysis,
- 3) geological interpretation and lithium potential (final report),
  - a) incorporate data into the broader geological and hydrogeological framework,
  - b) advance the understanding of geological controls and natural variability of lithium in formation waters,
  - c) preliminary assessment of aquifer volumes, deliverability and economic viability of lithium extraction.

### Phase 1: Co-Ordination and Scoping

The co-ordination and scoping phase has been completed, with details provided in Wilson et al. (2022). The preliminary well scoping methodology, detailed in Wilson et al. (2022), took into consideration a number of geological and hydrogeological factors to focus sampling efforts on up to 20 geological formations with adequate aquifer potential. The selected intervals spanned Devonian to Cretaceous

strata, with formations comprising both clastic- and carbonate-dominant lithologies.

In addition to the work undertaken to devise the preliminary program, the first phase of work also included the commencement of the engagement process with key operators of wells producing from the target formations (Wilson et al., 2022).

### Phase 2: Field Sampling and Data Analysis

Logistical planning for individual sampling programs at key operator sites formed the first steps of the second phase of the project. To date, the program has partnered with key operators who have agreed to facilitate access to their production infrastructure for brine sampling. The project team is grateful for their participation. These operators are Crescent Point Energy Corp., Enercapita Energy Ltd., Erikson National Energy Inc., ISH Energy Ltd., Ovintiv Inc., Shell Canada Limited, Tourmaline Oil Corp. and Whitecap Resources Inc.

Sixty-two samples have been collected and sampling continues at the key operator sites. It is noted that there is an overall decrease in total attainable sample numbers compared to the original sampling targets for the program. This is due to challenges encountered while undertaking such a large-scale, operationally complex program, which are dis-

cussed in subsequent sections. These challenges included the variable suitability of the infrastructure type at the sampling sites and the complications encountered while sampling during a pandemic. The project team strives to collect additional samples, as the schedule allows, and continues to maintain ongoing discussions with additional operators in the area.

### Phase 3: Geological Interpretation and Lithium Potential

The final deliverable for this project, which forms the third and last phase of work, is a preliminary, high fidelity and vetted database, which will serve as the foundation for additional formation-water chemistry studies in BC. Ideally, it will aid and inform regulatory policy considerations, as well as act as a catalyst to further brine resource exploration and development. This database will be accompanied by a final report, which will describe the data in the broader geological context of northeastern BC. The final report will include but not be limited to water chemistry mapping, graphical analysis and initial geochemical and enrichment interpretations of concentrated minerals and metals in formation-water brines.

#### Sampling Methods and Analytical Suite

To achieve the project goals, it is important to ensure that the sampling and data collection methods used in this program conform to necessary standards and follow rigorous QA-QC procedures. This objective is addressed through the following key operations:

- 1) assemble and quality check well data prepopulated for each infrastructure type and sample location, capturing key metadata of importance to the project and checking with operators for accuracy
- 2) use standardized sampling procedures
- 3) use a nationally accredited laboratory, which has significant expertise in analyzing oil and gas field brines with specific applications to lithium and other metal concentration assessment
- 4) adhere to standardized QA-QC methodologies
- 5) document chain of custody procedures

#### Metadata Collection

Metadata parameters are considered those parameters that are not explicitly analyzed but collected prior to and as part of the program activities. This includes sampling locations, sample collection dates, stratigraphic and depth intervals, infrastructure types used for sampling, as well as additional details on specific conditions of sampling. These parameters are organized into three main categories corresponding to their order of collection:

- 1) prefield metadata collection and confirmation
- 2) field metadata collection
- 3) postfield metadata quality checks

The full list of metadata parameters is shown in Table 1. All metadata parameters are collected as available. In cases where certain information is unavailable, a best effort approach is made to document the circumstances involved.

#### Sampling Methodology and Procedures

A standardized sampling procedure was devised and implemented for the program, which involved sampling at four key infrastructure types: 1) production wellhead, 2) oil separator, 3) treater, and 4) onsite production-stream storage tank, under certain circumstances. In general, the preference is to sample at isolated ‘in-test’ separators, however, in practice, this is not always feasible depending on the operation’s infrastructure and production configuration. Variations in infrastructure configuration accounted for the majority of unforeseen sampling constraints and the inability to sample at some sites led to a reduction in the sample numbers originally proposed. The main problem encountered was that many operations in northeastern BC have ‘wet-metered’ configurations with little or no means of isolating production from individual wells or zones. Measures were taken to adapt the sampling procedures to include additional sampling options to attain a reasonable sample coverage.

Of utmost importance during sampling is safety. There is an inherent risk in oilfield sampling that necessitates rigorous safety requirements. All oilfield sampling programs must comply with WorkSafeBC requirements and limits (WorkSafeBC, 2022), as well as operator-specific safety standards and procedures. The following descriptions are illustrative of the procedural sampling methodologies for data integrity but do not include the full safety procedures.

##### Wellhead Sampling

Sampling at the wellhead involves collecting a fluid sample from a sampling port at the wellhead production assembly. For this project, an oilfield wellhead is defined as any mechanism fitted onto a well that has structural and pressure-containing interface capabilities, and includes at least one valve to isolate the well from the atmosphere. The surface pressure control is provided by a master valve, which is installed on the production tubing located above the casing bowl. Wellheads can have multiple isolation valves and chokes to control fluid flow. Wellheads are typically attached to a surface casing bowl that is welded/attached to the surface casing or surface conductor pipe, which has been cemented in place to ensure adequate well structural integrity.

Wellhead sampling is conducted after the necessary safety precautions are observed, such as testing and releasing wellhead pressure and properly opening infrastructure isolation valves.

**Table 1.** Metadata collection parameters for the field sampling program of the northeastern British Columbia lithium formation-water database project.

Phase	Data type	Metadata parameter
Prefield metadata collection and confirmation	Location	Unique well identifier (UWI)
		Global Positioning System co-ordinates, easting Global Positioning System co-ordinates, northing Ground elevation, metres above sea level (m asl) Operator company Producing field name
	Formation	Formation sampled (formation name) Formation member name (if available) Geological age (e.g., Devonian) geoSCOUT downhole temperature (degrees Celsius) Production zone, if known
		Well and infrastructure
	Completion	Well completion depth top (elevation m asl) Well completion depth base (elevation m asl) Most recent well intervention type and date: workover, fracking, etc.
		Production and fluids
Field metadata collection	Sampling and infrastructure	Sample ID(s) (prepopulated; coincides with chain of custody) Confirm if sample is sour (Y or N) Operator company Supporting operator: last name, first name Collection date, time Number of sample bottles Infrastructure type sampled (e.g., separator, wellhead, etc.) Infrastructure additional comment (single or multiwell, in test condition and running time) Sample temperature at collection (degrees Celsius) Degree of emulsification (approx. percentage, e.g., 10%) Description of sample: clear/cloudy, colour, emulsion, product, smell, gassy, turbid, etc. Field note / additional comments
Postfield metadata quality checks	Collection and transmittal details	Chain of custody (COC) number Date shipped Transit time Lab arrival date and time Date sample processed and analyzed Observations about sample when analyzed, if applicable

### Separator Sampling

Test separators are used in oilfields to measure the flow rates of various wells and collect water and hydrocarbon samples from one or more wells at a satellite location. Test separators for this sampling program will either be two phase or three phase. Two phase means that oil and water are separated from gas, whereas three phase means that oil, water and gas are each separated. For both two phase and three phase, a sampling valve on the separator tank should

be present, which can be opened to produce a fluid sample. Where feasible, the owner and operator will ensure that the wells flowing to the separator will be ‘into test’ at least 24 hours prior to sample collection to flush the lines and ensure no risk of contamination from other wells. For some infrastructure and production configurations, the only way to collect a sample is to collect a commingled fluid sample. Where this was the case, it was explicitly documented as such and was identified as representing only one formation

production interval despite being sourced from a group of wells.

### Treater Sampling

A heater treater uses heat, delivered by a burner and fire tube, to heat the liquid inside the tank, which accelerates the process of separation. Similar to a two-phase separator, the valves and piping will send the gas to either sales or flare and the oil will be sent downstream, in this case to storage tanks. Produced water is also separated at this tank and is sent downstream to a disposal well. A sampling valve is usually present on treaters to gain access to production fluids, which can be collected along the oil production stream.

### Onsite Production-Stream Tankage

Where present, onsite storage tanks may provide an additional means of sampling although these tanks may contain commingled fluids, which will need to be assessed for their degree of representation of discrete formation zones of interest. In these cases, sampling ports at the base of the tanks may provide access to the brine fraction of production fluids inside; the suitability and accessibility must be assessed in co-ordination with the well owner/operator. This infrastructure is considered as a last resort option for sample collection given that the formation waters will have equilibrated to surface pressure and temperature conditions, and therefore some additional margin of error may be introduced as chemical constituents equilibrate in such tanks.

### Sample Collection

Once infrastructure access to fluids is attained, sample collection is undertaken. The sampling procedure observed for this program conforms to the methods outlined in Lico et al. (1982), which is regarded as the foundational reference for oilfield formation-water and brine sampling. Water is collected in an intermediate 9 L carboy and if there is an oil-water mixture, approximately 8 L of water or emulsion is collected. Sample temperature is taken immediately after collection. The sample is then capped and contained in the sealed carboy and allowed to sit for a period of time to assess whether the emulsion breaks down on its own. Once the emulsion separates adequately, the spigot at the base of the carboy (where the denser formation water will separate out) is used to fill individual 1 L laboratory-provided standard oilfield sampling bottles. In total, three 1 L bottles are collected for the project, one primary unfiltered and unpreserved sample, one secondary or duplicate raw sample and one sample filtered through two filters, a prefilter and a 0.45 mm filter, and preserved with nitric acid. The secondary sample was collected to serve as a duplicate sample in accordance with the QA-QC procedures and will serve as a backup sample in the event of damage or integrity issues in transit. It may also be used for reruns if results from a primary sample are flagged for inconsistencies. The filtered

and preserved samples were collected to check for possible sample quality degradation in the raw unfiltered samples.

### Nationally Accredited Laboratory

The petroleum testing services at AGAT Laboratories Ltd., with laboratories in Fort St. John and Fort Nelson, BC, and an oilfield water laboratory in Calgary, Alberta, were selected for this project. A full suite of water chemistry analyses, including lithium-ion concentration, has been devised to capture routine brine chemistry for characterization, along with the full suite of dissolved metal parameters of interest to this study. The routine analysis includes pH, electrical conductivity, Ca, Mg, Na, K, Fe, SO<sub>4</sub>, Cl, Mn, carbonate, bicarbonate, NO<sub>3</sub>, NO<sub>2</sub>, NO<sub>3</sub><sup>+</sup>, NO<sub>2</sub><sup>-</sup>, N, alkalinity, hardness and calculated total dissolved solids (TDS). The dissolved metals analysis includes analysis for Al, Sb, As, Ba, Be, Bi, B, Cd, Ca, Cr, Co, Cu, Fe, Pb, Li, Mg, Mn, Mo, Ni, K, Se, Si, Ag, Na, S, Sr, Sn, Tl, Ti, U, V and Zn and has explicitly been selected to run on an inductively coupled plasma-optical emission spectrometry (ICP-OES) instrument (in contrast to standard ICP-mass spectrometry instruments) to mitigate requirements for analytical dilution and achieve better accuracy and precision for dissolved lithium and other sensitive parameters.

Support for this analytical program has been provided by the GSC, which has agreed to provide scientific input and share analytical costs in support of their parallel yet separate study, which will further analyze the collected samples for a suite of isotopic parameters.

### QA-QC Procedures

In accordance with Matrix standard practices, QA-QC protocols were followed for the sampling program. These QA-QC measures included the collection and analysis of duplicate samples, as well as a review of the results from the laboratory QC samples. Field blanks and trip blanks were prepared for the conducted sampling events.

To determine the reproducibility of analyses, a duplicate of a primary sample was analyzed. Duplicates were taken for each sampled formation or at every seventh collected sample (depending on the number of samples collected). All duplicate samples analyzed were judged to be acceptable, with all relative difference values less than 30% and acceptable charge balances within a 10% error.

A field blank is a sample of organic-free, laboratory-supplied de-ionized water that is exposed to the sampling environment and then submitted blind to the laboratory along with the other samples in the set. Field blanks are used to measure incidental or accidental sample contamination (i.e., artifacts or analytes detected by analysis but not present in the samples). The field blank does not need to be analyzed for every sampling event, but can be analyzed

should analytical data for the actual samples appear anomalous.

A trip blank is a sample of organic-free, laboratory-supplied de-ionized water that is used to determine whether or not cross-contamination of particular compounds has been introduced to the actual samples during sample transportation. The trip blank remains unopened and is not exposed to the sampling environment. The sample is submitted to the laboratory as a blind sample along with the other samples in the set. The trip blank does not need to be analyzed every time, but can be analyzed should analytical data for the actual samples appear anomalous.

### Chain of Custody Procedures

A standard chain of custody documentation procedure was used to capture sampling details and the details of relinquishing each sample for transit to the laboratory. This included information such as sampling time, bottle numbers, analytical requirements and transit times as part of the sample submissions. Copies of the signed forms were documented for each step.

## Preliminary Sampling Results and Challenges

### Well Sampling

At the time of writing, 62 samples had been collected and plans are to collect more than 100 additional samples by early 2023. The project timeline was extended to accommodate for challenges encountered during the sampling program. Table 2 and Figure 2 show the progress of the sampling program by formation/member.

In total, 26 formations/members of interest were targeted for the sampling project. Of these identified units, 13 formations/members have been sampled to date, with an additional three currently unrepresented formations slated for upcoming sampling (Table 2). Six formations/members are approved for access but have not been sampled to date as details and confirmations are under consideration. Four formations/members did not have adequate infrastructure access to conduct sampling over the project timeframe. The details of the vetting of the original wells by formation/member can be found in Wilson et al. (2022).

Stratigraphic coverage to date has been successful as samples have been collected from a number of key formations in Devonian, Triassic and Cretaceous units. In general, the Triassic and Cretaceous units have a greater number of wells accessible for sampling in the project area. Unfortunately, sampling from some Paleozoic units that are the stratigraphic equivalents to lithium-enriched formations in Alberta and Saskatchewan has not been possible to date because of operational constraints. These units in BC include the Keg River and Shunda formations, and opportunities to

obtain samples from these formations will continue to be pursued, however, sampling limitations are expected to persist for these wells.

The results of the sample analyses will be released following an exclusivity period (six months after the end of the sampling field program) granted to the participants of the program. However, it can be reported that the anonymized values of notable lithium concentrations range from low values of 0.1 mg/L to approximately 100 mg/L. The higher concentrations reported to date are within the range of technical limits for direct lithium extraction (DLE) technologies (Grant, 2022), and are interpreted to warrant additional investigations for lithium brine resource potential in north-eastern BC.

### Program Challenges and Adaptations

To date, the attained sample numbers are lower than initially anticipated. This highlights a number of important challenges encountered in a large-scale program of this scope. These include unforeseen circumstances encountered during the proposed project timeline. Three key challenges were identified during the course of the project:

- 1) infrastructure configuration and well access limitations, which together filtered a significant number of wells from the original proposed well list
- 2) changes and limitations to the BC Mineral Tenure Act regulatory environment during the operator engagement phase
- 3) external factors—the COVID-19 pandemic and the subsequent surge in energy prices led to a number of schedule postponements

The infrastructure and operational configurations had a considerable effect on the suitability of sampling sites, particularly with respect to obtaining representative isolated (i.e., not commingled) zone and well source samples. In general, such configuration information and operational knowledge is not readily available through public data sources and is only evident upon conversations with local field operators. A significant number of candidate wells were filtered out because grouped production from multiple wells within a producing field were commingled directly into a production stream without field or well level separation. Variations of this grouped production setup are often referred to as wet-metered and offer limited discrete sampling opportunities compared to traditional onsite separators. In northeastern BC, many operators choose a wet-metered configuration to minimize remote operation and equipment costs. As the original well lists were vetted by operators, exceptions were made to collect the most representative sample base, given some of the infrastructure limitations. This was done under the premise that well-documented commingled fluid samples from a target formation were better than the alternative of not being able to

Table 2. Progress of the northeastern British Columbia lithium formation-water sampling program by formation/member.

Geological age	Formation/member	Samples collected to date (number of samples)	Sampling underway (number of samples)	Potential for additional sampling approved but details under consideration with operators (A-denotes unconfirmed numbers)	Confirmed sample totals	Sampling access restricted <sup>1</sup> - ongoing efforts to secure access (X-denotes restricted access)
Cretaceous	Dunvegan					X
Cretaceous	Cadotte			A		
Cretaceous	Spirit River/Notikewin			A		
Cretaceous	Bluesky		1	A	1	
Cretaceous	Gething	2	2	A	4	
Cretaceous	Cadomin/Chinkeh	2	15	A	17	
Cretaceous	Nikanassin			A		
Jurassic	Rock Creek					X
Jurassic	Nordegg			A		
Triassic	Baldonnel/Pardonet	3		A	3	
Triassic	Charlie Lake	9		A	9	
Triassic	Coplin	4	1	A	5	
Triassic	Boundary	5	1	A	6	
Triassic	Halfway	14		A	14	
Triassic	Doig		21	A	21	
Triassic	Montney (undifferentiated)	3		A	3	
Triassic	Upper Montney	8	8	A	16	
Triassic	Middle Montney	3	8	A	11	
Permian	Belloy			A		
Mississippian	Debolt	3		A	3	
Mississippian	Shunda					X
Mississippian	Pekisko		4	A	4	
Devonian	Jean Marie	3	4	A	7	
Devonian	Fort Simpson/Muskwa	3	3	A	6	
Devonian	Slave Point			A		
Devonian	Keg River/Pine Point					X
<b>Subtotals</b>		<b>62</b>	<b>68</b>	<b>~20-50</b>	<b>130</b>	
					<b>Potential total samples:</b>	<b>170</b>

<sup>1</sup>Restrictions exist due to numerous sampling challenges, such as operator well availability, operator capacity, infrastructure configurations and schedule limitations

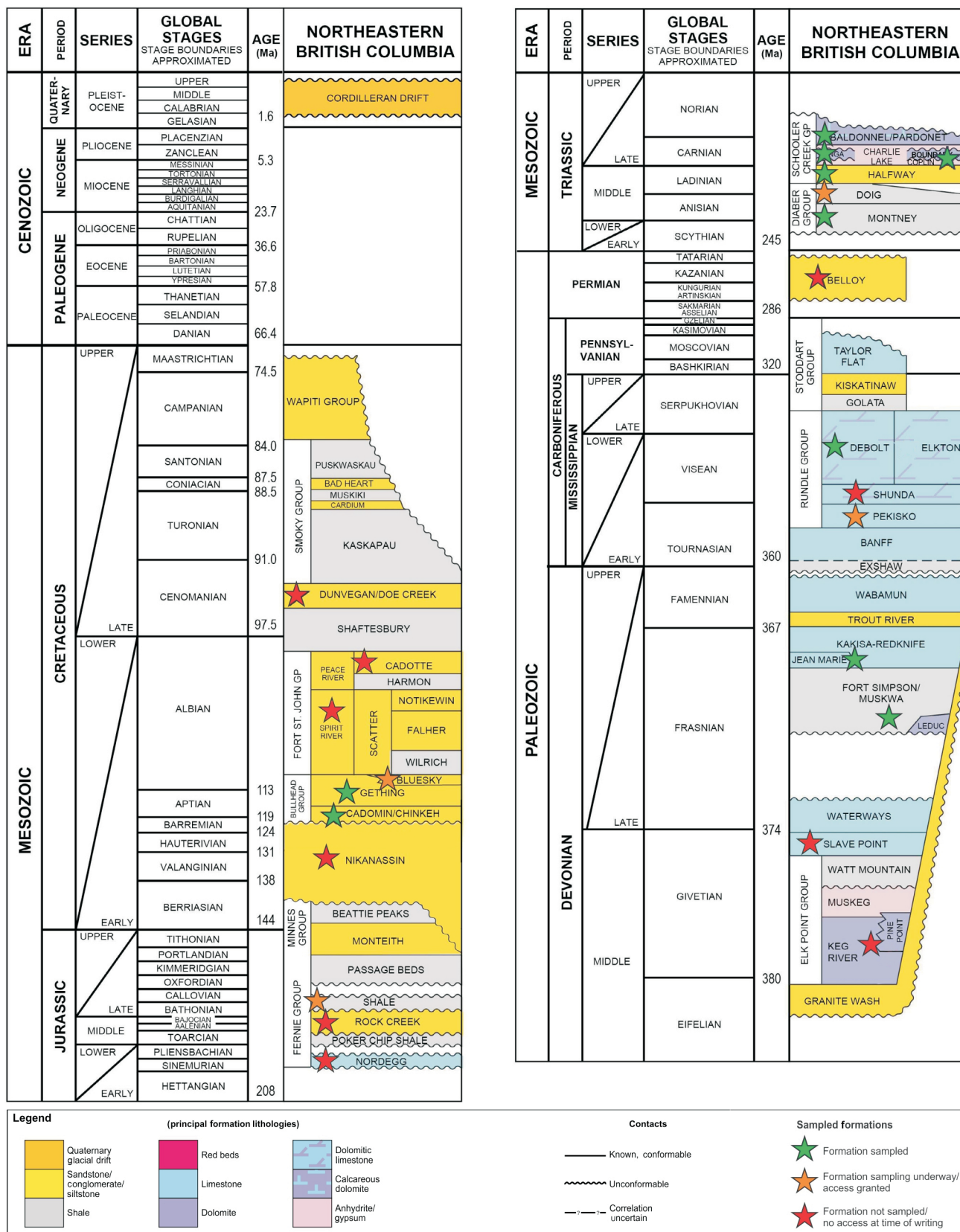


Figure 2. Stratigraphic column of northeastern British Columbia showing sample distribution (modified and reproduced with permission from Core Laboratories Petroleum Services, 2017).

collect samples at all. These exceptions, documented in the metadata collection, allowed for commingled fluid sampling where the commingled production stream was known to be producing from the same or equivalent formation interval. Special care was taken to ensure none of these exceptions had any commingled production from different stratigraphic zones. This measure helped to mitigate this filtering effect on the well lists available for each formation.

Another significant challenge, which arose part way through the project, was a change in the interpretation and application of provincial Mineral Tenure Act regulations pertaining to minerals dissolved in subsurface brines. This change significantly impacted whether operators and project proponents decided to participate in the program. Ultimately, a vast majority of the participating operators supported the need for data collected in projects of this nature, choosing to participate in the project despite these regulatory challenges.

Lastly, the project was conducted during the COVID-19 pandemic, which introduced a number of additional logistical challenges. It drove stricter health and safety policies and requirements of some of the larger operators participating in the program. In order to facilitate and minimize the burden to operators, they were given the option to have their local staff collect samples for the program. In these cases, all the metadata and chain of custody documentation was provided to the operator along with instructions for the standard sampling operating procedure. The project team documented this in the metadata collection and worked with operators to capture the necessary information and samples for the program. Also, during the pandemic, surges in energy prices led to increased production at oil facilities already impacted by a reduced work force. This affected the ability of some operators to be able to participate in the program.

## Conclusions

Subsurface brine resource exploration is accelerating in North America as the demand outlook for critical minerals and metals points to shortfalls before the end of the decade. Currently a window of opportunity exists to evaluate and identify the potential to develop these new resources. Characterizing the chemistry of formation waters in northeastern British Columbia is an important first step to inform regulatory policy considerations, de-risk early exploration activities to incentivize investment and development, as well as support the academic advancement of knowledge on resource prospects such as geothermal and dissolved mineral production, particularly for critical minerals and metals. The database and final report from this project will assist in these activities and help support the development

of a broader critical minerals and metals industry in British Columbia and Canada.

## Acknowledgments

The authors would like to acknowledge financial support from Geoscience BC, Northern Development Initiative Trust, Geological Survey of Canada and LithiumBank Resources Corp. along with the technical support of the advisors on this project's Advisory Committee. The authors would also like to thank W.S. Donaldson at Canadian Discovery Ltd. for taking the time to review this paper.

Additionally, this project would not be possible without the participation of key operators who have agreed to participate in this program despite significant staffing constraints through the COVID-19 pandemic and an emerging period of high energy prices: Crescent Point Energy Corp., Enercapita Energy Ltd., Erikson National Energy Inc., ISH Energy Ltd., Ovintiv Inc., Shell Canada Limited, Tourmaline Oil Corp. and Whitecap Resources Inc. At all levels, these operating companies have provided invaluable support to enable the sampling activities of this program.

## References

- Blondes, M.S., Gans, K.D., Engle, M.A., Kharaka, Y.K., Reidy, M.E., Saraswathula, V., Thordsen, J.J., Rowan, E.L. and Morrissey, E.A. (2018): U.S. Geological Survey national produced waters geochemical database (ver. 2.3, January 2018); U.S. Geological Survey, URL <<https://doi.org/10.5066/F7J964W8>>.
- Core Laboratories Petroleum Services (2017): Stratigraphic correlation chart; Core Laboratories Petroleum Services, Geological Sciences Department, 1 p., URL <<https://www.spec2000.net/downloads/StratChart.pdf>> [March 2021].
- Eccles, D.R. and Berhane, H. (2011): Geological introduction to lithium-rich formation water with emphasis on the Fox Creek area of west-central Alberta (NTS 83F and 83K); Energy Resources Conservation Board, ERCB/AGS Open File Report 2011-10, 28 p., URL <<https://ags.aer.ca/publication/offr-2011-10>> [November 2022].
- Eccles, D.R. and Jean, G.M. (2010): Lithium groundwater and formation-water geochemical data (tabular data, tab delimited format); Energy Resources Conservation Board, ERCB/AGS Digital Data 2010-0001, URL <<https://ags.aer.ca/publication/dig-2010-0001>> [March 2021].
- Grant, A. (2022): After the DLE Cambrian Explosion; Jade Cove Partners, URL <<https://www.jadecove.com/research/dlecambrianexplosion>> [September 2022].
- Jensen, G.K.S. (2012): Initial results of a brine sampling project: investigating the mineral potential of brines in southeastern Saskatchewan; *in* Summary of Investigations 2012, Volume 1, Saskatchewan Geological Survey, Saskatchewan Ministry of the Economy, Miscellaneous Report 2012-4.1, Paper A-8, 8 p.
- Jensen, G.K.S. (2016): Results from the 2016 field season for the brine sampling project: investigating the mineral potential of brines in Saskatchewan; *in* Summary of Investigations 2016, Volume 1, Saskatchewan Geological Survey, Sas-

- katchewan Ministry of the Economy, Miscellaneous Report 2016-4.1, Paper A-3, 7 p.
- Jensen, G.K.S. and Rostron, B. (2017): Investigating the mineral potential of brines in Saskatchewan: results from the 2017 field season for the brine sampling project; *in* Summary of Investigations 2017, Volume 1, Saskatchewan Geological Survey, Saskatchewan Ministry of the Economy, Miscellaneous Report 2017-4.1, Paper A-1, 6 p.
- Kamienski, C.W., McDonald, D.P., Stark, M.W. and Papcun, J.R. (2004): Lithium and lithium compounds; *in* Kirk-Othmer Encyclopedia of Chemical Technology, American Cancer Society, 40 p.
- Lico, M.S., Kharaka, Y.K., Carothers, W.W. and Wright, V.A. (1982): Methods for collection and analysis of geopressured geothermal and oil field waters; U.S. Geological Survey, Geological Survey Water-Supply Paper 2194, 21 p.
- Lopez, G.P., Weiss, J.A. and Pawlowicz, J.G. (2020): Lithium content in groundwater and formation water (tabular data, tab-delimited format); Alberta Energy Regulator / Alberta Geological Survey, AER/AGS Digital Data 2019-0029, URL <[https://services2.arcgis.com/jQV6VMr2Loovu7GU/arcgis/rest/services/Lithium\\_Content\\_in\\_Formation\\_Water/FeatureServer](https://services2.arcgis.com/jQV6VMr2Loovu7GU/arcgis/rest/services/Lithium_Content_in_Formation_Water/FeatureServer)> [April 2021].
- Natural Resources Canada (2021): Critical minerals; Natural Resources Canada, URL <<https://www.nrcan.gc.ca/criticalminerals>> [October 2022].
- Wilson, T., Williams, C., Pelletier, E., Murfitt, D., Rakhit, K. and Abercrombie, H. (2022): Northeastern British Columbia lithium formation-water database: forging the plan, process and path (NTS 093P, 094A, B, G–J, O, P, part of 0931); *in* Geoscience BC Summary of Activities 2021: Energy and Water, Geoscience BC, Report 2022-02, p. 1–8, <[https://cdn.geosciencebc.com/pdf/SummaryofActivities2021/EW/Project%202021-001\\_EWSOA2021.pdf](https://cdn.geosciencebc.com/pdf/SummaryofActivities2021/EW/Project%202021-001_EWSOA2021.pdf)> [October 2022].
- WorkSafeBC (2022): OHS Guidelines part 23: oil and gas; WorkSafeBC, URL <<https://www.worksafebc.com/en/law-policy/occupational-health-safety/searchable-ohs-regulation/ohs-guidelines/guidelines-part-23#SectionNumber:G23.5>> [October 2022].

# Investigating Fault-Sealing Effects on Induced Seismicity and Pore-Pressure Distribution in Northeastern British Columbia (Parts of NTS 093P, 094A): Observations and Modelling

Z. Esmaeilzadeh<sup>1</sup>, Department of Geoscience, University of Calgary, Calgary, Alberta, zahra.esmaeilzadeh@ucalgary.ca

D.W. Eaton, Department of Geoscience, University of Calgary, Calgary, Alberta

---

Esmaeilzadeh, Z. and Eaton, D.W. (2023): Investigating fault-sealing effects on induced seismicity and pore-pressure distribution in northeastern British Columbia (parts of NTS 093P, 094A): observations and modelling; *in* Geoscience BC Summary of Activities 2022: Energy and Water, Geoscience BC, Report 2023-02, p. 11–20.

## Introduction

The objective of this study is to test a hypothesis that induced seismicity risk is elevated in areas of high lateral gradient in pore pressure within the Montney Formation. To do this, a residual pore-pressure anomaly map was constructed. The results of this analysis support a simplified interpretation of pore-pressure terranes within the Kiskatinaw Seismic Monitoring and Mitigation Area (KSMMA) and surrounding area and indicate that induced earthquakes occur preferentially in areas of high lateral pore-pressure gradient. This study also investigates the effects of a large pore-pressure contrast on fault activation and hydraulic-fracture propagation mechanisms. To capture different aspects of the physical processes, numerical modelling was performed using two different approaches. First, with Itasca Consulting Group, Inc.'s 3DEC<sup>TM</sup> distinct element code, a simplified slip-weakening friction model was used to characterize the influence of a lateral pore-pressure gradient and high permeability damage zone on fault activation. Hydraulic-fracturing simulation was also performed using Halliburton Energy Services' Grid Oriented Hydraulic Fracture Extension Replicator (GOHFER<sup>®</sup>) software.

The study area encompasses the Septimus oil and gas field, which includes the location of the November 30, 2018, local magnitude ( $M_L$ ) 4.5 earthquake, and the KSMMA in northeastern British Columbia (BC; Figure 1).

## Previous Work

Pore pressure is a measurement of the in situ fluid pressure in a porous medium. Overpressure in tight formations has been linked to elevated risk of induced earthquakes (Eaton and Schultz, 2018). Previous studies have proposed that pore pressure in the Montney Formation is strongly com-

partmentalized into fault-bounded domains of high, intermediate and low pore pressure (Fox and Watson, 2019). The existence of these fault-bounded domains has a significant impact on seismic risk (Enlighten Geoscience Ltd., 2021). Seismicity induced by enhanced oil recovery in the Eagle and Eagle West oil and gas fields of northeastern BC was also influenced by fault-bounded pressure compartments (Horner et al., 1994). Pre-existing faults play an important role in reservoir dynamics. Some structurally complex reservoirs are dissected by sealing faults, which represent pressure barriers that form the boundaries of individual pressure compartments, such as the Egret field in the North Sea (e.g., Wilson, 2015). In the case where a fault is a pressure seal, a difference in pore pressure will exist across the fault. Although activation of a sealing fault could give rise to fault-valve behaviour, in which a co-seismic increase in permeability leads to partial equilibration of the pressure difference (Sibson, 1992), there has been relatively little attention given to the influence of a pore-pressure contrast on fault activation during fluid injection (Esmaeilzadeh et al., 2022). On November 30, 2018, an earthquake sequence with a  $M_L$  4.5 mainshock and ensuing aftershocks (Babaie Mahani et al., 2019; Salvage and Eaton, 2022) were localized near a pressure domain boundary along the southern bounding fault of the Fort St. John Graben (FSJG). The event was located near two horizontal wells that were undergoing hydraulic fracturing treatment at the time of the earthquake. These two wells, which have a true vertical depth (TVD) difference of 38 m, exhibit an exceptionally large lateral difference in pore pressure, approximately 10 megapascals (MPa) or 4.5 kilopascals/m (kPa/m) when expressed as a pressure gradient. The existence of this large pore-pressure contrast between two closely spaced wells in the Lower Montney Member provides motivation to investigate the potential association between lateral gradient in pore pressure and induced seismicity risk.

Although previous studies have carried out numerical simulations of processes of fault activation by hydraulic fracturing and water disposal, to the authors' knowledge the in-

---

<sup>1</sup>The lead author is a 2022 Geoscience BC Scholarship recipient.

This publication is also available, free of charge, as colour digital files in Adobe Acrobat<sup>®</sup> PDF format from the Geoscience BC website: <http://geosciencebc.com/updates/summary-of-activities/>.

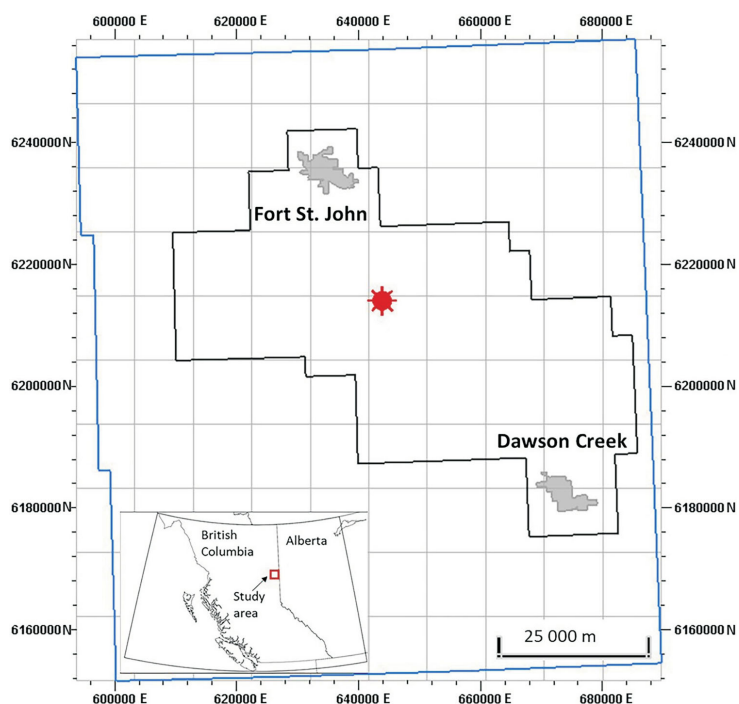


**Figure 1.** Location of the study area (blue outline) and Kiskatinaw Seismic Monitoring and Mitigation Area (black outline) in northeastern British Columbia. The star shows the approximate location of the November 30, 2018, earthquake sequence. All co-ordinates are in UTM Zone 10 North, NAD 83.

fluence on rupture processes of a large pore-pressure contrast across an impermeable fault has not been investigated using a numerical modelling approach. Rutqvist et al. (2013) conducted numerical simulation studies to assess the potential for injection-induced fault reactivation and notable seismic events associated with shale-gas hydraulic fracturing operations. Their modelling simulations indicate that if the fault is initially impermeable, hydraulic fracturing along the fault results in numerous small microseismic events along with the propagation, effectively preventing larger events from occurring (Rutqvist et al., 2013). Hu et al. (2018) built a 3-D model to simulate the stress field in Zhaziao, Leyi Township, China, which is associated with hydraulic fracturing. In their model the fault plane is set as nonpermeable. Thus, sliding is limited, shear displacement is only in the scale of millimetres and the calculated magnitude of the induced earthquakes is between moment magnitude ( $M_w$ )  $-3.5$  and  $-0.2$ . Zhang et al. (2020) presented a case study of fault reactivation and induced seismicity during multistage hydraulic fracturing in Sichuan Basin, China. Their modelling results showed that the aseismic deformation consumes a major part of the energy budget. The results indicate that lower injection rate and lower fluid viscosity would be helpful in reducing casing deformation but not in mitigating seismicity. Hemami et al. (2021) carried out a study to simulate the contribution of disposal wells to pore-pressure and stress perturbations in a fault zone near Prague, Oklahoma, at a depth of  $\sim 5000$  m under different

permeability structures. They constructed a coupled fluid-mechanical model to study the effect of saltwater injection on the fault reactivation and earthquake sequence. Their results suggest that the tendency of fault reactivation within deep crystalline basement increases when the fluid is pumped into a fault-bounded volume and a fault damage zone acts as a path for fluid to penetrate the deeper depth.

The purpose of this project is to test a working hypothesis, that induced seismicity risk is elevated in areas of high lateral gradient in pore pressure. A rationale for this hypothesis is that the existence of a high lateral gradient could indicate sealing faults that control distribution of overpressure in the Montney Formation. The goal of this study is to quantify the effects of pressure barriers on fault activation and hydraulic-fracture mechanism through numerical modelling, a topic that has received relatively little attention in the literature. The sensitivity of fault activation and fracture propagation is tested based on the presence or absence of a large pore-pressure difference, as well as the presence or absence of a highly fractured and permeable damage zone on both sides of the fault.

## Pore-Pressure Data and Mapping Method

This study uses pore-pressure data compiled by Enlighten Geoscience Ltd. (Enlighten; 2021), who performed a comprehensive study on pressure and stress mapping, and fault-slip potential analysis in the KSMMA. They used more than 3000 pressure data points within the Montney Formation in their study, including data from diagnostic fracture injection tests (DFITs), drillstem tests (DSTs) and reservoir pressure survey tests. Of these 3000 observations, 2022 are from the Upper Montney Member. All tests were subjected to quality control (QC) evaluation to remove poor quality tests, taking into account different gauge resolutions, and to exclude the outliers. For individual wells, the pressure data were extrapolated to the initial reservoir pressure to minimize the effects of production and fluid injection. The Enlighten dataset was augmented with 120 new bottom-hole pressure measurements within the Montney Formation, extracted using geoSCOUT (geoLOGIC systems ltd., 2022). From these new data, those with less than 10 days of shut-in duration prior to testing were excluded. In addition, pore-pressure measurements with a subhydrostatic gradient less than 6 kPa/m were excluded, leaving a total of 1782 data points for analysis. Next, gridded pore-pressure data were constructed using kriging (Figure 2). Also known as Gaussian process regression, kriging is a method of interpolation based on a Gaussian process governed by prior covariances. Under suitable assumptions of the prior, kriging

gives the best linear unbiased prediction (BLUP) at unsampled locations (Chung et al., 2019). The kriging method is widely used in the domain of spatial analysis. As shown in Figure 2, the gridded pore-pressure data contain a significant regional trend, which reflects the transition from an over-pressured regime in the deep basin (southwest of the study area) toward a normally pressured regime at the up-dip margin in the northeast. In the next step, a regional trend surface was removed by determining residual values based on quadratic regression using The Mathworks, Inc.'s MATLAB. Quadratic regression provided the highest regression coefficient compared to other methods for fitting the regional surface. Outliers were excluded using a median approach, in which outliers are defined as elements more than three scaled median absolute deviation (MAD) units from the median value. To remove the bull's-eye anomalies, smoothing of the data was performed by convolution using a two-dimensional low-pass filter (5 km). The smoothed data are shown in Figure 3. A mask has been applied to the map of the smoothed residual pore-pressure data to remove values that fall outside of the main well control.

### Pore-Pressure Analysis Results

The smoothed residual pore-pressure map in Figure 3 contains a number of clear anomalous features. The Saturn Low is a curvilinear relatively low pore-pressure terrane with a general east-west trend. The Septimus High and Doe High terranes flank the Saturn Low terrane to the north and south, respectively. Near the northwestern corner of the KSMMA, the Monias High terrane contains the highest residual pore-pressure values. The Dawson Low terrane is a north-northwest–south-southeast-trending anomaly in the southeastern part of the study area, mainly lying outside of the KSMMA. Figure 4 shows seismicity data overlain onto the pore-pressure residual map. The seismicity data were downloaded from the online catalogue maintained by the BC Oil and Gas Commission (2022) on October 13, 2022. The catalogue contained all seismic data from 2001 to October 13, 2022 and includes natural and induced earthquakes. In the central part of the KSMMA, it is evident that two prominent bands of seismicity (presumed induced) roughly flank the Saturn Low terrane, to the north and south. Seismicity in the northern part of the map region represents historical induced seismicity from the Eagle and Eagle West fields, north of Fort St. John. Overlaying seismicity onto the pore-pressure residual map reveals an apparent correlation between bands of seismicity and two positive

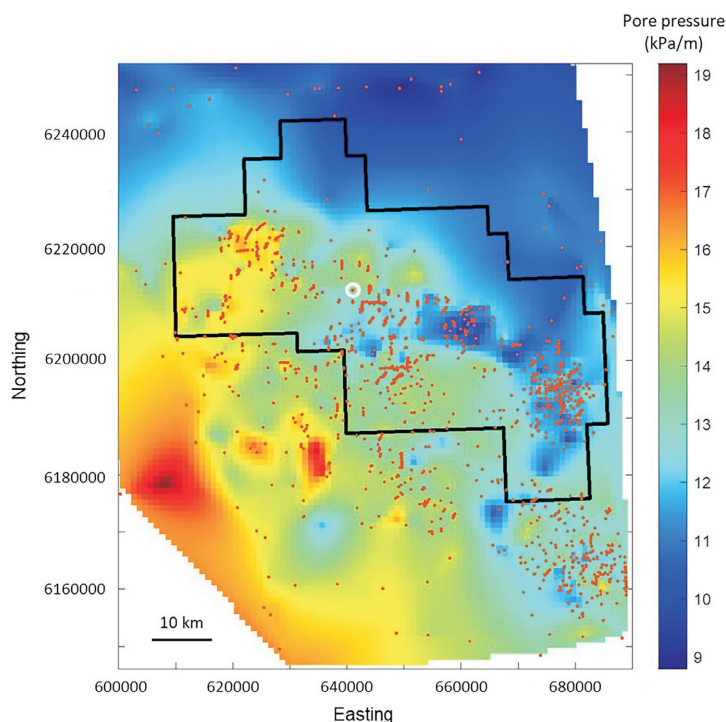


**Figure 2.** Pore-pressure gradient for the entire Montney Formation in the study area, computed by kriging. Orange dots show pore-pressure data points (from Enlighten Geoscience Ltd., 2021; geoLOGIC systems Ltd., 2022), the white circle shows the location of the two horizontal wells. Black outline shows the Kiskatinaw Seismic Monitoring and Mitigation Area. All co-ordinates are in UTM Zone 10 North, NAD 83. Abbreviation: kPa, kilopascal.

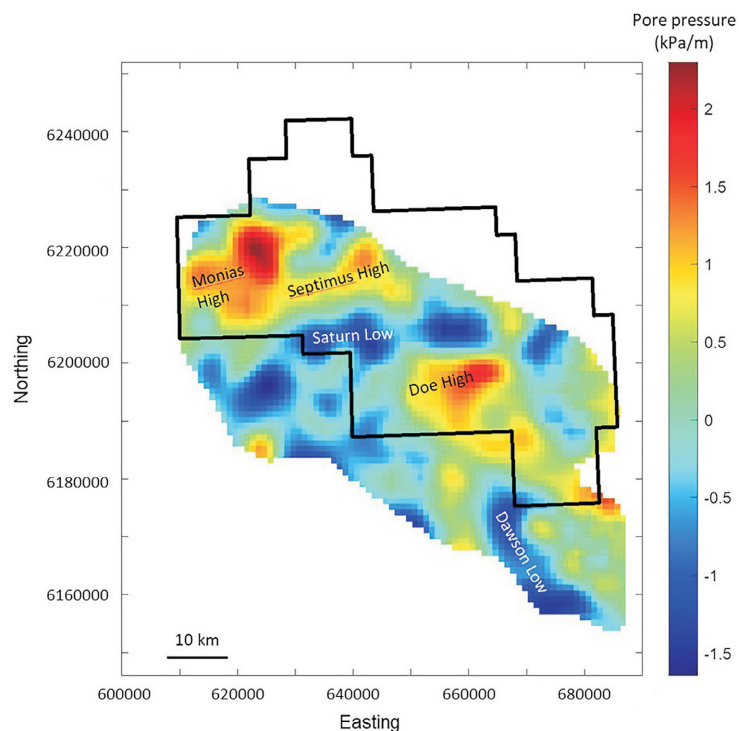


**Figure 3.** Smoothed pore-pressure residual map of the entire Montney Formation in the study area, masked by a polygon that encloses areas of high well control. Interpreted pore-pressure terranes are labelled. Black outline shows the Kiskatinaw Seismic Monitoring and Mitigation Area. All co-ordinates are in UTM Zone 10 North, NAD 83. Abbreviation: kPa, kilopascal.

east-west trends in the horizontal pore-pressure gradient data.

### 3DEC Model Geometry and Set Up

The first set of models was constructed using a three-dimensional numerical modelling code, 3DEC. Based on the numerical formulation of the distinct element method (Cundall and Strack, 1979), 3DEC simulates the mechani-

cal response of rock mass with discontinuities, such as fractures and faults (Israelsson, 1996). A rock formation in 3DEC is represented as an assembly of jointed blocks, and the interaction of the blocks is governed by the constitutive relation for the joints that determines force, displacement and failure. Each individual block is discretized into finite volume zones to allow block deformation. Fluid flow is simulated in flow planes defined through joints or within the block matrix. The fluid calculation is fully coupled with the mechanical deformation of the blocks. In this study, 3DEC was used to model the sensitivity of fault and fracture response to the presence of a sealing fault and/or damage zone.

The 3DEC model was configured as a rectangular block that is 500 m long, 500 m wide and 150 m high (Figure 5). A hydraulic fracture (HF) plane is located at the centre of the model. A fault plane with 90° dip runs through the model and obliquely intersects the HF plane. This fault orientation is close to optimal for shear slip. The HF plane and the fault plane are characterized by the Mohr-Coulomb constitutive relation. A pore-pressure difference was introduced to the two sides of the fault so that one side (pore pressure 1 [PP1], which is 38 MPa) had a 10 MPa overpressure relative to the other side (pore pressure 2 [PP2], which is 28 MPa). The permeability of the fault plane and immediate surrounding zone was configured as a fault core that acted as a pore-pressure barrier, with much lower permeability than the rock matrix. Surrounding high-permeability zones were specified as fault damage zones, which sandwiched the fault core. The width of each damage zone was 15 m and the width of the fault core was considered to be 1.5 m. The top and bottom portions of the HF plane and fault plane were configured to high tensile strength, leaving the centre portion of the planes (~120 m) as a weak corridor for hydraulic-fracture propagation. Two treatment stages were included in the simulation. The treatment stages were located on the HF plane, 25 m away from the intersection between the HF plane and the fault plane, outside of the damage zones. The first treatment stage (at well A) was in a low pore-pressure domain, and the second treatment stage (at well B) was in a high pore-pressure domain. Fluid injections were conducted at a constant injection rate. The simulated injection rates for the first and second treatment stages were 0.125 and 0.1 m<sup>3</sup>/s, respectively. The fluid injection of the second treatment stage started after the shut-in of the first treatment stage. In situ stresses were implemented for the model with the orientation of maximal horizontal stress parallel to the HF plane. Finally, the

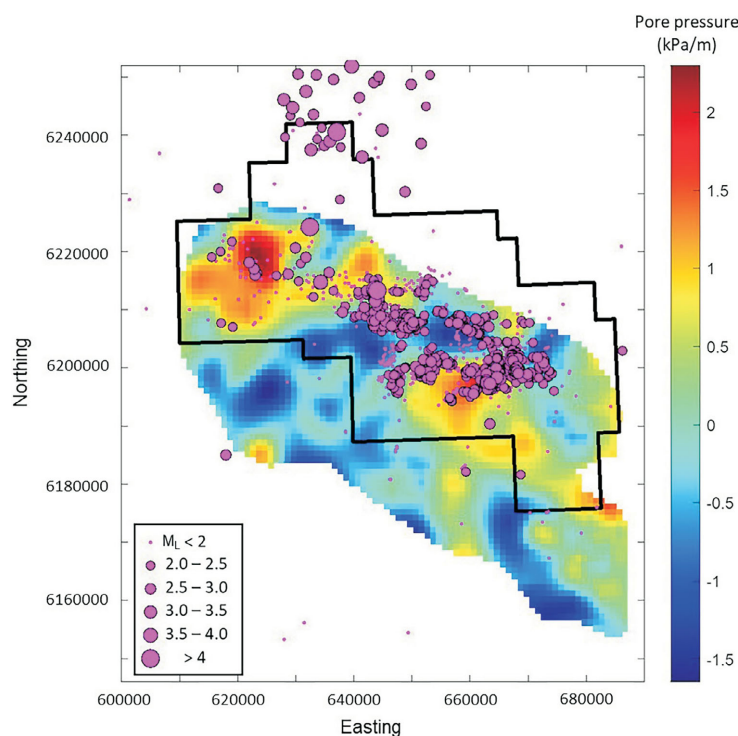


**Figure 4.** Seismicity data, 2001 to November 13, 2022 (from BC Oil and Gas Commission, 2022), overlain on smoothed pore-pressure residual map for the entire Montney Formation in the study area. Seismicity north of Kiskatinaw Seismic Monitoring and Mitigation Area (black outline) was induced by enhanced oil recovery in the Eagle and Eagle West oil and gas fields. All coordinates are in UTM Zone 10 North, NAD 83. Abbreviations: kPa, kilopascal;  $M_L$ , local magnitude.

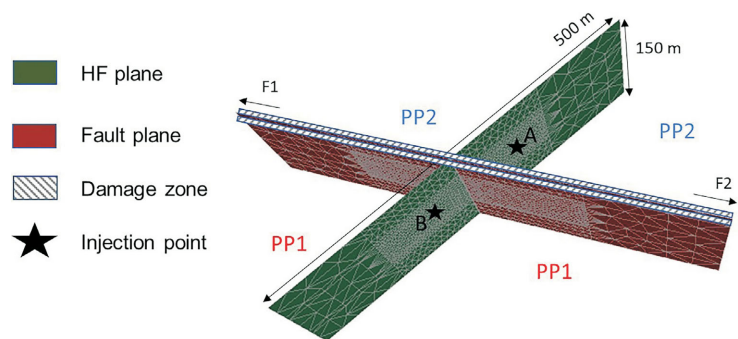


**Figure 5.** The 3DEC™ model geometry considered in this study. Abbreviations: A, well A; B, well B; F1, fault rupture propagation direction corresponding to an obtuse angle between the initial hydraulic fracture plane and the fault plane; F2, fault rupture propagation direction corresponding to an acute angle between the initial hydraulic fracture plane and the fault plane; HF, hydraulic fracture; PP1, pore pressure 1 (38 megapascals); PP2, pore pressure 2 (28 megapascals).

boundaries of the model were fixed, with zero displacement and velocity. The simulation time step was one second. The dimensions, fracture parameters and operational constraints were tuned based on the GOHFER model results presented in the next section, to maintain the consistency between the actual and numerical models.

Two simulation cases were undertaken to investigate the influence of pore-pressure contrast:

- Case 1: no damage zone, no pressure contrast; the pore pressure for both sides was PP2 (Figure 6)
- Case 2: presence of damage zone, strong pore-pressure contrast between sides (PP1 > PP2, 10 MPa overpressure; Figure 7)

### 3DEC Modelling Results

#### Case 1: No Damage Zone and No Pressure Contrast

The simulation results for the reference model (case 1), with neither a damage zone nor any pore-pressure contrast across the fault, are summarized in Figure 6. In this simulation, the presence of an impermeable (but weak) fault created a barrier that inhibited the propagation of the hydraulic

fracture. A final symmetric fracture geometry was obtained, and the slight difference in the fracture dimensions on both sides of the fault is probably due to stress shadowing effects caused during well B injection. The model predicts tensile opening of the fault plane, similar to field observations of the results of direct injection into a pre-existing fault (Guglielmi et al., 2015). However, in this model there was a preferred direction of fault rupture/opening, in the direction subtended by an obtuse angle between HF plane in well A and the fault plane.

#### Case 2: Damage Zone and Strong Pressure Contrast

The simulation results for the case 2 model, which is characterized by both a pressure contrast and a damage zone around the fault, are summarized in Figure 7. In this case, the fault was breached during well A injection. When the simulation run was complete, it ultimately produced a symmetrical HF pattern. Once again, the effect of the damage zone was a more diffuse fault opening. The damage zone seems to act as a permeable conduit in the absence of a pressure contrast and contributes to fracture development, whereas in the presence of a pressure gradient it allows fluid leakage.

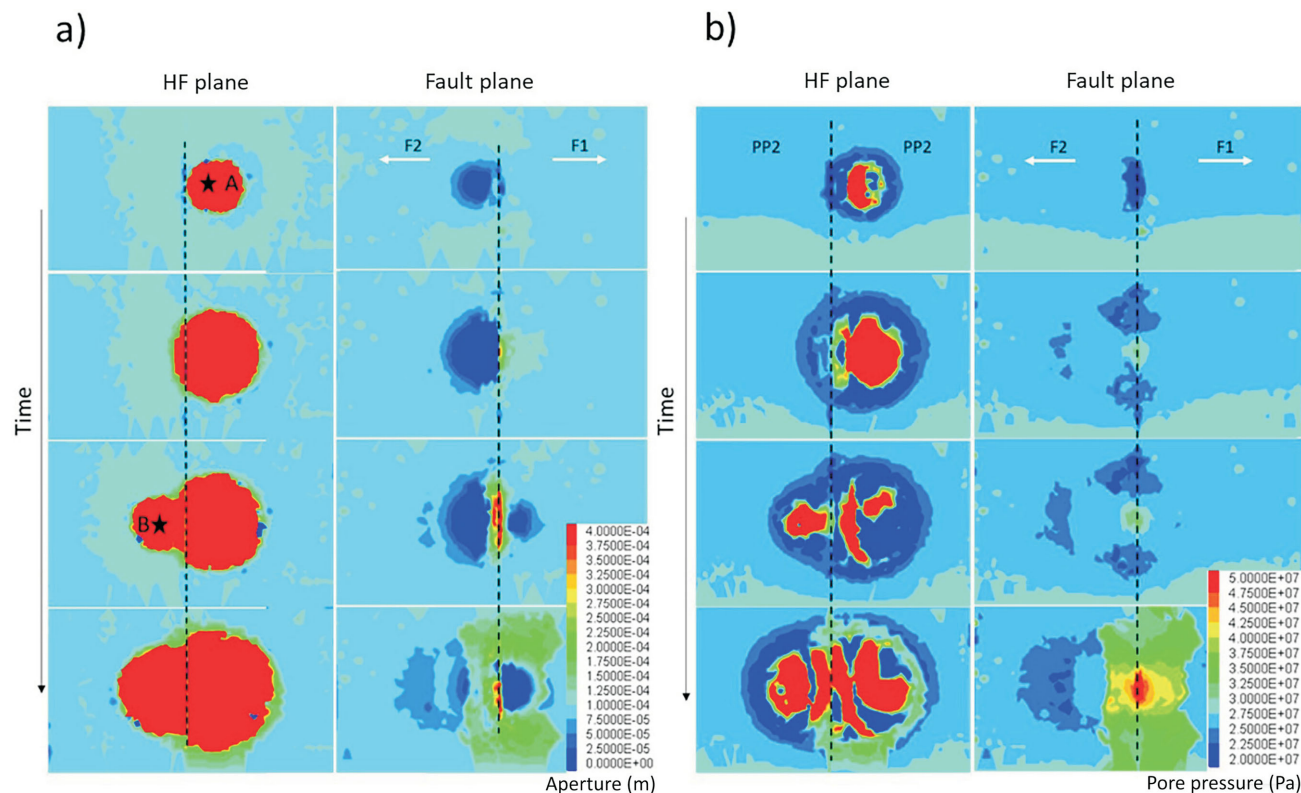


**Figure 6.** Results for case 1 model. **a)** The aperture for the hydraulic fracture plane and the fault plane. Stars indicate the location of injection points. The first two time periods are the start and the stop of the well A (A) injection, and the third and fourth time periods are the beginning and end of well B (B) injection. **b)** Pore pressure for the hydraulic fracture plane and the fault plane. The fault plane appears to inhibit hydraulic fracture growth. Fault aperture shows preferred growth in the F2 direction. Abbreviations: F1, fault rupture propagation direction corresponding to an obtuse angle between the initial hydraulic fracture plane and the fault plane; F2, fault rupture propagation direction corresponding to an acute angle between the initial hydraulic fracture plane and the fault plane; HF, hydraulic fracture; Pa, pascal; PP2, pore pressure 2 (28 MPa).

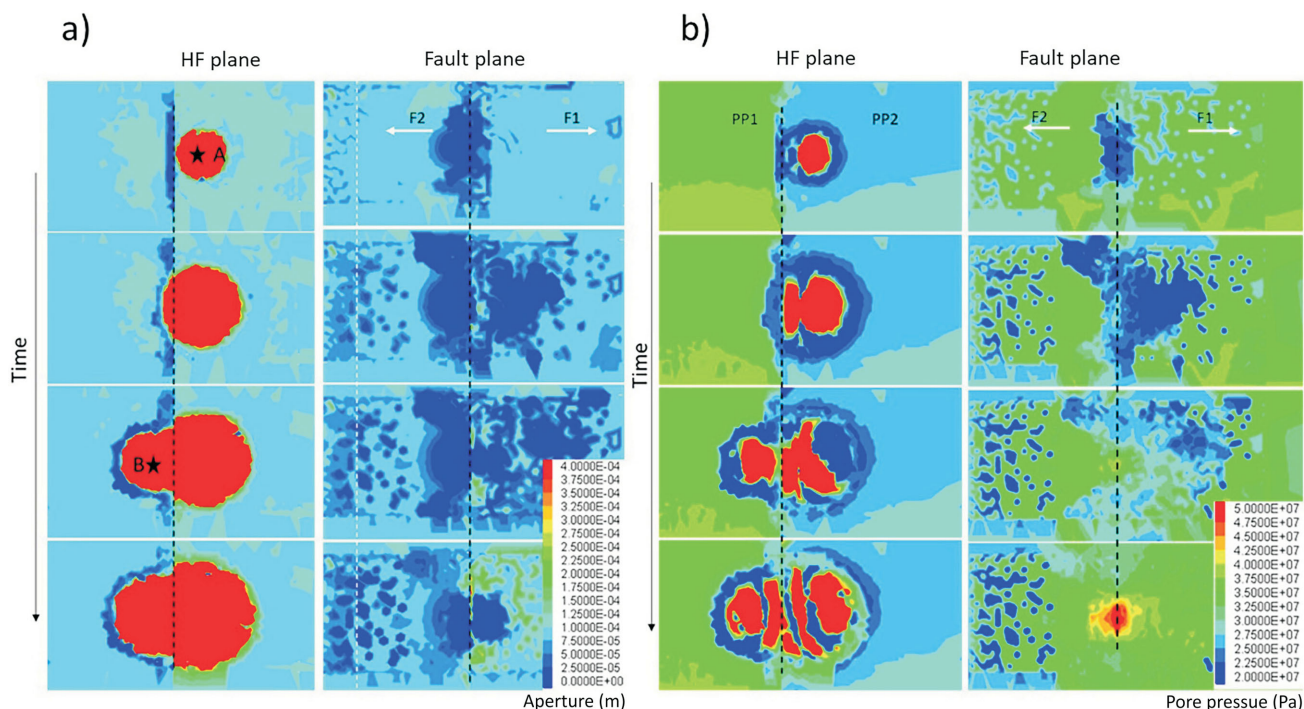


**Figure 7.** Results for case 2 model. **a)** The aperture for the hydraulic fracture plane and the fault plane. Stars indicate the location of injection points. The first two time periods are the start and the stop of the well A (A) injection, and the third and fourth time periods are the beginning and end of well B (B) injection. **b)** Pore pressure for the hydraulic fracture plane and the fault plane. The permeable damage zone appears to channel pore pressure along the fault, leading to the development of a more uniform fault aperture. Considerable leakage of overpressure is evident, from the high pore-pressure domain (PP1) into the lower pore-pressure domain (PP2). Abbreviations: F1, fault rupture propagation direction corresponding to an obtuse angle between the initial hydraulic fracture plane and the fault plane; F2, fault rupture propagation direction corresponding to an acute angle between the initial hydraulic fracture plane and the fault plane; HF, hydraulic fracture; Pa, pascal; PP1, pore pressure 1 (38 MPa); PP2, pore pressure 2 (28 MPa).

## Discussion

The sensitivity of the fault activation has been tested based on the presence or absence of a large pore-pressure difference, as well as the presence or absence of a highly fractured and permeable damage zone on both sides of the fault (four cases). Due to space limitations, only the results of cases 1 and 2 are presented in this paper. Although both a damage zone and pore-pressure contrast showed an increase in the magnitude of induced events, all of the models considered here produced similar final equivalent moment magnitudes of approximately  $M_w$  2.2 (Figure 8), with a generally decelerating moment release rate. The moment magnitude increases more rapidly during the initial stimulation, then subsequently slows down. Since a simplified slip-weakening model was used here, and dynamic rupture processes were not explicitly considered, the fault activation likely provides a better representation of slow (aseismic) fault slip. These small magnitude earthquakes perfectly match with the real seismicity pattern between the two HF horizontal wells.

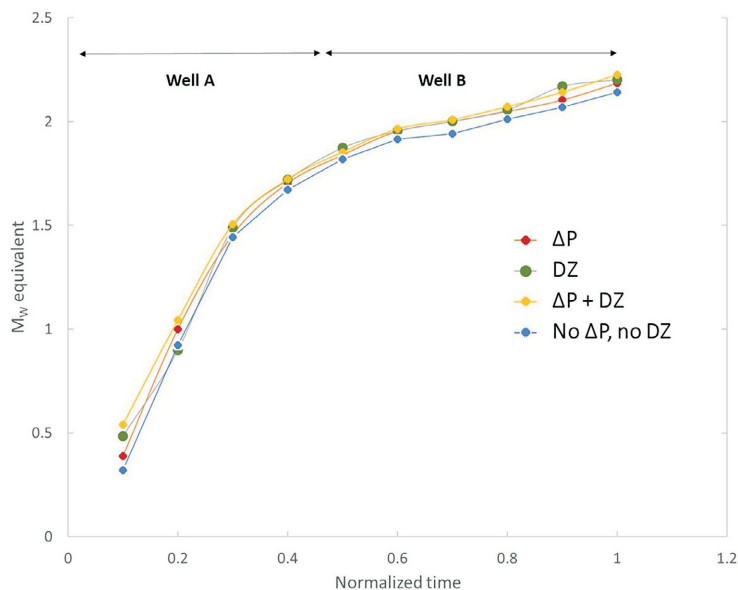


**Figure 8.** Evolution of cumulative equivalent moment magnitude ( $M_w$ ) versus normalized time, where one time unit is the duration of injection into one well. All of the models culminate with a  $M_w$  of approximately 2.2. Both pore-pressure contrast and permeable damage zone increase the event moment magnitudes. The amount of increase also depends on the fault dimensions and critical state. Abbreviations:  $\Delta P$ , lateral pore-pressure gradient; DZ, damage zone.

## GOHFER Hydraulic Fracturing Simulation

GOHFER is a planar 3-D geometry fracture simulator with a fully coupled fluid/solid transport simulator. GOHFER, developed by R. Barree in 1983, has been continually refined based on laboratory and field data. A grid structure is used to describe the entire reservoir and allows for vertical and lateral variations and bi-wing asymmetric fractures to model complex reservoirs. The grid is used for both elastic rock displacement calculations and finite difference fluid flow solutions. Proppant concentration, leakoff, width, pressure, viscosity and other variables are accounted for at each grid block. The in situ stress is internally calculated from pore pressure, Biot's coefficient and elastic moduli. The width solution is fully 3-D and local displacements are controlled by local pressures and rock properties. The fracture extension model in GOHFER is based on a formulation that expects the formation to fail in shear and be essentially decoupled.

For horizontal well simulations, a nearby vertical reference well with a full suite of logs is often used to characterize the properties of the medium. Here, the reference well is a ver-

tical well located 3 km northeast of the modelled treatment wells. The primary well logs imported for this study include neutron and density porosity (PHIN and PHID), gamma ray (GR), density (RHOB), resistivity (RESIST) and compressional sonic travel time (DTC). The grid properties and grid dimensions defined to set up the model are listed in Tables 1 and 2. A layered isotropic model was assumed for this study. The HF plane was confined by two stiff layers preventing out-of-zone fracture growth. A general pore-pressure offset of ~7 MPa was applied to reproduce the overpressure behaviour of the unconventional Montney reservoir at the target depths in the study area. To generate the 10 MPa pressure difference between the two wells, an additional pore-pressure offset was added along well B.

The stage pumping schedule for the actual hydraulic-fracturing job performed in this study is presented in Table 3 for well B. This well is considered close to the fault and completed in the high pressure zone. Slickwater and resin-coated sands with 40/70 mesh size were used as fracturing fluid and proppants. Seven stages were completed in well B. It was during the completion of the seventh stage on November 30, 2018, that the M<sub>L</sub> 4.5 mainshock occurred south of Fort St. John.

Due to space limitations, only the diagrams of the base case model (no pressure contrast, no damage zone) and the fracture model with damage zone and strong pressure contrast are shown here (Figure 9). The results of other simulation scenarios are presented in Table 4 for comparison. To calibrate the model, history matching was performed, calibrated by the breakdown pressure, injection rate, total proppant volume, pressure data, as well as total stress with the actual operational data.

**Table 1.** Grid dimensions used in the GOHFER<sup>®</sup> model.

Grid dimensions	
Node size (m)	5
Aspect ratio	2
Length (m)	4000
Transverse aspect ratio	2
Grid top (m)	1800
Grid bottom (m)	2500

**Table 2.** Grid properties used in the GOHFER<sup>®</sup> model.

Grid properties	
Rock density (kg/m <sup>3</sup> )	2650
Biot's coefficient	0.24
Compressional sonic travel time (μs/m)	195
Poisson's ratio	0.25
Static Young's modulus (GPa)	40
Pore pressure 1 (MPa)	38
Pore pressure 2 (MPa)	28
Water saturation (fraction)	0.3
Strain, microstrain	400
Matrix porosity (fraction)	0.1
Damage zone permeability (m <sup>2</sup> )	9.87 × 10 <sup>-16</sup>
Matrix permeability (m <sup>2</sup> )	9.87 × 10 <sup>-18</sup>
Process zone stress (fracture net stress; MPa)	7
Vertical stress (MPa)	59
Maximum horizontal stress (MPa)	128
Total stress (closure pressure; MPa)	42

Abbreviations: GPa, gigapascal; MPa, megapascal

## Fracture Geometry and Simulation Results

As expected, the nearby fault acted as a barrier against fracture propagation and prevented fracture growth beyond the fault. However, this sealing behaviour depends on the fault throw, injection rate, damage zone properties and the amount of lateral pore-pressure gradient (ΔP) across the fault. Faults with a small vertical offset may not completely seal the fracture plane. Thus, in the intervals where the layer is still connected on both sides of the fault, the fluid can penetrate to the other side. The amount of penetration, however, depends on the injection rate. If a damage zone is present, fluid leakage (in the presence of ΔP) into the permeable pathways leads to a shorter fracture. Finally, a sealing fault with a large pressure contrast produces an asym-

**Table 3.** Pumping schedule for well B, used in the GOHFER<sup>®</sup> model.

Average fluid injection rate (slickwater and proppant) (m <sup>3</sup> /min)	Maximum fluid injection rate (m <sup>3</sup> /min)	Volume of slickwater (m <sup>3</sup> )	Volume of slickwater and proppant (m <sup>3</sup> )	Volume of acid (m <sup>3</sup> )	Proppant tonnage (t)
6.2	6.2	1175.8	1213.4	9	98

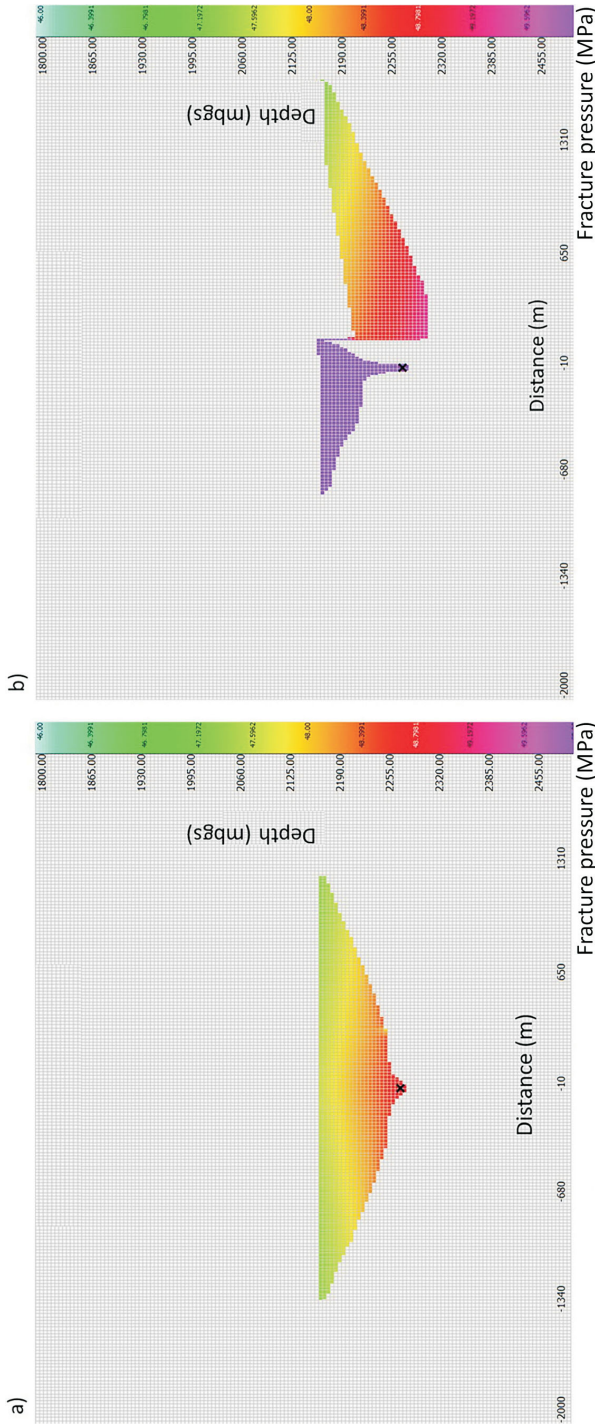


**Figure 9.** Hydraulic-fracture geometry in well B in terms of fracture pressure. **a)** Model with no fault and no pore-pressure contrast. The final fracture geometry is a symmetrical bi-wing fracture with an upward growth tendency in a layered medium. **b)** Model with a damage zone ( $9.87 \times 10^{-16} \text{ m}^2$  permeability) and a strong pore-pressure contrast. Pressure difference across the fault leads fracture propagation into the low-pressure side. Damage zone permeability controls leakoff rate and the final fracture length. The 'x' indicates the location of the stage treatment. Abbreviations: mbgs, metres below ground surface; MPa, megapascal.

**Table 4.** Hydraulic fracturing results of the stage treatment of well B for different simulation scenarios, used in the GOHFER<sup>®</sup> model. Abbreviations:  $\Delta P$ , lateral pore-pressure gradient; DZ, damage zone; MPa, megapascal; perm., permeability.

Simulation scenario	Gross fracture length (m)	Proppant cutoff length (m)	Estimated flowing fracture length (m)	Fracture height (m)	Average proppant concentration (kg/m <sup>2</sup> )	Average conductivity (m <sup>2</sup> *m)	Cumulative fluid lost (m <sup>3</sup> )	Flowing area (m <sup>2</sup> )	Propped area (m <sup>2</sup> )	Efficiency (%)	Width (mm)
No fault, no $\Delta P$ , no DZ	1270	40	9	115	0.4	$2.37 \times 10^{-16}$	80	4076	18400	50	4
50 m throw normal fault, no $\Delta P$ , no DZ	1420	70	9	115	0.41	$1.48 \times 10^{-16}$	81	4012	32200	50	4
No $\Delta P$ , DZ perm. of $9.87 \times 10^{-16} \text{ m}^2$	1370	50	17	115	0.4	$1.97 \times 10^{-16}$	91	7732	23000	44	4
No $\Delta P$ , DZ perm. of $9.87 \times 10^{-15} \text{ m}^2$	1430	80	37	125	0.48	$1.58 \times 10^{-16}$	94	18642	40000	42	4
No fault, no DZ, only $\Delta P$	1820	50	7	115	0.42	$2.37 \times 10^{-16}$	80	3033	23000	51	4
$\Delta P$ , no DZ	1910	50	7	115	0.41	$2.37 \times 10^{-16}$	80	3176	23000	51	4
$\Delta P$ + DZ perm. of $9.87 \times 10^{-16} \text{ m}^2$	1740	20	14	115	0.47	$3.65 \times 10^{-16}$	87	6568	9200	46	4
$\Delta P$ + DZ perm. of $9.87 \times 10^{-15} \text{ m}^2$	1500	20	39	115	0.3	$2.57 \times 10^{-16}$	107	18082	9200	34	5
Sensitivity, fracture net stress of 20 MPa, DZ perm. of $9.87 \times 10^{-16} \text{ m}^2$	2990	30	17	115	0.78	$4.54 \times 10^{-16}$	66	7998	13800	59	12
Sensitivity, matrix perm. of $9.87 \times 10^{-20} \text{ m}^2$ , DZ perm. of $9.87 \times 10^{-16} \text{ m}^2$	2520	20	9	110	0.46	$3.75 \times 10^{-16}$	30	4120	8800	81	4

metric fracture, with most of the fracture length being in the low-pressure domain. Therefore, fault structural properties, operational constraints, damage zone permeability and  $\Delta P$  are all important parameters controlling the fault-sealing behaviour. Hydraulic-fracture geometry in well B is shown in Figure 9. Table 4 summarizes the simulation results of the stage treatment in well B for different scenarios. Additional sensitivity analysis was performed on matrix permeability and fracture net pressure based on values reported in core data and DFIT reports. The average matrix permeability is  $\sim 9.87 \times 10^{-18} \text{ m}^2$  based on well log calculations and most core values, however, some core data suggest lower permeabilities (in the range of  $9.87 \times 10^{-20} \text{ m}^2$ ) in some regions. Also, the fracture net stress, defined here as the difference between instantaneous shut-in pressure (ISIP) and closure pressure in the DFIT tests, shows two average values of 7 and 20 MPa. Therefore, understanding the role of matrix transmissibility and fracture net stress in hydraulic fracture geometry is important (Table 4).

## Conclusions

The Kiskatinaw Seismic Monitoring and Mitigation Area is situated within a transition region between overpressured and normally pressured regimes for the Montney unconventional hydrocarbon system. Localized vestiges of overpressure, such as the Monias High, Septimus High and Doe High terranes, are interpreted to be bounded by sealing faults. Areas of relative pore-pressure lows, such as the Saturn Low terrane, are interpreted as areas in which permeable pathways exist, which allowed depressurization of the Montney Formation during exhumation. This study has attempted to test a working hypothesis that elevated induced seismicity risk is coincident with high lateral gradient in pore pressure. This study provides robust statistical evidence that induced seismicity occurs preferentially in areas of high lateral pore-pressure gradient.

The 3DEC modelling results show that both damage zone and pore-pressure contrast influence the fault activation. Additionally, they both increase the magnitude of induced seismicity. The presence of a damage zone around the fault appears to channel pore pressure along the fault, leading to a more uniform distribution of fault aperture and pore pressure than in the absence of a damage zone where the fault opening is concentrated near the hydraulic-fracture fault intersection.

Hydraulic-fracture modelling results indicate that the presence of a fault, regardless of its sealing behaviour and damage zone properties, affects hydraulic-fracture geometry due to stress variation around the fault. Fault-sealing behaviour depends on the amount of pressure difference, stress shadowing effects from previous stages, fault throw, injection rate and damage zone permeability. Based on these model results, the order of importance of the param-

eters affecting the development of a fracture network in the presence of a fault is as follows: stress shadowing > lateral pore-pressure gradient > fault-sealing effects. When there is a lateral pore-pressure gradient across the fault, the fracture pressure at the fault intersection is higher than when there is no pressure difference across the fault. Effects of a damage zone are more pronounced when there is a lateral pore-pressure gradient across the fault. Finally, damage zone permeability is more important than lateral pore-pressure gradient in terms of the effects on fluid loss and proppant concentration. Higher fracture net stress increases the fracture dimensions in the presence of a pressure barrier and damage zone. Low matrix permeability increases the fracture half-length and decreases the fracture height in the presence of a pressure barrier and damage zone. Both impermeable rock and high stress fractures reduce the cumulative fluid loss.

## Acknowledgments

This work was funded by a Natural Sciences and Engineering Research Council of Canada's Alliance grant and a scholarship from Geoscience BC. Special thanks to BC Oil and Gas Commission for providing data used in this work. geoLOGIC systems ltd. is thanked for their contribution of data and software used in this study. All geoLOGIC systems ltd. data and software is © 2022. The authors would like to thank Schlumberger Canada Limited for providing access to Petrel software under academic licence, and Halliburton Energy Services for providing an academic licence for GOHFER<sup>®</sup> fracture modelling software. The authors are grateful to Itasca Consulting Group, Inc. for providing a research licence for 3DEC<sup>™</sup>. The authors appreciate their peer reviewer, N. Orr, at CNRL, for taking the time and effort necessary to provide insightful guidance. All sponsors of the Microseismic Industry Consortium are sincerely thanked for their financial support.

## References

- Babaie Mahani, A., Kao, H., Atkinson, G.M., Assatourians, K., Addo, K. and Liu, Y. (2019): Ground-motion characteristics of the 30 November 2018 injection-induced earthquake sequence in northeast British Columbia, Canada; *Seismological Research Letters*, v. 90, no. 4, p. 1457–1467.
- BC Oil and Gas Commission (2022): Seismic events magnitude 1.5 and greater in NEBC [BCOGC-76037]; BC Oil and Gas Commission, URL <<https://www.bcogc.ca/data-reports/data-centre/?category=77352>> [October 2022].
- Chung, S.Y., Venkatramanan, S., Elzain, H.E., Selvam, S. and Prasanna, M. (2019): Supplement of missing data in groundwater-level variations of peak type using geostatistical methods; Chapter 4 *in* GIS and Geostatistical Techniques for Groundwater Science, S. Venkatramanan, M.V. Prasanna and S.Y. Chung (ed.), Elsevier Inc., Amsterdam, The Netherlands, p. 33–41.
- Cundall, P.A. and Strack, O.D. (1979): The development of constitutive laws for soil using the distinct element method; *in* Numerical Methods in Geomechanics, Aachen, 1979,

- W. Wittke (ed.), A.A. Balkema, Rotterdam, The Netherlands, v. 1, p. 289–317.
- Eaton, D.W. and Schultz, R. (2018): Increased likelihood of induced seismicity in highly overpressured shale formations; *Geophysical Journal International*, v. 214, no. 1, p. 751–757.
- Enlighten Geoscience Ltd. (2021): Pressure, stress and fault slip risk mapping in the Kiskatinaw Seismic Monitoring and Mitigation Area, British Columbia; report prepared for the BC Oil and Gas Research and Innovation Society, Final Report ER-Seismic-2020-01, 81 p.
- Esmailzadeh, Z., Eaton, D. and Wang, C. (2022): Numerical modeling of hydraulic fracture propagation and fault activation in the presence of a sealing fault and highly permeable damage zone—a case study of the Montney Formation in British Columbia; SPE/AAPG/SEG Unconventional Resources Technology Conference, June 20–22, 2022, Houston, Texas, Paper no. URTEC-3723715-MS.
- Fox, A.D. and Watson, N.D. (2019): Induced seismicity study in the Kiskatinaw Seismic Monitoring and Mitigation Area, British Columbia; report prepared for the BC Oil and Gas Commission, 51 p., URL <<https://www.bcogc.ca/files/reports/Technical-Reports/final-report-enlighten-geoscience-kssma-phase-1-study-2019w-appendices-links.pdf>> [October 2022].
- geoLOGIC systems ltd. (2022): geoSCOUT version 8.3.0.0; geoLOGIC systems ltd., URL <<https://www.geologic.com/products/geoscout/>> [September 2022].
- Guglielmi, Y., Cappa, F., Avouac, J.-P., Henry, P. and Elsworth, D. (2015): Seismicity triggered by fluid injection–induced aseismic slip; *Science*, v. 348, no. 6240, p. 1224–1226.
- Hemami, B., Masouleh, S.F. and Ghassemi, A. (2021): 3d geomechanical modeling of the response of the Wilzetta Fault to saltwater disposal; *Earth and Planetary Physics*, v. 5, no. 6, p. 559–580.
- Horner, R.B., Barclay, J.E. and MacRae, J.M. (1994): Earthquakes and hydrocarbon production in the Fort St. John area of northeastern British Columbia; *Canadian Journal of Exploration Geophysics*, v. 30, no. 1, p. 39–50.
- Hu, J., Cao, J.-X., He, X.-Y., Wang, Q.-F. and Xu, B. (2018): Numerical simulation of fault activity owing to hydraulic fracturing; *Applied Geophysics*, v. 15, no. 3, p. 367–381.
- Israelsson, J.I. (1996): Short descriptions of UDEC and 3DEC; *Developments in Geotechnical Engineering*, v. 79, p. 523–528.
- Rutqvist, J., Rinaldi, A.P., Cappa, F. and Moridis, G.J. (2013): Modeling of fault reactivation and induced seismicity during hydraulic fracturing of shale-gas reservoirs; *Journal of Petroleum Science and Engineering*, v. 107, p. 31–44.
- Salvage, R.O. and Eaton, D.W. (2022): The influence of a transitional stress regime on the source characteristics of induced seismicity and fault activation: evidence from the 30 November 2018 Fort St. John ML 4.5 induced earthquake sequence; *Bulletin of the Seismological Society of America*, v. 112, no. 3, p. 1336–1355.
- Sibson, R. (1992): Implications of fault-valve behaviour for rupture nucleation and recurrence; *Tectonophysics*, v. 211, no. 1–4, p. 283–293.
- Wilson, A. (2015): Dynamic fault-seal breakdown–investigation in the North Sea Egret Field; *Journal of Petroleum Technology*, v. 67, no. 10, p. 65–66.
- Zhang, F., Yin, Z., Chen, Z., Maxwell, S., Zhang, L. and Wu, Y. (2020): Fault reactivation and induced seismicity during multistage hydraulic fracturing: microseismic analysis and geomechanical modeling; *SPE Journal*, v. 25, no. 2, p. 692–711.

# Northeast BC Geological Carbon Capture and Storage Atlas: A Key Step Toward Net Zero Emissions (NTS 093I, O, P, 094A, B, G–J, N–P)

R.N. Hughes, Geoscience BC, Vancouver, British Columbia, [hughes@geosciencebc.com](mailto:hughes@geosciencebc.com)

---

Hughes, R.N. (2023): Northeast BC Geological Carbon Capture and Storage Atlas: a key step toward net zero emissions (NTS 093I, O, P, 094A, B, G–J, N–P); in Geoscience BC Summary of Activities 2022: Energy and Water, Geoscience BC, Report 2023-02, p. 21–30.

## Introduction

For British Columbia (BC) to reduce carbon emissions and ultimately reach net zero emissions by 2050 (CleanBC, 2018, 2021b), a number of initiatives and technologies have been and must continue to be deployed. Geological carbon capture and storage (CCS) can be utilized to help reduce the level of carbon dioxide (CO<sub>2</sub>), a greenhouse gas, in the atmosphere by sequestering CO<sub>2</sub> in the subsurface. Using CCS can also enable low-carbon energy initiatives at surface, including hydrogen production from existing natural gas reserves (CleanBC, 2021a).

A recent study supported by Geoscience BC has identified, assessed, mapped and catalogued the best geological CO<sub>2</sub> sequestration targets and CO<sub>2</sub> storage potential in the area of northeastern BC that is underlain by the Western Canada Sedimentary Basin (Figure 1). The project was designed to

- identify and undertake a preliminary quantification of the storage potential of the best CO<sub>2</sub> sequestration targets in northeastern BC to help enable CCS and low-carbon energy projects, from small to large scale;
- provide key information to enable improved decision making for policy and regulatory makers, and industry;
- recommend future CCS evaluation steps in northeastern BC; and
- provide a template and methodology that can be applied to help assess CO<sub>2</sub> sequestration storage potential in other geological basins in BC, particularly those in proximity to the largest CO<sub>2</sub> emission sites in the province.

The final report for the project, *Northeast BC Geological Carbon Capture and Storage Atlas* (Canadian Discovery Ltd., 2023), was released by Geoscience BC in early 2023, along with maps in both PDF and shapefile format, and a fulsome database of oil and gas pool and aquifer data. This paper summarizes the key project activities, outcomes and outputs.

---

*This publication is also available, free of charge, as colour digital files in Adobe Acrobat® PDF format from the Geoscience BC website: <http://geosciencebc.com/updates/summary-of-activities/>.*

## Project Overview

The *Northeast BC Geological Carbon Capture and Storage Atlas* published by Geoscience BC is a follow up to the seminal work of Bachu (2006) and was completed in partnership with the B.C. Centre for Innovation & Clean Energy and the BC Hydrogen Office (BC Ministry of Energy, Mines and Low Carbon Innovation). Technical work for the project was undertaken by Canadian Discovery Ltd. Primary goals of the project were to identify the best CO<sub>2</sub> sequestration targets in northeastern BC, and to present the findings in easy-to-use maps and tables.

The study assessed two types of subsurface storage targets: depleted gas pools (i.e., >90% depleted), and deep saline aquifers. The injection of CO<sub>2</sub> into oil pools for enhanced oil recovery was not considered for this project. The study reviewed existing data to filter, assess, rank and map the best CO<sub>2</sub> sequestration candidates for each of 12 subsurface formations (or groups of formations in some cases). Depleted pool data was obtained from the BC Oil and Gas Commission (2021). Aquifer data was largely derived from Geoscience BC Report 2021-14 *Wastewater Disposal in the Maturing Montney Play Fairway of Northeastern British Columbia* (Petrel Robertson Consulting Ltd., 2021) and supplemented by the technical work of Canadian Discovery Ltd.

Pool and aquifer data were vetted for CO<sub>2</sub> storage suitability criteria, including cutoffs for porosity and permeability, and sufficient depth, temperature, pressure and trapping for effective storage. After vetting, 12 subsurface formations were deemed suitable for CO<sub>2</sub> storage. In some cases, equivalent or proximal formations were grouped for ease of mapping and reporting. Storage candidates with initial reservoir pressures greater than 7500 kilopascals and temperatures greater than 31.1°C (the critical point for CO<sub>2</sub>) were flagged as having supercritical CO<sub>2</sub> storage potential. At supercritical conditions, CO<sub>2</sub> has high density like a liquid, but low viscosity like a gas—ideal for injection and storage of higher volumes of CO<sub>2</sub> as compared to storage in gaseous phase. Where appropriate, the mapped boundary of gaseous to supercritical phase has been annotated on formation maps.

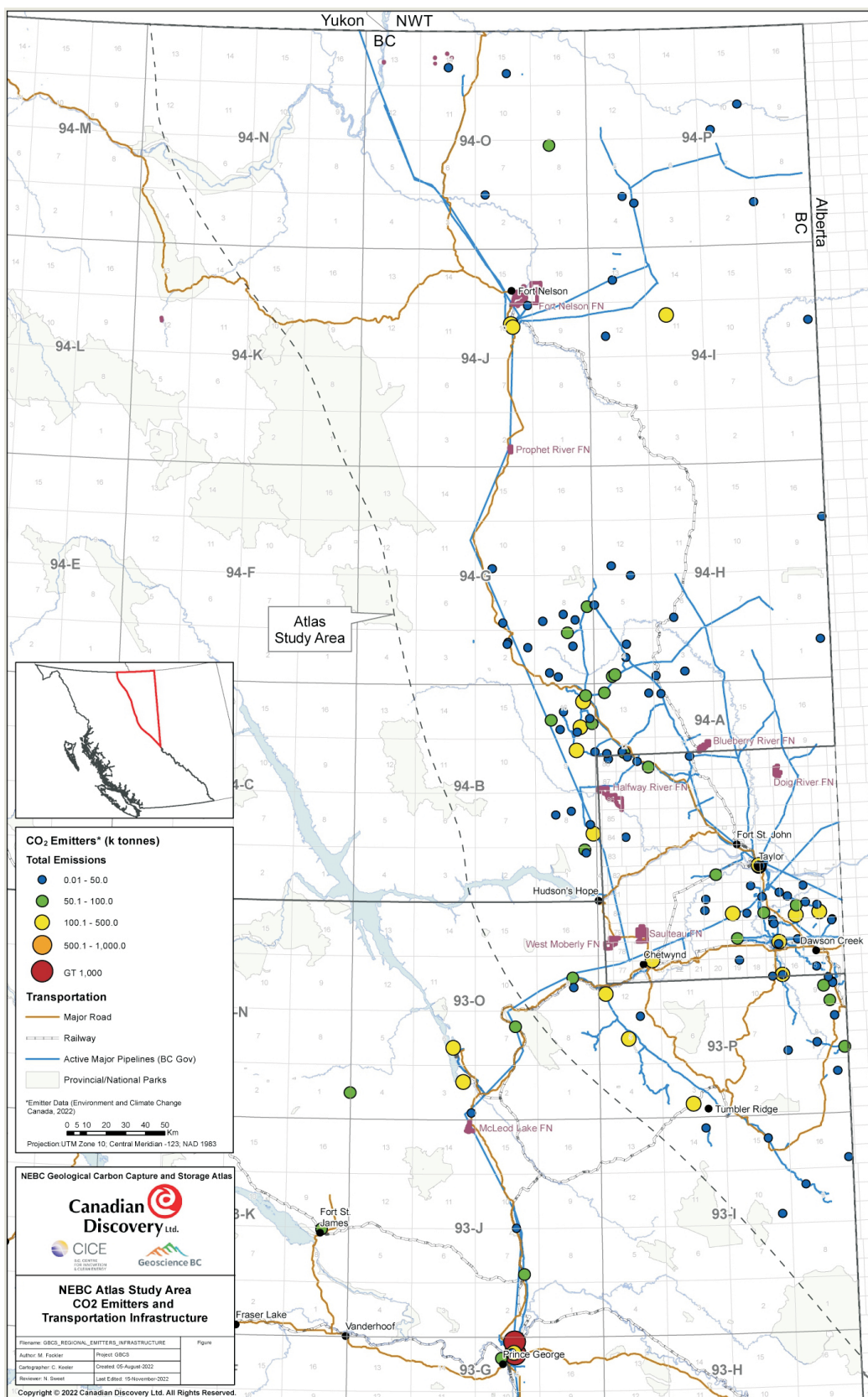


**Figure 1. Northeast BC Geological Carbon Capture and Storage Atlas project study area. Carbon dioxide (CO<sub>2</sub>) emitters are shown as coloured circles, with circle size and colour proportional to annual CO<sub>2</sub> emission volumes. Abbreviations: FN, First Nation(s); Gov, Government; GT, greater than; NEBC, northeastern British Columbia.**

Calculations of theoretical and effective CO<sub>2</sub> storage potential for pools and aquifers are provided in the report. Theoretical storage is the mass of CO<sub>2</sub> that can be stored using the reservoir volumes of the produced hydrocarbons for pools, and the mapped pore volume and CO<sub>2</sub> density for aquifers. Effective storage is the storage potential for CO<sub>2</sub> after accounting for various reservoir conditions and fluid properties. Given that terminology varies across jurisdictions, and also changes over time, the term ‘storage potential’ has been used for this project and is broadly related to the ‘storage resources’ category of the Society of Petroleum Engineers’ storage resources management system (Society of Petroleum Engineers, 2017). The term ‘capacity’ applies to specific pools or aquifer areas that have undergone extensive storage evaluation, beyond that provided in this study. For regional aquifers, given their large areal extent and that injected CO<sub>2</sub> has to displace fluid in place, the calculations for effective storage potential are provided on a 10<sup>th</sup> percentile (P10; low), 50<sup>th</sup> percentile (P50; mean) and 90<sup>th</sup> percentile (P90; high) basis, as a function of percent of total theoretical storage potential. To determine an estimated effective storage potential for P10, P50 and P90, an E<sub>saline</sub> or storage efficiency factor was applied to total theoretical storage potential values. The efficiency factor values used were similar to those in the U.S. Department of Energy, National Energy Technology Laboratory’s carbon utilization and storage publications (Gray, 2010, 2012, 2015): 0.5% for P10, 2.0% for P50 and 5.4% for P90.

As mentioned, detailed site-specific calculations and modelling is required to define specific CO<sub>2</sub> storage capacity volumes.

## Results

The study generated a written report, which provides background information on CCS basics and the methodologies

### Belloy Favourability Attributes

Top 10 Depleted Pool Total Capacity	51 Mt	●
Aquifer Storage (P50)	158 Mt	●
Seal Containment Risk	Variable	●
Lithology	Dolomitic sandstone	●
Porosity	8-24%	●
Permeability	10-1000mD	●
Depth (TVD)	800-2,900m	●
Net Reservoir Thickness	5-45m	●

**Figure 2.** Example of table of favourability attributes from the *Northeast BC Geological Carbon Capture and Storage Atlas* (Canadian Discovery Ltd., 2023). For each formation, circles indicate whether an attribute is considered generally favourable (green) or has risk and requires additional work (yellow). Abbreviations: Belloy, Belloy Formation; mD, millidarcy; Mt, megatonne; P50, 50<sup>th</sup> percentile; TVD, true vertical depth.

used to vet and calculate theoretical and effective CO<sub>2</sub> storage potential. A stand-alone chapter is provided for each of the 12 formations that have identified storage potential in northeastern BC. Each formation chapter provides summary results, including a brief overview; a table of favourability attributes (Figure 2); a structure map (Figure 3), which also has the gas phase to supercritical boundary annotated; an aquifers and depleted pools effective CO<sub>2</sub> storage potential map (Figure 4); a table of the top 25 depleted pools (ranked by effective storage potential), including metrics for each pool (Table 1); and a table of identified aquifer properties and storage potential, which includes P10, P50 and P90 effective storage potential calculations (Table 2). In addition, more detailed supporting information and mapping is provided in the formation chapters, including a geology summary, net porous isopach map of pools and aquifers, storage and trapping details, porosity-permeability correlations and hydrodynamics.

Importantly, the report includes a map of the total effective CO<sub>2</sub> storage potential calculation of the ‘stacked’ depleted pools with >5 megatonnes (Mt) of storage potential from all of the 12 formations mapped (Figure 5). As well, there is a similar stacked P50 effective CO<sub>2</sub> storage potential map for all identified aquifer storage areas in the study area (Figure 6). These maps identify areas and fairways of concentrated subsurface storage potential in northeastern BC and are useful in determining future carbon hub and hydrogen hub locations and parameters.

The report includes a chapter that provides detailed references and information regarding CCS, as well as links to BC hydrogen information, and a chapter that outlines recommendations for future research and evaluation work in northeastern BC and how it would be suitable for application to other geological basins in BC for CCS evaluation.

Finally, in addition to the main report, appendices provide supporting information including regional stratigraphy, storage calculations, a digital database for pool data, a digital database for aquifer data, and references and resources for CCS. There are PDF and digital shapefile documents for each suite of maps, all provided by formation in 12 subfolders.

### Calculated Effective CO<sub>2</sub> Storage Potential

The project has determined that there are numerous opportunities in northeastern BC for geological CCS in depleted pools and in deep saline aquifers. These sites are appropriate for CCS projects of small to large scale. The total estimated effective CO<sub>2</sub> storage potential of vetted depleted pools is approximately 1200 Mt. The total estimated P50 (mean) effective CO<sub>2</sub> storage potential of deep saline aquifers is approximately 3030 Mt, however, it is noted that aquifer effective storage potential values have a large range,

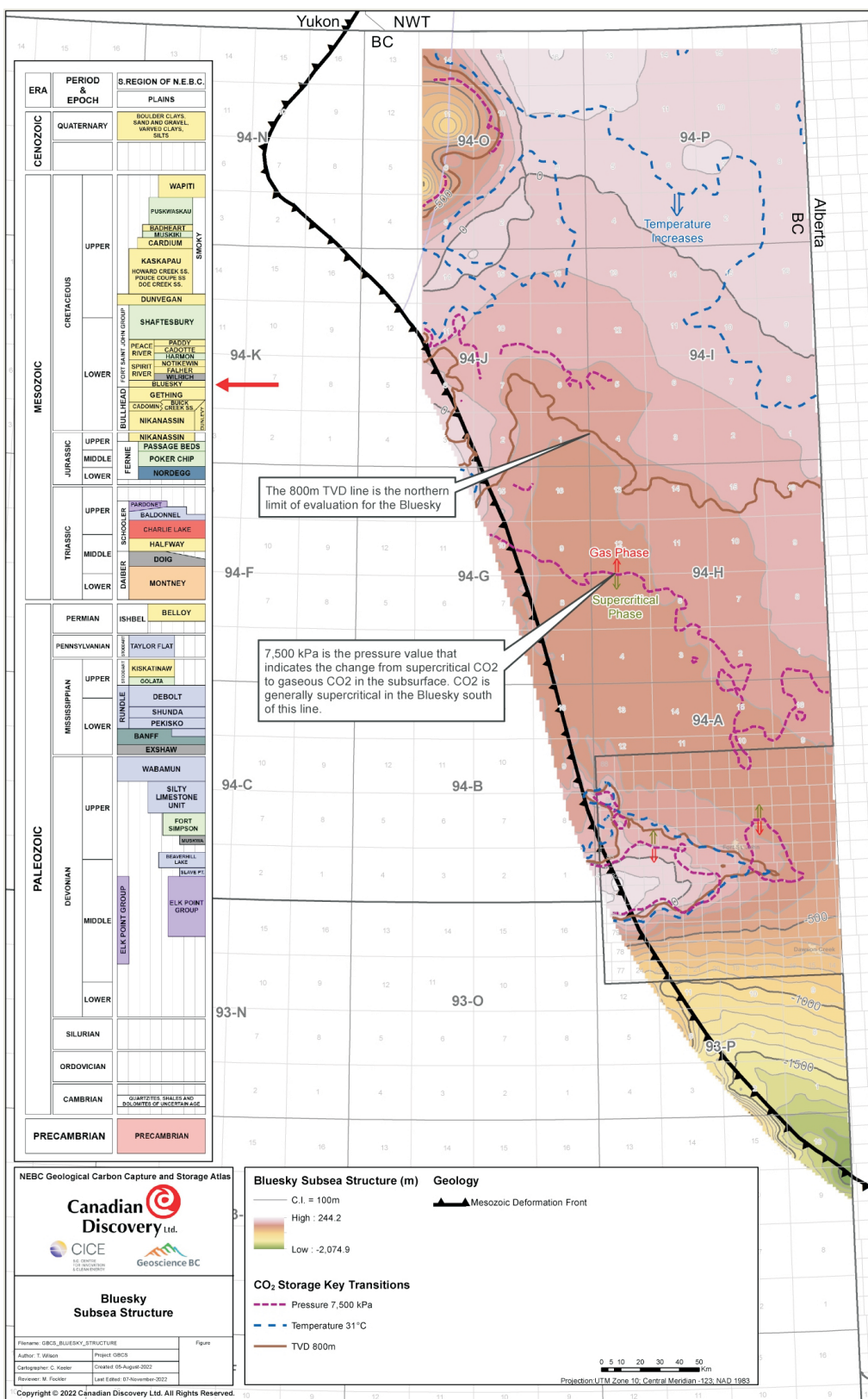


**Figure 3.** Example of structure map from the *Northeast BC Geological Carbon Capture and Storage Atlas* (Canadian Discovery Ltd., 2023). For each formation, lines are annotated for the 800 m depth cutoff, the 31°C cutoff and the supercritical conditions boundary. Stratigraphic column from BC Ministry of Energy, Mines and Low Carbon Innovation (2011). Abbreviations: Bluesky, Bluesky Formation; C.I., contour interval; CO<sub>2</sub>, carbon dioxide; kPa, kilopascal; NEBC, northeastern British Columbia; Pt., Point; S., southern; SS, sandstone; TVD, true vertical depth.

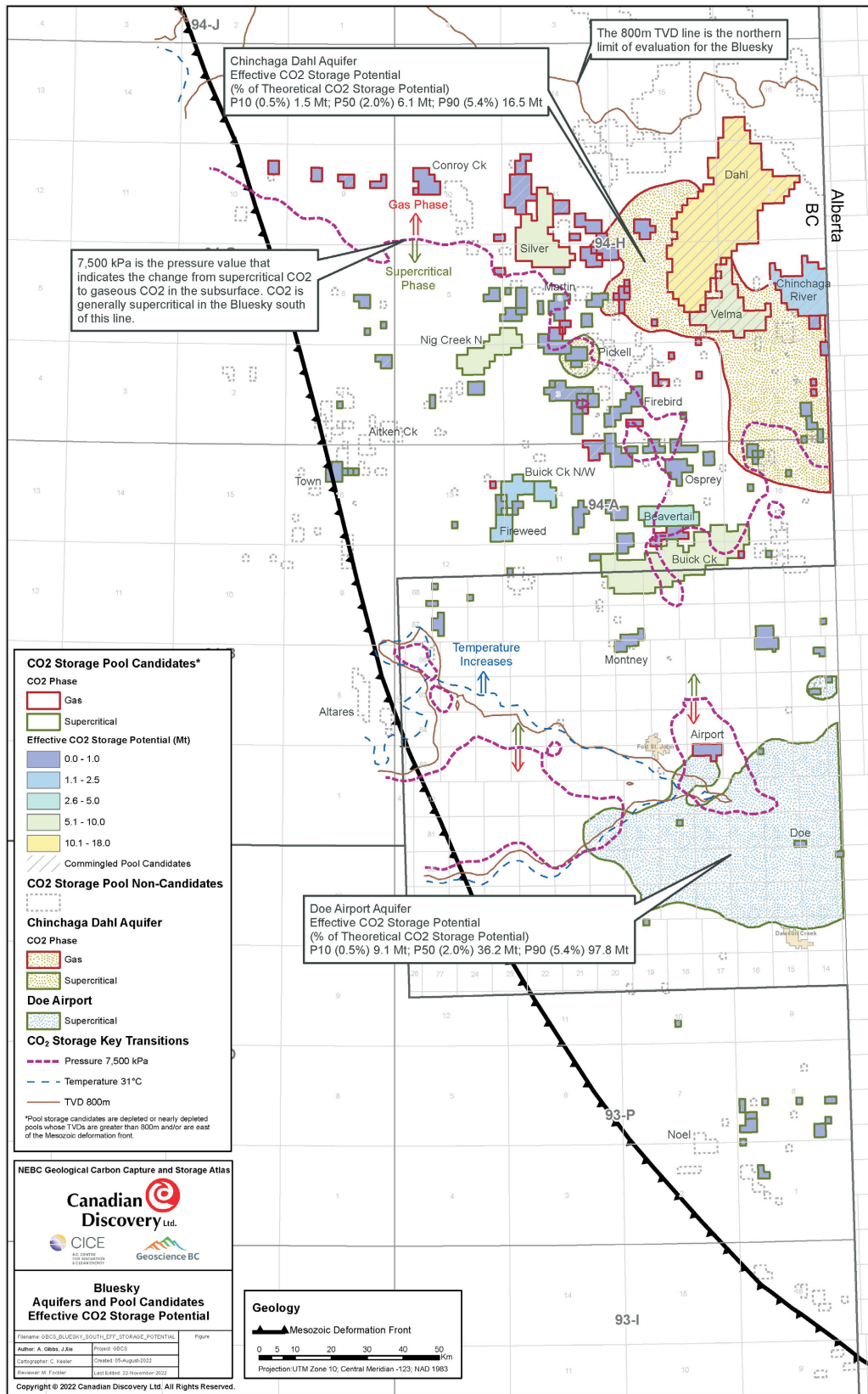


**Figure 4.** Example of aquifers and depleted pools candidates map from the *Northeast BC Geological Carbon Capture and Storage Atlas* (Canadian Discovery Ltd., 2023). For each formation, effective carbon dioxide (CO<sub>2</sub>) storage potential is mapped. Abbreviations: Bluesky, Bluesky Formation; Ck, Creek; kPa, kilopascal; Mt, megatonne; N, north; NEBC, northeastern British Columbia; P10, 10<sup>th</sup> percentile; P50, 50<sup>th</sup> percentile; P90, 90<sup>th</sup> percentile; TVD, true vertical depth; W, west.

**Table 1.** Example of top 25 depleted oil and gas pools table from the Northeast BC Geological Carbon Capture and Storage Alias (Canadian Discovery Ltd., 2023). For each formation, key reservoir metrics and carbon dioxide (CO<sub>2</sub>) storage potential are provided. Abbreviations: BC, British Columbia; kPa, kilopascal; Mt, megatonne.

Pool name	Pool type	Well count	Initial pressure (kPa)	Temperature (°C)	Average porosity (%)	CO <sub>2</sub> phase	Theoretical	
							CO <sub>2</sub> storage potential (Mt)	Effective CO <sub>2</sub> storage potential (Mt)
Dahl Bluesky Gething-A	Gas	198	6 564	51	15.0	Gas	20.6	18.0
Buick Creek Bluesky C	Gas	130	7 714	48	14.0	Supercritical	11.4	10.0
Nig Creek North Bluesky A	Gas	38	10 332	58	13.7	Supercritical	8.1	7.1
Silver Bluesky A	Gas	37	6 971	59	14.4	Gas	7.6	6.6
Velma Bluesky Gething-A	Gas	41	6 692	53	15.6	Gas	6.1	5.4
Beavertail Bluesky A	Gas	16	7 770	48	12.0	Supercritical	5.1	4.5
Buick Creek West Bluesky A	Gas	12	9 388	54	9.0	Supercritical	2.5	2.1
Buick Creek North Bluesky A	Gas	10	9 080	51	8.9	Supercritical	2.0	1.7
Fireweed Bluesky B	Gas	11	9 062	53	13.5	Supercritical	1.9	1.6
Chinchaga River Bluesky Gething-Detrital-A	Gas	116	6 549	48	17.3	Gas	2.4	1.5
Osprey Bluesky A	Gas	10	7 475	49	12.8	Supercritical	1.1	0.9
Pickell Bluesky Gething-A	Gas	16	7 957	51	11.2	Supercritical	1.0	0.8
Montney Bluesky A	Gas	7	8 715	49	13.7	Supercritical	0.9	0.8
Conroy Creek Bluesky A	Gas	11	5 626	60	15.2	Gas	0.9	0.8
Noel Basal Bluesky B	Gas	2	24 155	77	6.5	Supercritical	0.9	0.8
Fireweed Bluesky A	Gas	4	9 168	53	10.4	Supercritical	0.9	0.8
Tommy Lakes Bluesky A	Gas	6	5 575	56	13.5	Gas	0.8	0.7
Firebird Bluesky A	Gas	13	7 699	53	14.7	Supercritical	1.0	0.6
Martin Bluesky A	Gas	7	8 215	60	16.6	Supercritical	0.7	0.6
Siphon East Bluesky A	Gas	11	8 025	49	14.6	Supercritical	2.3	0.6
Ladyfern Bluesky M	Gas	3	7 449	43	19.4	Supercritical	0.8	0.5
Buick Creek Bluesky A	Gas	6	7 660	48	10.8	Supercritical	0.5	0.5
Noel Basal Bluesky J	Gas	2	28 268	86	8.1	Supercritical	0.5	0.5
Nig Creek Bluesky C	Gas	6	10 199	61	11.4	Supercritical	0.7	0.4
Town Bluesky D	Gas	9	10 392	60	13.0	Supercritical	0.5	0.4

**Table 2.** Example of aquifer properties and storage potential table from the Northeast BC Geological Carbon Capture and Storage Alias (Canadian Discovery Ltd., 2023). For each formation, key aquifer reservoir metrics and effective carbon dioxide (CO<sub>2</sub>) storage potential on a 10<sup>th</sup> percentile (P10; low), 50<sup>th</sup> percentile (P50; mean) and 90<sup>th</sup> percentile (P90; high) basis are provided. Abbreviations: BC, British Columbia; MPa, megapascal; Mt, megatonne.

Aquifer name	Type	Thickness range (m)	Pressure range (MPa)	Temperature range (°C)	Porosity range (%)	CO <sub>2</sub> phase	P10			P50			P90		
							effective storage potential at 0.5% (Mt)	effective storage potential at 2.0% (Mt)	effective storage potential at 5.4% (Mt)	effective storage potential at 0.5% (Mt)	effective storage potential at 2.0% (Mt)	effective storage potential at 5.4% (Mt)	effective storage potential at 0.5% (Mt)	effective storage potential at 2.0% (Mt)	effective storage potential at 5.4% (Mt)
Chinchaga-Dahl Regional System	Aquifer	2–10	5.7–7.9	43–60	9–21	Mostly gas	1.5	6.1	16.5						
Doe-Airport Regional System	Aquifer	2–40	6.6–11.1	27–56	8–22	Mostly supercritical	9.1	36.2	97.8						

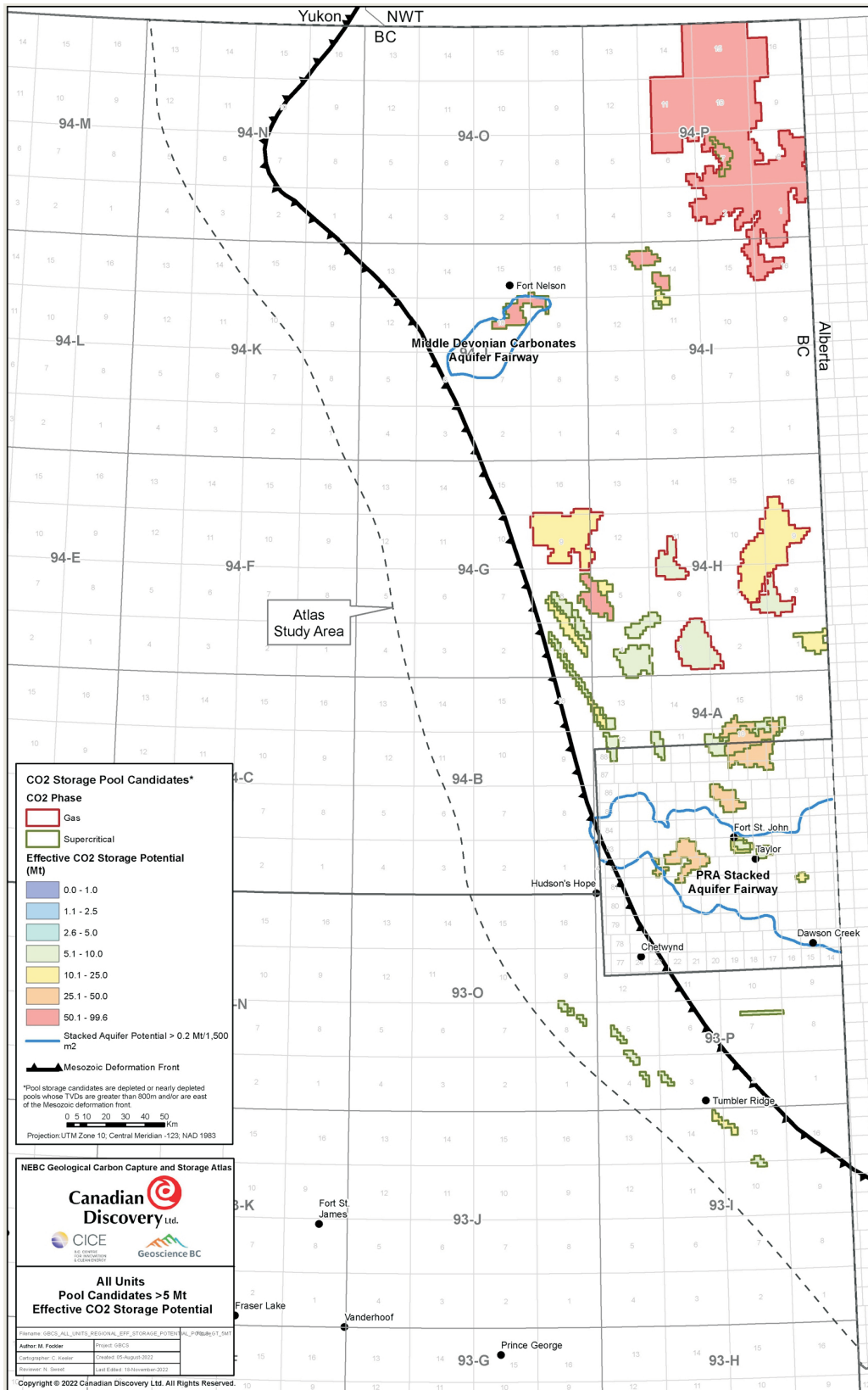


**Figure 5.** Depleted pools with greater than 5 megatonnes (Mt) of effective carbon dioxide (CO<sub>2</sub>) storage potential in northeastern British Columbia. This is a summary map that combines the largest pools from all 12 formations mapped (reproduced from Canadian Discovery Ltd., 2023). Stacked aquifer fairways are also annotated on the map. Abbreviations: GT, greater than; Mt, megatonne; NEBC, northeastern British Columbia; PRA, Peace River Arch; TVD, true vertical depth.

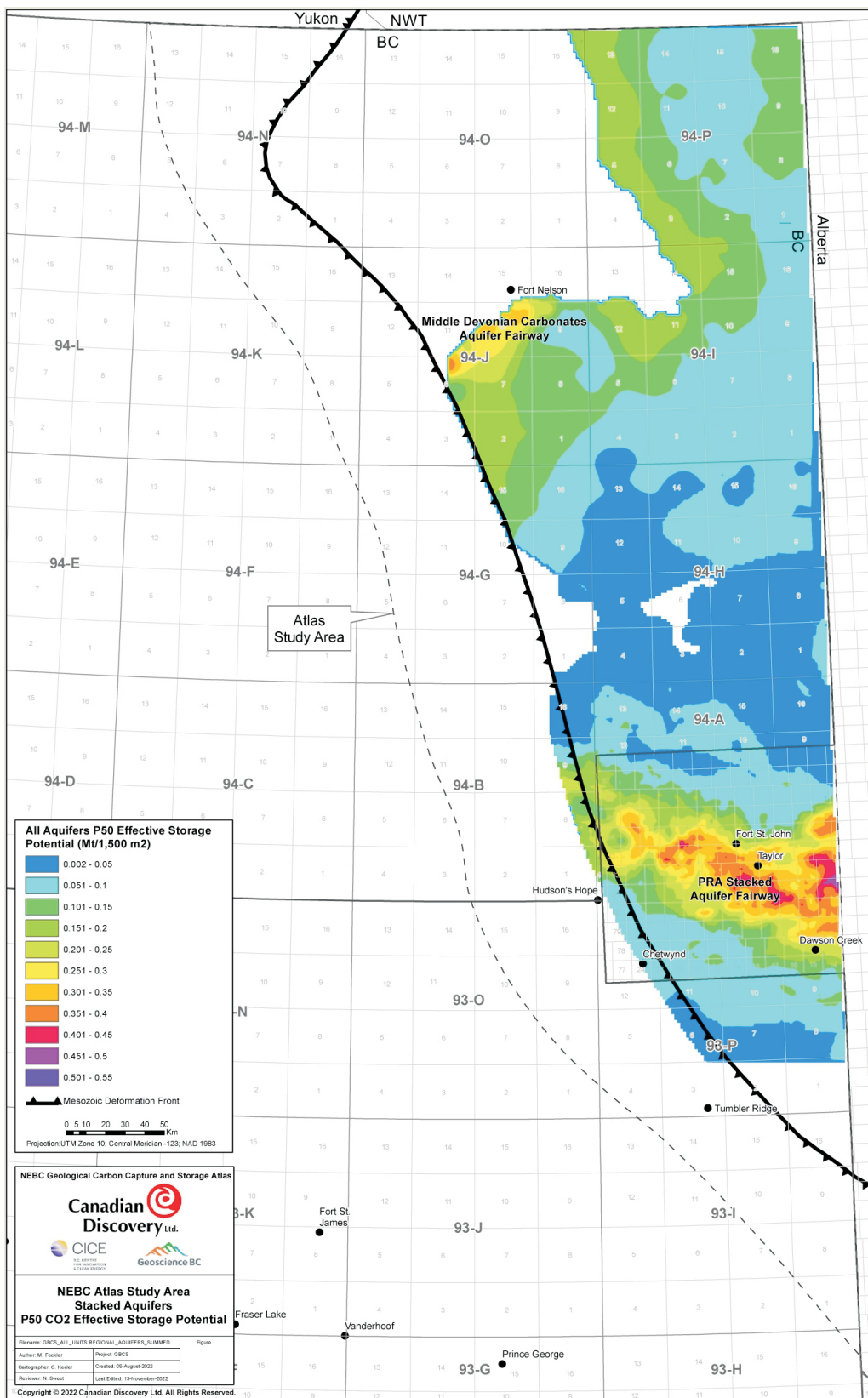


**Figure 6.** Total estimated effective carbon dioxide (CO<sub>2</sub>) storage potential of stacked aquifers (for 50<sup>th</sup> percentile; P50) in northeastern British Columbia. This is a summary map that combines the aquifer storage potential from all 12 formations mapped (reproduced from Canadian Discovery Ltd., 2023). Note that not all formations have storage aquifers available. Abbreviations: Mt, megatonne; NEBC, northeastern British Columbia; PRA, Peace River Arch.

from 758 to 8182 Mt. Combined, the total depleted pool and P50 aquifer effective CO<sub>2</sub> storage potential is approximately 4230 Mt.

For depleted pools, CCS favourable storage fairways have been identified in the region north and northeast of Fort St. John, and in the northeastern corner of the study area (Figure 5). For aquifers, CCS favourable storage fairways have been identified in the Dawson Creek to Fort St. John region and south of Fort Nelson (Figure 6).

It is noted that defining site-specific CO<sub>2</sub> sequestration capacities will require considerable additional investigation and detailed modelling.

## Conclusions

The *Northeast BC Geological Carbon Capture and Storage Atlas* provides a summary of the best geological carbon dioxide (CO<sub>2</sub>) sequestration sites in northeastern British Columbia, in depleted gas pools and in deep saline aquifers. Total calculated effective CO<sub>2</sub> storage potential, including 50<sup>th</sup> percentile calculations for aquifers, is greater than 4000 megatonnes in the study area, which is enough storage potential to consider carbon hub or hydrogen hub development. Strategic areas of carbon capture and storage potential have been identified as storage fairways.

The study report and associated maps provide data in easy-to-use summary format, but also provide more detailed supporting information and databases. The study provides a key dataset that identifies the best zones and areas for carbon capture and storage and low-carbon hydrogen development, but recognizes that additional detailed research and work is required in northeastern British Columbia before reaching development decisions, particularly for carbon hub or hydrogen hub development.

The study provides information that can help guide regulations and policies, and is a template for evaluation of other geological basins in British Columbia.

## Acknowledgments

The author is grateful to N. Sweet of Canadian Discovery Ltd. for her assistance in reviewing this paper.

## References

Bachu, S. (2006): The potential for geological storage of carbon dioxide in northeastern British Columbia; *in* Summary of Activities 2006, BC Ministry of Energy, Mines and Low Carbon Innovation, p. 1–48, URL <[https://www2.gov.bc.ca/assets/gov/farming-natural-resources-and-industry/natural-gas-oil/petroleum-geoscience/geoscience-reports/2006/og\\_rpt2006bachu.pdf](https://www2.gov.bc.ca/assets/gov/farming-natural-resources-and-industry/natural-gas-oil/petroleum-geoscience/geoscience-reports/2006/og_rpt2006bachu.pdf)> [November 2022].

BC Ministry of Energy, Mines and Low Carbon Innovation (2011): Stratigraphic correlation chart northeastern British Columbia and adjacent parts of Alberta, Yukon and Northwest Territories; BC Ministry of Energy, Mines and Low Carbon Innovation, URL <[http://www2.gov.bc.ca/gov/DownloadAsset?assetId=E286DEE42F0D41C8A94F9B12EE2E01EB&filename=20111\\_nebc\\_strat\\_column.pdf](http://www2.gov.bc.ca/gov/DownloadAsset?assetId=E286DEE42F0D41C8A94F9B12EE2E01EB&filename=20111_nebc_strat_column.pdf)> [November 2022].

BC Oil and Gas Commission (2021): Annual oil, gas and by-products reserves estimates tables prepared by the Oil and Gas Commission; BC Oil and Gas Commission, URL <<http://www.bcogc.ca/data-reports/reservoir-management/reserves/>> [November 2022].

Canadian Discovery Ltd. (2023): Northeast BC Geological Carbon Capture and Storage Atlas; Geoscience BC, Report 2023-04, 168 p., URL <<https://www.geosciencebc.com/projects/2022-001/>>.

CleanBC (2018): Highlights report; Government of British Columbia, 15 p., URL <[https://news.gov.bc.ca/files/CleanBC\\_HighlightsReport\\_120318.pdf](https://news.gov.bc.ca/files/CleanBC_HighlightsReport_120318.pdf)> [November 2022].

CleanBC (2021a): BC hydrogen strategy – a sustainable pathway for B.C.’s energy transition; Government of British Columbia, 37 p., URL <[https://www2.gov.bc.ca/assets/gov/farming-natural-resources-and-industry/electricity-alternative-energy/electricity/bc-hydro-review/bc\\_hydrogen\\_strategy\\_final.pdf](https://www2.gov.bc.ca/assets/gov/farming-natural-resources-and-industry/electricity-alternative-energy/electricity/bc-hydro-review/bc_hydrogen_strategy_final.pdf)> [November 2022].

CleanBC (2021b): Roadmap to 2030; Government of British Columbia, 68 p., URL <[https://www2.gov.bc.ca/assets/gov/environment/climate-change/action/cleanbc/cleanbc\\_roadmap\\_2030.pdf](https://www2.gov.bc.ca/assets/gov/environment/climate-change/action/cleanbc/cleanbc_roadmap_2030.pdf)> [November 2022].

Environment and Climate Change Canada (2022): Canada’s official greenhouse gas inventory; Government of Canada, URL <<https://www.canada.ca/en/environment-climate-change/services/climate-change/greenhouse-gas-emissions/inventory>> [November 2022].

Gray, K. (2010): Carbon sequestration atlas of the United States and Canada (3<sup>rd</sup> edition); U.S. Department of Energy, 161 p., URL <<https://doi.org/10.2172/1814019>>.

Gray, K. (2012): Carbon utilization and storage atlas (4<sup>th</sup> edition); U.S. Department of Energy, 129 p., URL <<https://doi.org/10.2172/1814016>>.

Gray, K. (2015): Carbon storage atlas (5<sup>th</sup> edition); U.S. Department of Energy, 113 p., URL <<https://doi.org/10.2172/1814017>>.

Petrel Robertson Consulting Ltd. (2021): Wastewater disposal in the maturing Montney play fairway of northeastern British Columbia; Geoscience BC, Report 2021-14, 236 p., URL <[https://cdn.geosciencebc.com/project\\_data/GBCReport2021-14/GBCR%202021-14%20Wastewater%20Disposal%20in%20the%20Matuering%20Montney%20Play%20Fairway%20of%20NEBC.pdf](https://cdn.geosciencebc.com/project_data/GBCReport2021-14/GBCR%202021-14%20Wastewater%20Disposal%20in%20the%20Matuering%20Montney%20Play%20Fairway%20of%20NEBC.pdf)> [November 2022].

Society of Petroleum Engineers (2017): CO<sub>2</sub> storage resources management system; Society of Petroleum Engineers, 47 p., URL <[https://www.spe.org/media/filer\\_public/0d/3e/0d3efcb5-57a8-4db2-ac94-6a1be0de61df/srms\\_sep2022\\_w\\_errata.pdf](https://www.spe.org/media/filer_public/0d/3e/0d3efcb5-57a8-4db2-ac94-6a1be0de61df/srms_sep2022_w_errata.pdf)> [November 2022].



# Three-Dimensional Reconstruction of the Georgia Basin and Potential for Carbon Dioxide Sequestration in the Lower Mainland, Southwestern British Columbia (Parts of NTS 092G/01–03)

M. Nazemi<sup>1</sup>, Department of Earth Sciences, Simon Fraser University, Burnaby, British Columbia, maziyar\_nazemi@sfu.ca

S. Dashtgard, Department of Earth Sciences, Simon Fraser University, Burnaby, British Columbia

---

Nazemi, M. and Dashtgard, S. (2023): Three-dimensional reconstruction of the Georgia Basin and potential for carbon dioxide sequestration in the Lower Mainland, southwestern British Columbia (parts of NTS 092G/01–03); in Geoscience BC Summary of Activities 2022: Energy and Water, Geoscience BC, Report 2023-02, p. 31–46.

## Introduction

Steady increases in atmospheric carbon dioxide (CO<sub>2</sub>) were first recognized by Keeling (1960), and annual peak concentrations have only increased since (Ewald, 2013; Keighley and Maher, 2015). Although CO<sub>2</sub> is produced naturally, recent (1800s until present) increases are predominantly attributed to human activity (Keighley and Maher, 2015) and specifically to the use of carbon-based resources such as coal, oil and natural gas (methane). Higher CO<sub>2</sub> concentrations affect Earth's atmosphere by increasing the natural greenhouse effect, thereby exerting a warming influence on the planet's surface (Bachu, 2003). As Earth's climate warms, extreme weather events such as heat domes, tropical cyclones, elevated precipitation and flooding are expected to occur more frequently and with greater intensity (Flannigan and Wagner, 1991). As these events threaten infrastructure critical to society, concerns regarding the impacts of climate change on society have understandably increased (Bratu et al., 2022). Nevertheless, CO<sub>2</sub> emissions will continue to rise, as the effort to transition to a carbon-neutral global economy is expected to take decades (U.S. Energy Information Administration, 2021).

Finding practical solutions to decrease carbon emissions while simultaneously maintaining our standard of living and expanding the standard of living of developing countries demands economical and novel solutions. To this end, capturing and sequestering CO<sub>2</sub> underground is the most viable approach to reducing CO<sub>2</sub> emissions over the short to medium term (Intergovernmental Panel on Climate Change, 2014). Carbon capture and storage (CCS) removes CO<sub>2</sub> from industrial sources and injects it underground into suitable geological formations (Bachu et al., 1994; Kaszuba et al., 2003; Bachu and Gunter, 2005; Kharaka et

al., 2006; Shukla et al., 2010; Underschultz et al., 2011; Stephenson et al., 2019; Pearce et al., 2021). In most cases, CCS is used in regions with significant hydrocarbon production (Lane et al., 2021). In areas with limited oil and gas exploration, CCS is largely ignored, owing to assumptions that underground storage is not viable.

The Lower Mainland of British Columbia (referred to herein as LMBC) has been evaluated previously for hydrocarbon potential and natural gas storage, and represents a readily accessible and potentially economically feasible locale to store CO<sub>2</sub> (Gordy, 1988; Hannigan et al., 2001). However, no significant effort has been expended yet to evaluate the feasibility of CCS in the LMBC. Sedimentary strata below the LMBC are poorly understood, particularly at depth, and the geological context (e.g., interpretation of depositional environments and facies analysis) of these strata has not been examined in detail. To address this knowledge gap, the proposed research aims to place the strata below the LMBC in geological context, assess these strata for their reservoir potential, and build an integrated three-dimensional (3-D) static geological model of the strata. These data will then be used to estimate the storage capacity and long-term fate of injected CO<sub>2</sub>. The geological model will be used to define subsurface geohazards (e.g., faults).

## Study Area

The strata underlying the LMBC belong to the Georgia Basin, which is a northwest-southeast-oriented structural and topographic depression. The Georgia Basin extends over 18 000 km<sup>2</sup> and encompasses the Strait of Georgia, eastern Vancouver Island, the Fraser River Lowland and the northwestern portion of the State of Washington, United States (Figure 1; Molnar et al., 2010). The fill of the Georgia Basin comprises three major tectonostratigraphic clastic sedimentary packages: the mainly Upper Cretaceous Nanaimo Group, the Paleogene Huntingdon Formation, and the Neogene Boundary Bay Formation (Figure 1; Monger, 1990; Groulx and Mustard, 2004; Molnar et al., 2010).

---

<sup>1</sup>The lead author is a 2022 Geoscience BC Scholarship recipient.

This publication is also available, free of charge, as colour digital files in Adobe Acrobat® PDF format from the Geoscience BC website: <http://geosciencebc.com/updates/summary-of-activities/>.

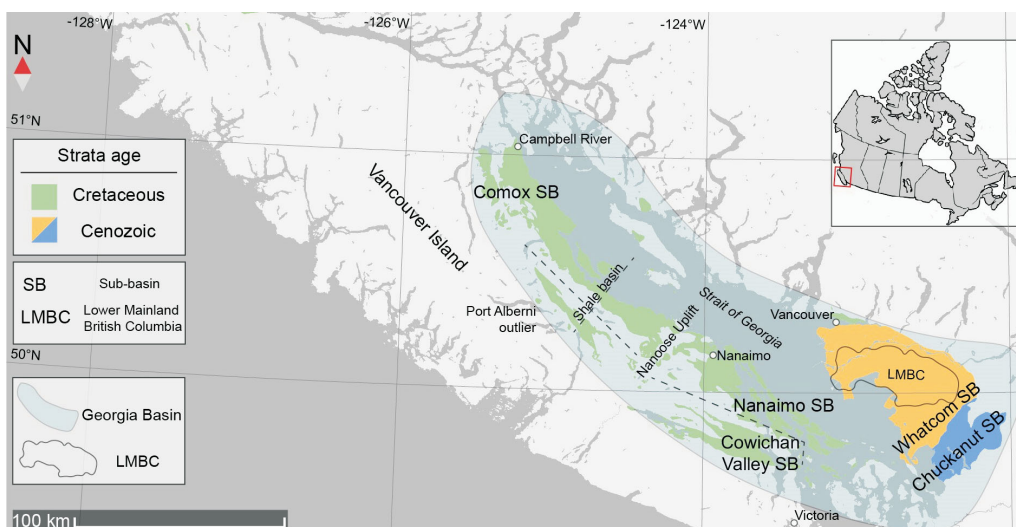


**Figure 1.** Location map of the Georgia Basin and Lower Mainland of British Columbia, Canada, and simplified geological map of southwestern British Columbia, Canada. Outcrop areas in the Georgia Basin include Upper Cretaceous Nanaimo Group strata exposed in the Comox, Nanaimo and Cowichan Valley sub-basins (green); Paleogene and Neogene strata in the Whatcom sub-basin (orange); and Paleogene and Neogene strata in the Chuckanut sub-basin (blue). The inset figure shows the location of the larger map within the context of the province of British Columbia and the rest of Canada (Huang et al., 2022).

The LMBC encompasses metropolitan Vancouver, the Fraser River Lowland, and the flanks of the surrounding mountainous regions (Figure 1). The region is home to over 60% of British Columbia’s (BC) population (>3 000 000) and is Canada’s third-largest urban region. The LMBC is

bounded by the Coast Mountains to the north, the Cascade Mountains to the east, and the Canada–US international border to the south. Population centres in the LMBC are also major industrial hubs, with several large carbon emitters therein.

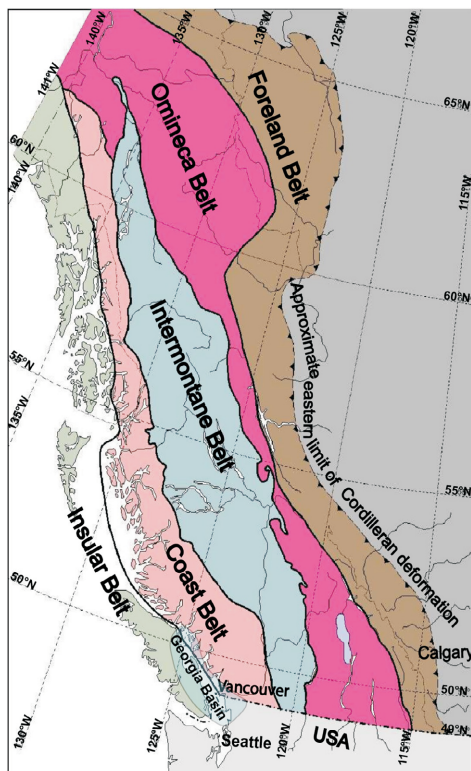


**Figure 2.** Morphogeological belts of the Canadian Cordillera (from Wheeler et al., 1991).

## Geological Background

### Tectonic Setting and Basin Type

The Canadian Cordillera is divided into five morphological belts. From west to east, these include the Insular, Coast, Intermontane, Omineca and Foreland belts (Figures 2, 3; Monger and Price, 2002). Each belt is characterized by a distinct combination of landforms, rock types, metamorphic grade and structural style (Gabrielse and Yorath, 1991). The southern Canadian Cordillera was established through the accretion of two superterranes, which also equate to two of the morphological belts (Figures 2, 3). The eastern Intermontane Superterrane accreted in the Middle Jurassic, and the western Insular Superterrane accreted in the Early Cretaceous (Monger, 1991a, b; Zelt et al., 2001). These two superterranes are separated by the Coast Belt or Coast Plutonic Complex (CPC), which is a high-grade metamorphic and plutonic belt that probably formed when the Insular Superterrane was accreted to the western margin of North America in the Early Cretaceous (Monger et al., 1994).

The Georgia Basin is a Cretaceous to Cenozoic fore-arc basin that straddles the boundary between the Insular Superterrane and the CPC (Figures 1, 2; England, 1991; England and Bustin, 1998; Monger and Price, 2002). Based on the

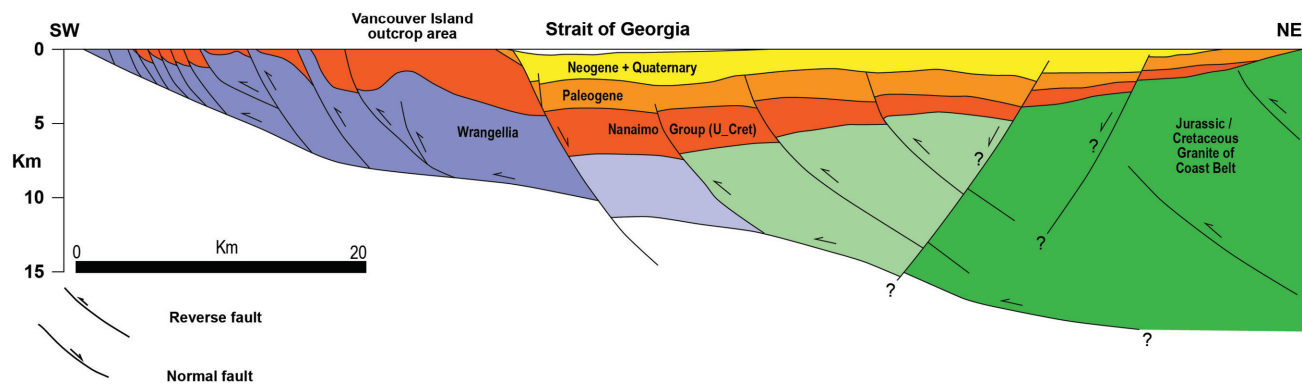


**Figure 3.** Idealized structural cross-section of the southern Georgia Basin based on LITHOPROBE data, modified after England and Bustin (1998), England and Calon (1991) and Gordy (1988). Question marks along the fault surfaces indicate interpreted locations. Paler shades of purple and green are used on the strata below the Strait of Georgia, but they are still part of the Wrangellia (purple) and Jurassic/Cretaceous (green) sequences. Abbreviations: NE, northeast; SW, southwest; U\_Cret, Upper Cretaceous.

structural evolution of the Canadian Cordillera, previous workers have posited that the Georgia Basin was developed in the arc-trench gap between Wrangellia and North America, and overlies the eastern portion of Wrangellia and the western portion of the CPC (Figure 1; Muller and Jeletzky, 1970; Bustin and England, 1991; England, 1991; England and Calon, 1991).

The Georgia Basin has been interpreted variably as a fore-arc basin, a strike-slip basin, and a foreland basin (Muller and Jeletzky, 1970; Pacht, 1984; England, 1989; Monger and Journeay, 1994; Mustard and Monger, 1994). Monger (1991a) postulated that the Georgia Basin developed in a foreland setting, with associated west-verging thrust faults, crustal thickening and regional uplift of the CPC. England and Calon (1991) suggested that Nanaimo Group sedimentation occurred in a fore-arc setting, and was associated with Late Cretaceous subduction and convergence in the CPC. Recognition of multiple source areas for Cretaceous sedimentary rocks, including areas west of the Georgia Basin, suggests the fore-arc basin model is most applicable, and that is the model adhered to herein. The Georgia Basin has been identified as an ‘anomalous’ fore-arc basin, owing to the preservation of thick successions of paralic and shallow-marine strata (Dickinson and Seely, 1979; Miall, 1984; Hamblin, 2012; Kent et al., 2020). Preserving thick successions of shallow-marine proximal facies could reflect a more oblique convergent character for the Georgia Basin. However, recent studies of fore-arc basins globally have identified thick basal successions of terrestrial and shallow-marine strata in similar fore-arc settings, suggesting shallow-marine strata are common in these basins and particularly in ridged fore arcs (Takano et al., 2013; Jones, 2016; Takano and Tsuji, 2017; Kent et al., 2020).

The siliciclastic fill of the Georgia Basin attains a thickness locally in excess of 6 km (England and Bustin, 1998). Late (and possibly Early) Cretaceous through to modern sedimentary strata comprises the fill (Figure 3; Hannigan et al.,

2001). The Georgia Basin comprises five sub-basins (Figure 1; Mustard and Monger, 1994; England and Bustin, 1998; Hannigan et al., 2001; Huang et al., 2019, 2022; Kent et al., 2020; Giroto, 2022). The Nanaimo sub-basin encompasses the southeast coast of Vancouver Island, the adjacent Strait of Georgia and the Gulf Islands. The Comox sub-basin is situated farther north, along the east-central coast of Vancouver Island and the adjacent Strait of Georgia. The Cowichan Valley sub-basin was defined as a separate sub-basin on the basis of its strata having an unknown relationship to the rest of the Nanaimo Group. Later studies incorporated the Cowichan Valley sub-basin into the Nanaimo sub-basin, with no reason given for this revision (Clapp, 1913). The Cowichan Valley sub-basin was redefined by Huang et al. (2022) and Giroto (2022) as a separate sub-basin, based on strata near the basal unconformity yielding substantially different detrital zircon age populations and maximum depositional ages than strata in the Comox and Nanaimo sub-basins.

The Chuckanut and Whatcom sub-basins include the Fraser Delta and northwestern Washington, respectively (Figure 1; Hannigan et al., 2001; Kent et al., 2020). Nanaimo Group sedimentary strata exist within the Whatcom sub-basin, and these strata are overlain by Paleogene sediments of the Huntingdon Formation, Neogene sediments of the Boundary Bay Formation, and Quaternary sediments of Fraser River (Figure 4; Zelt et al., 2001). The Chuckanut sub-basin is separated from the Whatcom sub-basin by the Lummi Island fault, which accommodates more than 1.5 km of southward displacement (Miller, 1963; Johnson, 1985). The fill of the Chuckanut sub-basin comprises the Chuckanut Formation, Boundary Bay Formation, and overlying Quaternary deposits (Figures 1, 4).

## General Stratigraphy

The basement of the Georgia Basin comprises predominantly Wrangellia. Wrangellia itself comprises the Sicker

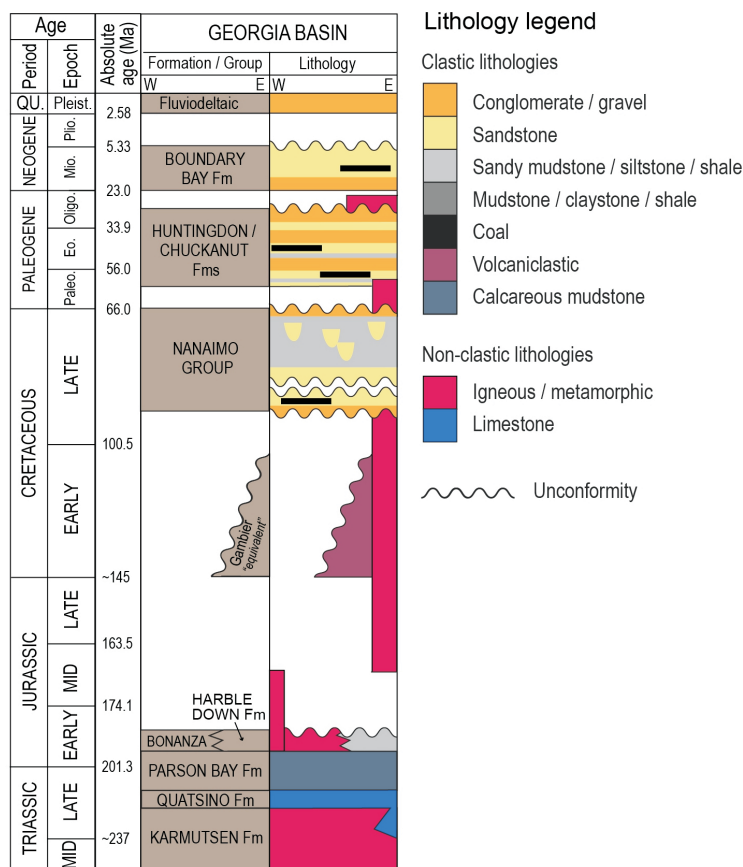


**Figure 4.** Simplified stratigraphic column for the Georgia Basin (with data from Haggart, 1992, 1993; Hannigan et al., 2001; Bain and Hubbard, 2016; Englert et al., 2018; Huang et al., 2019; Kent et al., 2020). Potential reservoir strata occur in coarse clastic rocks of the Huntingdon and Boundary Bay formations, and the Nanaimo Group. Abbreviations: E, east; Eo., Eocene; Fm, Formation; Fms, formations; MID, Middle; Mio., Miocene; Oligo., Oligocene; Paleo., Paleocene; Pleist., Pleistocene; Plio., Pliocene; QU., Quaternary; W, west.

arc, a Silurian to Devonian island arc; the Karmutsen Formation, a Triassic mid-ocean-basalt plateau; the Bonanza arc, a Jurassic bimodal arc; and sedimentary rocks associated with these features (Huang et al., 2022). The eastern Georgia Basin is flooded by the CPC, a middle Jurassic to Eocene continental arc (Monger and Journeay, 1994), and the Gambier Group, which is a sequence of Lower Cretaceous volcanogenic sedimentary and volcaniclastic rocks (Figure 4; Lynch, 1991; Lynch, 1992; Monger and Journeay, 1994). The mainly Upper Cretaceous to lowermost Paleocene fill of the Georgia Basin comprises the 4 km thick Nanaimo Group (Figures 3, 4; Mustard, 1991; Mustard et al., 1994; England and Bustin, 1998; Huang et al., 2022). The Nanaimo Group is divided informally into the lower and upper Nanaimo groups, with the lower Nanaimo Group comprising predominantly continental to shallow-marine strata in sedimentologically isolated sub-basins, including the Comox, Nanaimo and Cowichan Valley sub-basins (Figure 1; Giroto, 2022; Huang et al., 2022). The Comox and Nanaimo sub-basins are divided into lithostratigraphic formations, which alternate between

dominantly coarse- and fine-grained strata. The lower Nanaimo Group in the Comox sub-basin encompasses the Comox and Trent River formations, whereas in the Nanaimo sub-basin, it comprises the Sidney Island, Barnes Island, Comox, Haslam, Extension, Pender and Protection formations (Figure 5; Giroto, 2022). The transition between the lower and upper Nanaimo Group represents the unification of the isolated sub-basins into a single basin, and the initiation of basin-wide, deep-marine sedimentation (England, 1991; Mustard, 1991; Mustard and Monger, 1994; Kent et al., 2020; Giroto, 2022). The upper Nanaimo Group includes the Cedar District, De Courcy, Northumberland, Geoffrey, Spray and Gabriola formations (Figure 5; Mustard and Monger, 1994; Huang et al., 2019, 2022; Kent et al., 2020). The Nanaimo Group is exposed predominantly in eastern Vancouver Island, but these strata also occur in the subsurface under the Strait of Georgia and below the LMBC (Figures 3, 4). The subsurface distribution and character of Nanaimo Group strata are poorly understood, owing to limited data.

The Huntingdon Formation in BC, and the time-equivalent Chuckanut Formation in Washington, comprise the main Paleogene fill of the Georgia Basin (Figure 4; Vance, 1975; Johnson, 1984; England and Hiscott, 1992; Hannigan et al., 2001). Paleogene strata are dominated by continental deposits both in the Canadian and American extents of the Georgia Basin (Johnson, 1984, 1991; Mustard and Monger, 1994; Hannigan et al., 2001). Paleogene and Cretaceous strata are intruded locally by Oligocene dikes and sills in the Vancouver area (Figure 4; Mustard et al., 1994). In the LMBC, the Huntingdon Formation disconformably overlies the upper Nanaimo Group (Figures 3, 4; Mustard et al., 1994).

In the Whatcom sub-basin, there is a thick succession of mainly Miocene sediments that are distinct from older Cenozoic sediments (Hopkins, 1966, 1968; Rouse et al., 1990; Mustard and Rouse, 1991; Mustard et al., 1994). These strata are referred to as the Boundary Bay Formation (Mustard et al., 1994). The Boundary Bay Formation is exposed mainly in scattered outcrops along the lower Fraser River valley, and east and northeast of Bellingham in Washington (Figure 1; Hannigan et al., 2001).

### Exploration History and Regional Studies

The Georgia Basin has been the subject of scientific investigations for over 140 years, initially due to large bituminous coal resources discovered in the basin between 1850 and the early 1900s, and later due to its potential for signifi-

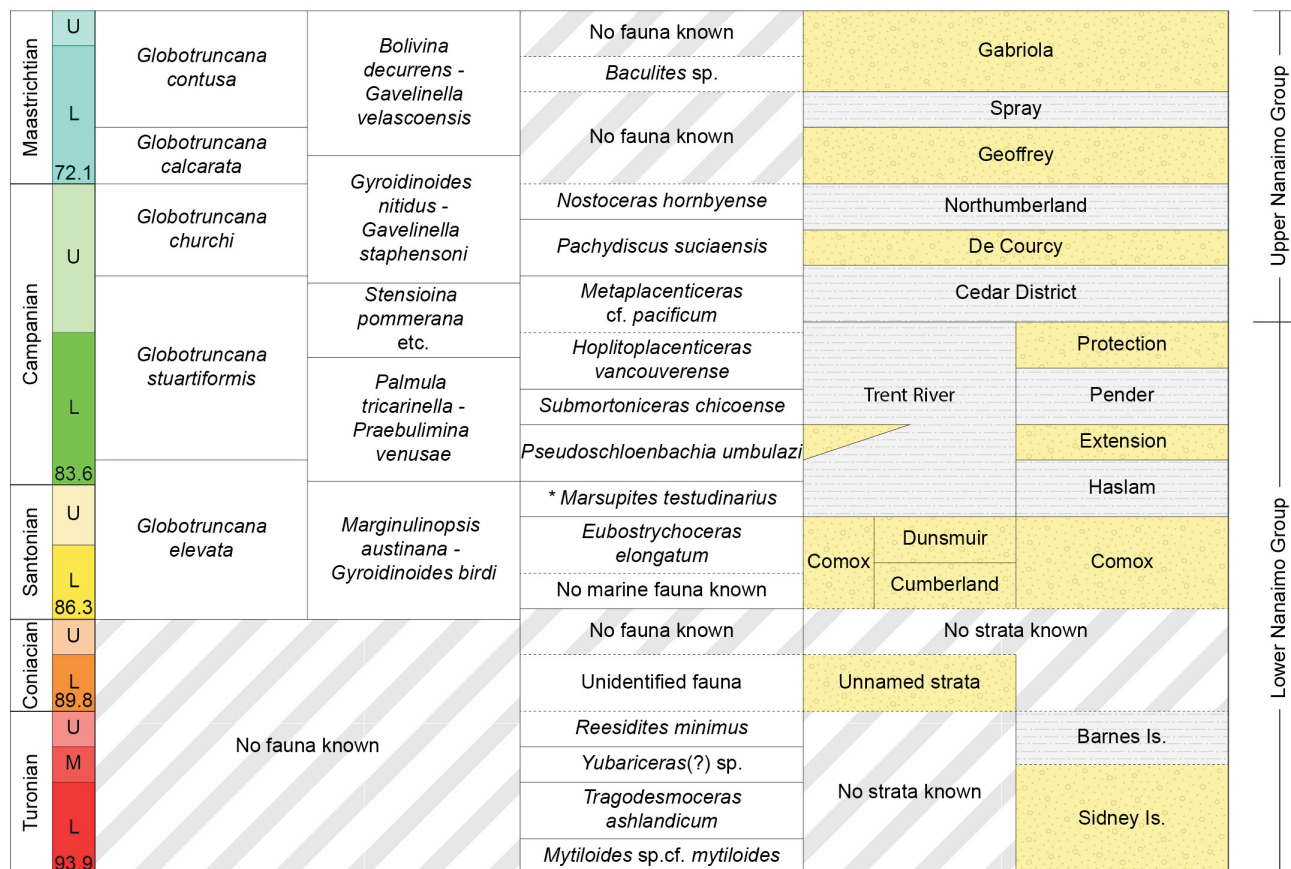


**Figure 5.** Nanaimo Group lithostratigraphy in the Nanaimo and Comox sub-basins (Mustard et al., 1994; Haggart et al., 2005) including foraminiferal (Sliter, 1973; McGugan, 1979) and molluscan biozones (Muller and Jeletzky, 1970; Haggart et al., 2005; Ward et al., 2012; Haggart and Graham, 2018). In the formation column, yellow indicates strata that comprise dominantly sandstone and/or conglomeratic intervals, and grey indicates dominantly mudstone and shale (Huang et al., 2022). Abbreviations: Is., Island; L, Lower; M, Middle; U, Upper.

cant hydrocarbon accumulations (Bustin and England, 1991; Bustin, 1995).

Exploration surveys (e.g., geological, seismic, gravimetric, magnetic) and drilling for hydrocarbons has been conducted intermittently in the basin since the early 1920s, with little tangible success. The first petroleum exploration wells were drilled prior to the acquisition of the first seismic lines, with the first well drilled in Whatcom County, Washington, in 1901, and the first well in the Fraser Valley, Canada, drilled in 1906 (Johnston, 1923; McFarland, 1983). Out of all the wells drilled for oil and gas exploration within the Georgia Basin (particularly in the Canadian part), only 40 wells have known location and drilling information (Figure 6). Twenty-three of the drilled wells within the Canadian part of the Georgia Basin have wireline log data (10 wells in the LMBC and 13 wells on Vancouver Island; Figure 6).

The first basin-scale exploration survey was a regional aeromagnetic geophysical survey, led by the Geological Survey of Canada in 1955. In 1959, a gravity survey was conducted by Petcal Ltd., which encompassed most of the Fraser Valley and west of Abbotsford. In 1959, the first

large-scale seismic reflection survey was acquired by Richfield Oil Corporation. The coverage of the seismic reflection survey extended from Abbotsford to the Strait of Georgia, and between the Fraser River and the United States border. In 1977, a seismic program was conducted by BC Gas (now FortisBC), to assess the potential for underground gas storage in the LMBC; this program involved acquiring 322 km of two-dimensional (2-D) seismic lines. Geophysical surveys outside of the LMBC include surveys in the United States, the Strait of Georgia, and on Vancouver Island. In the United States, CGG (Companie Général Géophysique) acquired seismic reflection data in 1985 in Whatcom County. In 1962, Canadian Superior Oil Ltd. acquired roughly 245 km of gas-exploder seismic data in the Strait of Georgia. Soon after, the British American Oil Company Ltd. acquired a 1150 km long gas-exploder marine seismic survey in the Strait of Georgia. An extensive marine seismic program was performed by Texaco Exploration Canada in the Strait of Georgia from 1968 to 1969 that acquired 300 km of marine seismic data. In 1987, British Petroleum Resources Canada Ltd. acquired 160 km of seismic surveys on eastern Vancouver Island. Following that survey, two wells were drilled into seismically defined

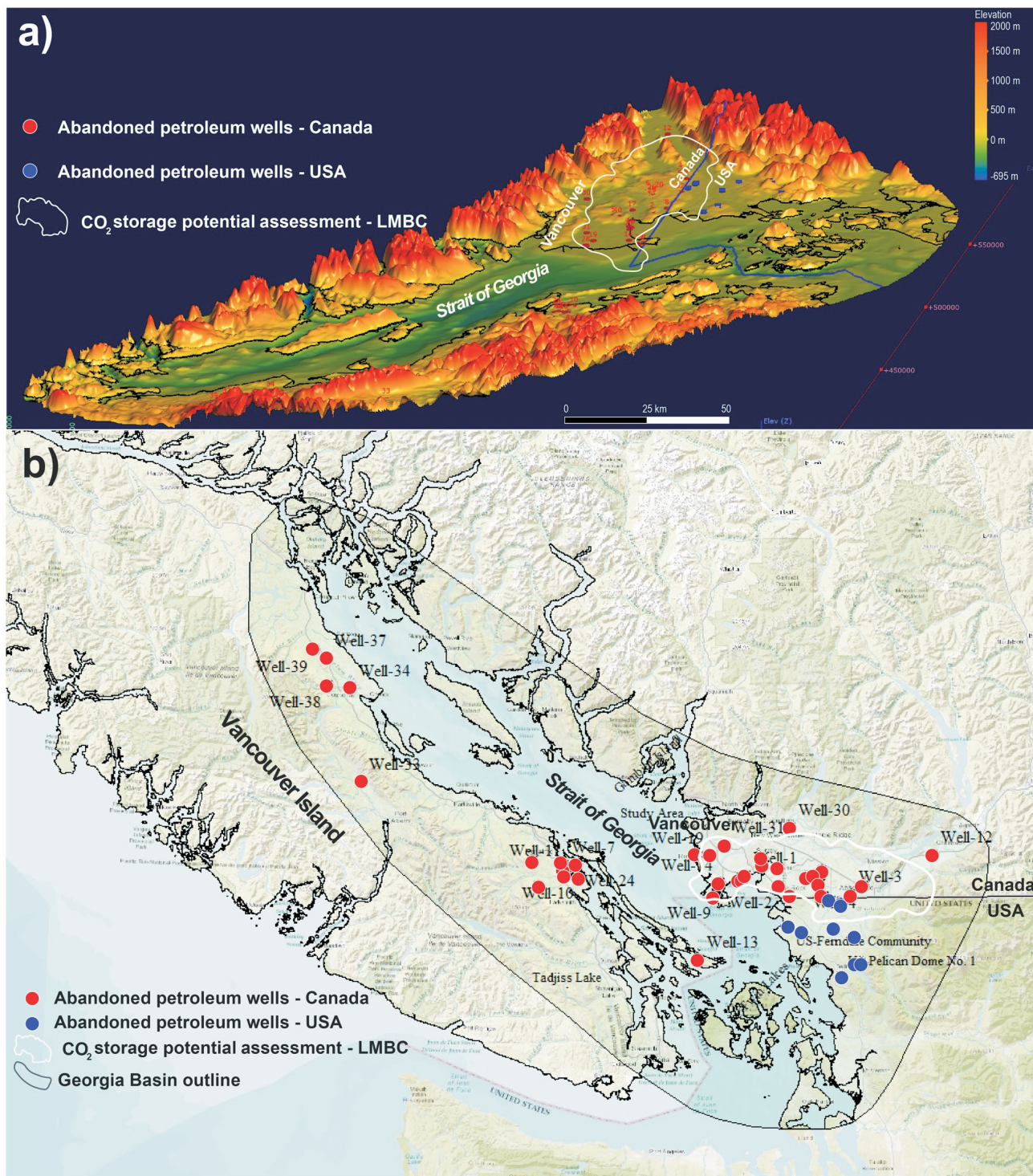


**Figure 6. a)** Digital elevation model and bathymetry of the Georgia Basin. **b)** Location of drilled wells in the Georgia Basin for which drilling data (e.g., hole location, kelly bushing, depth, etc.) are available. Among the 40 wells in the Georgia Basin with drilling data, only 23 have wireline log data: 10 in the Lower Mainland of British Columbia (LMBC), and 13 on Vancouver Island.

structures. Offshore seismic data acquired in the Strait of Georgia remain difficult to find.

## Petroleum Geology

### Reservoir Potential of Mesozoic and Cenozoic Strata in the LMBC

The Nanaimo Group contains the oldest strata inferred to have significant reservoir potential within the Georgia Basin (England, 1991; Hannigan et al., 2001). In general, the Nanaimo Group's lithoformations comprise alternating sequences of coarse-grained (sandstone- and conglomerate-dominated) and fine-grained (mudstone-dominated) units (England and Bustin, 1998; Kent et al., 2020; Huang et al., 2022). This simplified stratigraphy remains reasonably accurate for the lower Nanaimo Group in recently developed genetic stratigraphic frameworks (Kent et al., 2020; Giroto, 2022; Huang et al., 2022). However, in the upper Nanaimo Group, the position of lithoformations is mainly dependent on the architecture of the turbidite system, and hence, is more variable (Bain and Hubbard, 2016; Englert et al., 2018; Huang et al., 2022). Thick sandstone and conglomerate units are potential reservoirs within the Nanaimo Group (England and Bustin, 1998; Hannigan et al., 2001). There are also minor thin sandstone or conglomerate beds within fine-grained units that could potentially act as reservoirs.

A wide array of depositional environments are represented in the Nanaimo Group. Neritic to bathyal marine depositional environments are represented by deep-marine turbidites, submarine fans, and slope facies. Shallow-marine and littoral facies record marginal-marine deposition (Mustard et al., 1994; Katnick and Mustard, 2003; Johnstone et al., 2006; Hamblin, 2012; Giroto, 2022). The lower Nanaimo Group is dominated by coastal, paralic and nonmarine deposition, and the upper Nanaimo Group is dominated by deep-marine and submarine-fan complexes (Giroto, 2022; Huang et al., 2022).

The Paleogene Huntingdon and equivalent Chuckanut formations are fluvial- and alluvial-type clastic deposits (Johnson, 1984; Gilley, 2003). In the subsurface, the Huntingdon Formation is interpreted as a thick fluvial sequence with laterally accreting meandering channels in a sand-dominated floodplain (Mustard et al., 1994; Gilley, 2003). Medium- to coarse-grained sandstone and conglomerate are the principal rock types, with lesser shale, mudstone, siltstone and lignite (Gilley, 2003). Potential reservoir facies include coarse clastic deposits (Hannigan et al., 2001). Feldspars and lithic fragments in Paleogene sandstones are less degraded, contain less silica cement, and show less compaction than Nanaimo Group sandstones (Hannigan et al., 2001; Gilley, 2003). Reservoir-quality rocks are more likely to occur in Cenozoic sedimentary rocks than in the Nanaimo Group (Hannigan et al., 2001).

The Boundary Bay Formation consists of interbedded sandstone, mudstone, and lesser amounts of conglomerate and coal (Figure 4; Gordy, 1988; Mustard et al., 1994; Gilley, 2003). Porous sandstone units are generally thin, with most varying between 0.6 and 5 m in thickness. There are locally 10 m thick reservoir-quality sandstone units that are interpreted as fluvial channel deposits. Gordy (1988) indicated that prospective sandstones in southwestern BC vary in porosity from 8 to 34%, with an average of 15%. In Washington, porous sandstone has an average porosity of 12–15%. There is evidence of secondary fracture porosity due to significant water and gas flows below 2000 m depth and where primary matrix porosity is negligible.

### Seal Potential of Mesozoic and Cenozoic Strata

Geological storage of CO<sub>2</sub> must be designed such that the CO<sub>2</sub> cannot escape from the porous rock into which it is injected; therefore, structural trapping of CO<sub>2</sub> plays a crucial role. Injecting into porous and permeable strata should occur below an interval of laterally extensive and thick, low-permeability strata that will act as an impermeable seal and will prevent upward buoyant migration of CO<sub>2</sub>. In general, adequate lateral and top seals for Cretaceous reservoirs are provided by numerous interbedded and overlying shale and mudstone units in the Georgia Basin (Hannigan et al., 2001). Structural seals are also present in the Georgia Basin and in the LMBC, and could act as a seal where sandstone and shale units are in fault contact. Seal potential is probably reduced for Paleogene strata due to their overall high sand content (England, 1991).

## Objectives

The primary objective of the proposed research is to assess the CO<sub>2</sub> storage potential of sedimentary strata underlying the LMBC. The primary objective will be achieved through four sub-objectives, which are outlined below.

### Sub-Objective 1: Facies Characterization and Petrophysical Formation Evaluation of Cenozoic Strata Below the LMBC

Sub-objective 1 focuses on sedimentary facies characterization, petrophysical formation evaluation, integration of wireline logs and sedimentary facies, and paleogeographic mapping of the Huntingdon and Boundary Bay formations in the subsurface below the LMBC. Available drillcore data from relevant intervals across the LMBC will be examined from sedimentologic, ichnologic and stratigraphic perspectives. Identification of sedimentary facies will be done using both qualitative and quantitative parameters, including mineral composition, stratification, sedimentary structures, bioturbation, and grain-size distribution observed in cored intervals. Sedimentary facies will be grouped into facies associations, and facies associations will be used to interpret paleoenvironments (i.e., facies analysis) and to

guide genetic stratigraphic correlations across the study area. Stratigraphic correlations and facies associations will be correlated to well-log signatures, and the combined dataset will be used to map the distribution of lithological units in the subsurface.

In addition to the steps outlined above, petrophysical formation evaluation of the Huntingdon and Boundary Bay formations will be completed. Petrophysical data that will be acquired and/or calculated include total porosity (PHIT), effective porosity (PHIE), shale volume ( $V_{shale}$ ), volume fractions of lithology, horizontal permeability ( $K_h$ ) and vertical permeability ( $K_v$ ). Most of these properties will be derived from well logs, with the exception of horizontal and vertical permeability, which will be derived from available core analysis data.

Finally, facies mapping and petrophysical data will be integrated, to identify the sedimentary strata and stratigraphic intervals with the greatest available pore volumes and highest potential for long-term CO<sub>2</sub> storage. The data derived under sub-objective 1 (and 2) will form the backbone of the static reservoir model (sub-objective 3), including predicting the distribution and nature of permeable strata below the LMBC.

### Sub-Objective 2: Facies Characterization and Petrophysical Formation Evaluation of the Upper Cretaceous Strata Below the LMBC

Sub-objective 2 involves sedimentary facies characterization, petrophysical formation evaluation, integration of wireline logs and sedimentary facies, and paleogeographic mapping of the Nanaimo Group in the subsurface below the LMBC. The data to be collected under sub-objective 2, and the methodology employed, is similar to that of sub-objective 1. However, paleogeographic mapping of the Nanaimo Group differs in that sedimentary facies must be linked to the paleogeographic maps constructed previously for both the lower and upper Nanaimo groups (Bain and Hubbard, 2016; Englert et al., 2018; Kent et al., 2020; Giroto, 2022). This will result in a more complete paleogeographic picture of the Nanaimo Group throughout the Georgia Basin.

### Sub-Objective 3: 3-D Static Geological Modelling of the Georgia Basin Below the LMBC

The aim of sub-objective 3 is to produce a 3-D static geological model for the Georgia Basin below the LMBC, and these data will be used to depict the 3-D distribution of reservoirs and seals. The model will combine all subsurface geological data, and will build extensively on the results and outputs from sub-objectives 1 and 2. In addition to these data, available 2-D seismic data, seismic maps, drill-stem test data and water chemistry information will be in-

corporated in Schlumberger Limited's (Schlumberger) Petrel software.

Construction of the regional static geological model involves three phases: 1) structural modelling, 2) facies modelling, and 3) property modelling (co-dependent on facies modelling).

The structural framework includes all the interpreted faults below the LMBC, as well as structure on interpreted stratigraphic horizons and reservoir layers. The structural model will be constructed in the depth domain using data from drilled wells with geological markers, seismic maps of stratigraphic horizons, and maps of faults derived from seismic data and wells. The extent of structural mapping within and beyond the study area will be determined based on available and resolvable geophysical data and the maximum depth of wells drilled in the region.

Facies modelling will form the interface between geological phenomena and reservoir characterization, and will occur before modelling porosity and permeability. Lateral and vertical facies changes directly control reservoir quality; hence, it is necessary to resolve facies trends and build them into the geological model. For this, facies defined in sub-objectives 1 and 2 will be spatially modelled across the LMBC.

Finally, property modelling involves modelling the parameters calculated from petrophysical formation evaluation and drillcore logs (mainly PHIE and permeability). These parameters will be modelled using results from sub-objectives 1 and 2.

The regional static model generated under sub-objective 3 will enable a reconciliation of differences and an estimation of uncertainty in both the static model and in future dynamic (fluid flow) modelling. The 3-D model is essential for accurately predicting fluid (CO<sub>2</sub>) flow behaviour through reservoir simulations.

### Sub-Objective 4: Fault Mapping and Identification of Geohazards Below the LMBC

Sub-objective 4 focuses on mapping the distribution and patterns of faults that are only expressed in the subsurface below the LMBC, and assessing their potential as geohazards. The LMBC is situated over an active tectonic zone, and yet the positions of faults within the region are not mapped in detail, especially where they have no surface expression. Each of these surfaces represents a potential slipface that could reactivate during an earthquake, so mapping the position of faults with no visible fault trace will give a better sense of the geohazard risks for the residents of BC's Lower Mainland.

## Methods

The datasets that will be used in this research include drill-core data, geophysical well logs, drillstem test results, water chemistry analysis, 2-D seismic lines and seismic maps. These data will be analyzed using one of four methods: 1) core and facies analysis, 2) petrophysical formation evaluation, 3) 3-D static geological modelling, and 4) seismic interpretation.

### Core and Facies Analysis

Core logging will be done on the five wells in the LMBC for which drillcore is available. Approximately 190 m of core exist between the five wells (Figure 7). Core descriptions will be used to conduct facies analysis, define sedimentary environments, construct paleogeographic maps, and make genetic stratigraphic correlations through the sedimentary strata below the LMBC. Sedimentary facies will be classi-



**Figure 7.** Photos of core from a well drilled in the Lower Mainland of British Columbia (core 5, with unique well identifier [UWI] of A-017-B/092-G02; BC Oil and Gas Commission, 2022): **a)** cored interval from 1386.9 to 1390.8 m, showing the finely layered sandstone typical of this area; **b)** close-up of core 5 from depth of 1387.30 m, illustrating the relatively coarse-grained nature of the rock.

fied according to their textural, sedimentological and ichnological characteristics. Textural observations include lithology, grain size, grain sorting and roundness. Sedimentological data includes bedding, physical sedimentary structures, cementation and lithological accessories (e.g., macerated plant material). Ichnological information includes ichnogenera, trace-fossil sizes and diversity, bioturbation intensity using the BI-scale of Taylor and Goldring (1993), and the distribution of burrowing between beds. These data will be used to generate paleoenvironmental interpretations. Porosity and permeability values derived from cored intervals will be correlated to facies. Core logs and porosity-permeability data will form the main datasets for sub-objectives 1 and 2.

### Petrophysical Formation Evaluation

Wireline log data (Figure 8) from 10 wells in the LMBC will be used to derive petrophysical parameters, and these data will be incorporated into sub-objectives 1, 2 and 3. Wireline logs will be calibrated to remove artefacts from wireline data acquisition to obtain the best possible petrophysical calculations. In this regard, several quality-assurance steps will be applied to the logs, including depth calibration through depth shifts, log normalization, and the removal of outliers. Core-to-well log-depth shifts will be reviewed and adjusted if necessary. Outliers include intervals with null or missing values (i.e., missing core); intervals with obvious postdepositional overprints (fractures observed in core); and intervals characterized by caliper-indicated washouts or bad wellbore conditions.

Finally, petrophysical data, including PHIT, PHIE,  $V_{\text{shale}}$ , volume fraction of lithology and predicted permeability, will be calculated via petrophysical formation evaluation using Schlumberger's Techlog software.

### Seismic Interpretation

Seismic data are essential for sub-objectives 3 and 4, and available seismic data include 2-D seismic data and interpreted seismic maps of stratal surfaces and faults beneath the LMBC (Figure 9). A basin-wide structural interpretation of the strata underlying the LMBC is limited because of the absence of 3-D seismic data, and poor quality or sparse availability of 2-D seismic data. There are approximately 22 km of 2-D seismic lines available that will be reprocessed and interpreted. In addition, two maps that were constructed using an array of 2-D seismic lines have been digitized. The surfaces on these maps were digitized using Neuralog's NeuraMap software and incorporated into the geological model. The maps are in two-way-travel-time, and will be converted to depth using synthetic wavelet models built from sonic well logs using wells that intersect seismic lines. Stratigraphic horizons and faults below the study area will be picked and interpreted through Schlumberger's Petrel software.

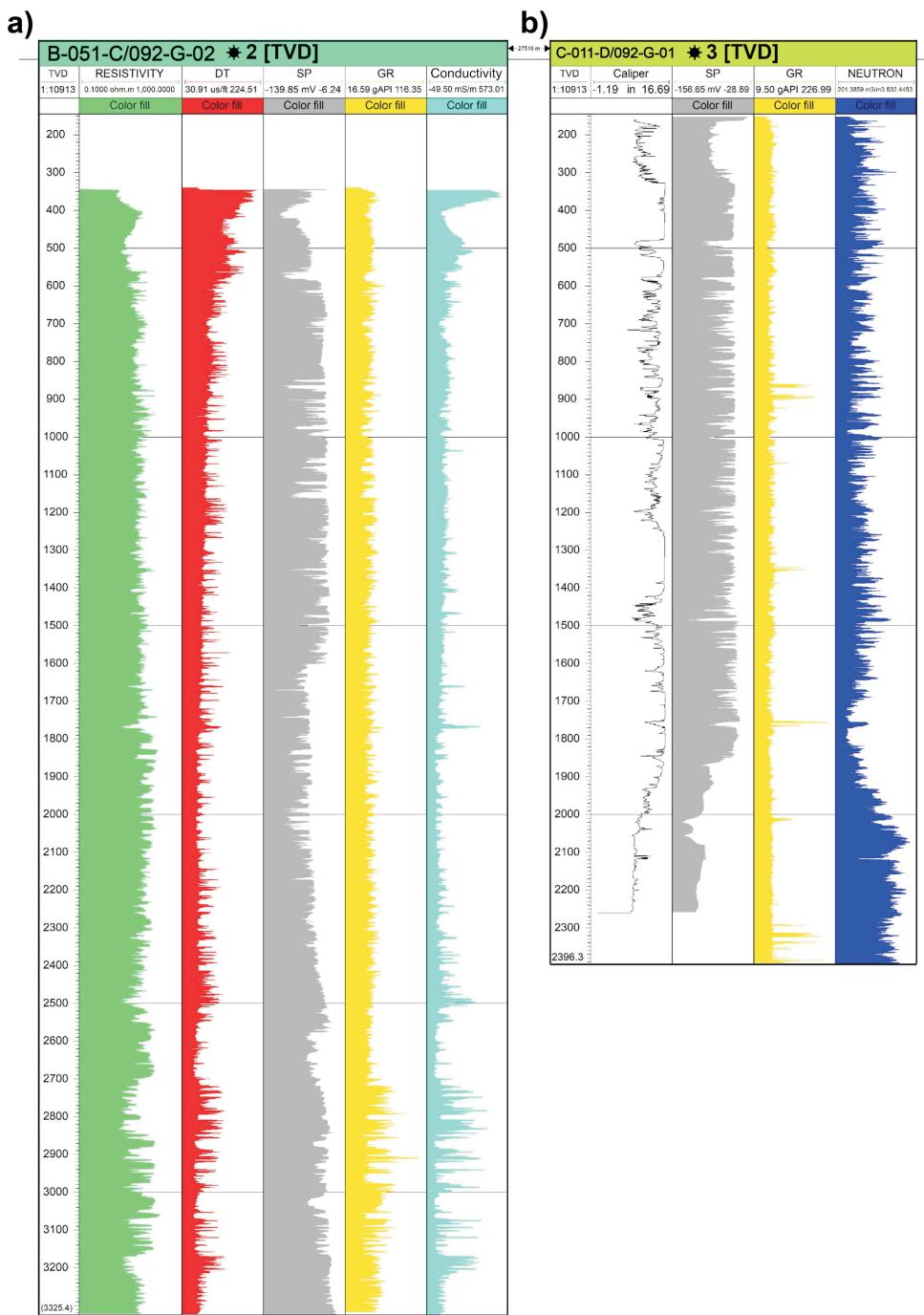


**Figure 8.** Two of the available wireline logs for wells drilled in the Lower Mainland of British Columbia: **a)** wireline log from unique well identifier B-051-C/092-G-02, and **b)** wireline log from unique well identifier C-011-D/092-G-01 (BC Oil and Gas Commission, 2022). Both logs are corrected for true vertical depth (TVD), given in metres. Abbreviations: DT, sonic log; gAPI, API gamma-ray unit; GR, gamma ray; mS/m, millisiemens per metre; mV, millivolt; SP, spontaneous potential.

Seismic interpretation and the resultant maps are key data needed to identify both CO<sub>2</sub> injection and storage locations and areas with high geohazard risks. Among the most important seismic outputs are the distribution, thickness and depth of potential reservoirs and seals; the fault architecture below the LMBC; and identification of potential reservoir connectivity across faults. Regional seismic interpre-

tation is necessary for the development of an accurate 3-D geological model.

### 3-D Static Geological Modelling

The 3-D static geological model integrates various data, including core data; geophysical logs and petrophysical data;

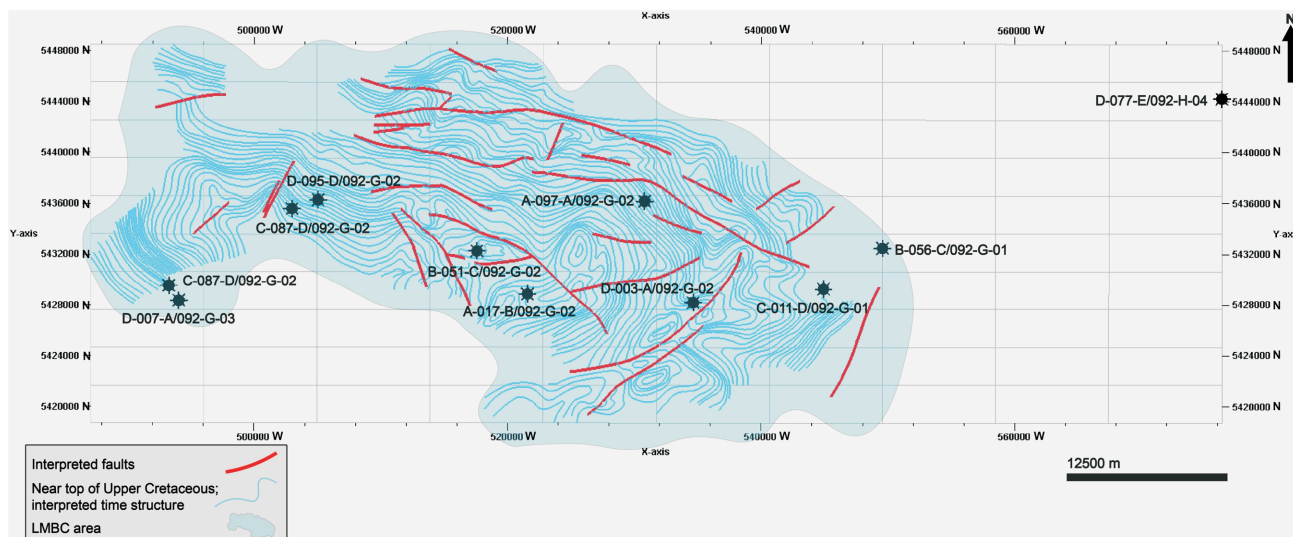


**Figure 9.** Seismic time structure map of the Upper Cretaceous and the interpreted faults in the Lower Mainland, British Columbia (LMBC). Also shown are the locations of wells (unique well identifiers; BC Oil and Gas Commission, 2022) from which data were obtained. The digitized version of the interpretation of the Upper Cretaceous horizon and faults in the LMBC area was prepared using Schlumberger Limited’s Petrel software.

drillstem test results and water chemistry data, well tops, and 2-D seismic data; structural surfaces from seismic surveys and wells; and paleogeographic reconstruction maps of depositional environment systems. These data will be built into a probabilistic distribution of facies and rock properties. Construction of the 3-D static geological model comprises three phases, including structural modelling, facies modelling, and property modelling (Figure 10). The sequential workflow applied to build the 3-D regional static model is as follows:

- 1) Stratigraphic surfaces and major fault structures mapped from seismic data will be the input for structural modelling, and the resulting structural framework should enable identification of potential structural traps. The potential factors in defining the grid increment and orientation are the well locations and distribution, the geometry of structures, fault elongation and geometry, boundary/edge of the grid, variography analysis of seismic inversion data, and the behaviour of the reservoir. Structural modelling involves several steps, including defining the fault framework (seismic-interpreted faults, fault naming, matching well markers and interpreted faults, and fault-model quality control); defining the structural framework boundary; stratigraphic and reservoir layer modelling; and constructing the geological grid.
- 2) A 3-D facies model will be constructed from facies defined in cored intervals (sub-objectives 1 and 2) and then mapped regionally using wireline log signatures. Facies models will be guided by the trends recognized in paleogeographic reconstructions developed in sub-objectives 1 and 2, to guide interpre-

tations of facies trends in the subsurface where no core, wireline or seismic data exist. Facies modelling comprises three main tasks: i) well log up-scaling to grid cells (facies data of wells will be scaled-up in the 3-D grid by averaging the facies log values in the grid cells);

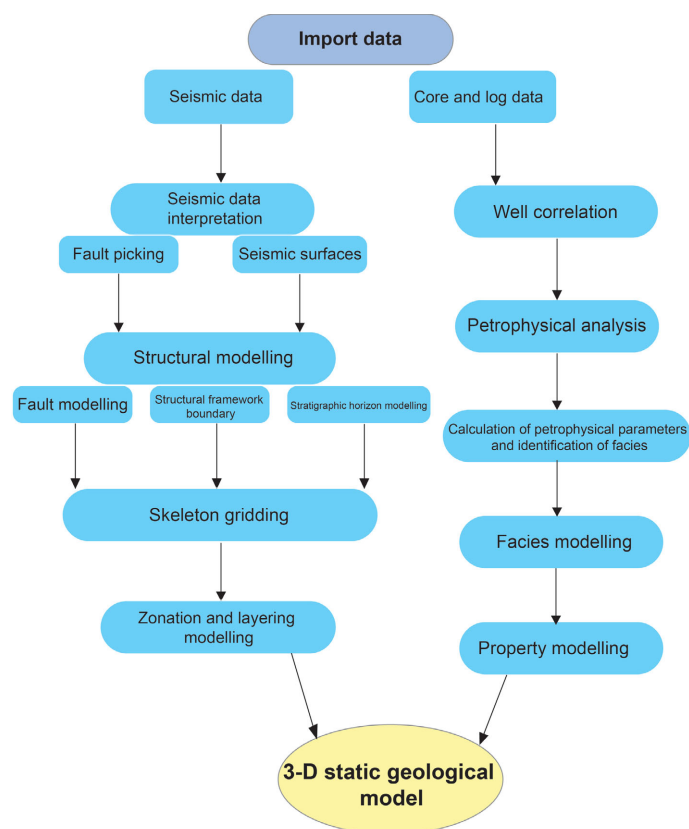


**Figure 10.** Flow chart of the three-dimensional (3-D) static geological modelling process.

- ii) data analysis; and iii) the facies modelling process. Facies data are usually modelled geostatistically using Sequential Indicator Simulation (SIS) algorithms.
- 3) Property modelling includes modelling effective porosity and permeability distribution in 3-D. Effective porosity will be based on facies-based PHIE values, which are derived from the petrophysical formation evaluation analysis in sub-objectives 1 and 2. Permeability values will also be facies-based, and will be derived from core analysis and permeability prediction via formation evaluation analysis. Property modelling includes three main tasks: i) well log up-scaling to grid cells (PHIE and permeability data of wells will be scaled-up in the 3-D grid by averaging their log values in the grid cells); ii) data analysis; and iii) the property modelling process.

Petrophysical data are usually modelled geostatistically by two methods in Petrel, including Sequential Gaussian Simulation (SGS) and Gaussian Random Function Simulation (GRFS). In the property modelling step, the GRFS method will be used to propagate the porosity and permeability values at facies level into the 3-D model. The property model will be populated using the GRFS method, using variograms, correlation coefficients and trends, to constrain the vertical and lateral distribution of properties. The GRFS method has advantages over the SGS method, as it is faster to run and it provides more accurate results compared to SGS.

## Conclusion

In conclusion, carbon dioxide (CO<sub>2</sub>) concentration is increasing, and it tremendously influences Earth's atmosphere by intensifying the natural greenhouse effect, exerting a warming influence on the planet's surface. As Earth's climate warms, extreme weather events (e.g., heat domes, tropical cyclones, elevated precipitation, and flooding) occur with greater intensity, raising individuals' concerns about their safety and the safety of their property. Finding practical solutions to decrease carbon emissions while simultaneously maintaining our standard of living and expanding the standard of living of developing countries demands economical and novel solutions. Accordingly, capturing, and sequestering CO<sub>2</sub> underground is the most viable approach to reducing CO<sub>2</sub> emissions over the short to medium term.

British Columbia's Lower Mainland has been assessed previously for hydrocarbon potential and natural gas storage, and these results demonstrated that the area is a readily accessible and potentially economically feasible locale to store CO<sub>2</sub>. Nevertheless, not much effort has been made to evaluate the feasibility of carbon capture and storage in the Lower Mainland. Sedimentary strata below the Lower Mainland (at depth) are poorly understood, and the geological context (e.g., depositional environment and facies

analysis) of these strata has not been examined in detail. Therefore, this research aims to evaluate the feasibility of carbon capture and storage through several related steps, including facies characterization and petrophysical formation evaluation of Cenozoic and Upper Cretaceous strata below the Lower Mainland, three-dimensional static geological modelling of the Georgia Basin below the Lower Mainland, and fault mapping and identification of geohazards in the same area. Applying these steps will lead to placing the strata below the Lower Mainland in a geological context, assessing these strata for their reservoir potential, and building an integrated three-dimensional static geological model of the strata. These data will then be used to estimate the storage capacity and long-term fate of injected carbon dioxide. The geological model will also be used to define subsurface geohazards (e.g., faults).

## Acknowledgments

The lead author would like to thank Geoscience BC for providing financial support through the Geoscience BC scholarship. A special thank you to J. MacEachern for providing comments that improved the quality of this paper.

## References

- Bachu, S. (2003): Screening and ranking of sedimentary basins for sequestration of CO<sub>2</sub> in geological media in response to climate change; *Environmental Geology*, v. 44, no. 3, p. 277–289.
- Bachu, S. and Gunter, W.D. (2005): Overview of acid-gas injection operations in western Canada; *in* Proceedings of the 7<sup>th</sup> International Conference on Greenhouse Gas Control Technologies, September 5–9, 2004, Vancouver, British Columbia, E.S. Rubin, D.W. Keith and C.F. Gilboy (ed.), Elsevier, p. 443–448.
- Bachu, S., Gunter, W. and Perkins, E. (1994): Aquifer disposal of CO<sub>2</sub>: hydrodynamic and mineral trapping; *Energy Conversion and Management*, v. 35, no. 4, p. 269–279.
- Bain, H.A. and Hubbard, S.M. (2016): Stratigraphic evolution of a long-lived submarine channel system in the Late Cretaceous Nanaimo Group, British Columbia, Canada; *Sedimentary Geology*, v. 337, p. 113–132.
- BC Oil and Gas Commission (2022): Well lookup and reports; BC Oil and Gas Commission, URL <<http://www.bcogc.ca/online-services>> [September 2022].
- Bratu, A., Card, K.G., Closson, K., Aran, N., Marshall, C., Clayton, S., Gislason, M.K., Samji, H., Martin, G., Lem, M., Logie, C.H., Takaro, T.K. and Hogg, R.S. (2022): The 2021 western North American heat dome increased climate change anxiety among British Columbians: results from a natural experiment; *The Journal of Climate Change and Health*, v. 6, art. 100116.
- Bustin, R. (1995): Organic maturation and petroleum source rock potential of Tofino Basin, southwestern British Columbia; *Bulletin of Canadian Petroleum Geology*, v. 43, no. 2, p. 177–186.
- Bustin, R. and England, T. (1991): Petroleum source rock potential of the Nanaimo Group, western margin of the Georgia Basin, southwestern British Columbia; *in* Current Research,

- Part A, Geological Survey of Canada, Paper 91-1A, p. 143–145.
- Clapp, C.H. (1913): Geology of the Victoria and Saanich map areas, Vancouver Island, British Columbia; Geological Survey of Canada, Memoir 36, 143 p.
- Dickinson, W. and Seely, D. (1979): Structure and stratigraphy of forearc regions; AAPG Bulletin, v. 63, no. 1, p. 2–31.
- England, T.D.J. (1989): Late Cretaceous to Paleogene evolution of the Georgia Basin, southwestern British Columbia; M.Sc. thesis, Memorial University of Newfoundland, 560 p.
- England, T. (1991): Late Cretaceous to Paleogene structural and stratigraphic evolution of Georgia Basin, southwestern British Columbia: implications for hydrocarbon potential; Washington Geology, v. 19, no. 4, p. 10–11.
- England, T. and Bustin, R. (1998): Architecture of the Georgia Basin, southwestern British Columbia; Bulletin of Canadian Petroleum Geology, v. 46, no. 2, p. 288–320.
- England, T. and Calon, T. (1991): The Cowichan fold and thrust system, Vancouver Island, southwestern British Columbia; Geological Society of America Bulletin, v. 103, no. 3, p. 336–362.
- England, T. and Hiscott, R. (1992): Lithostratigraphy and deep-water setting of the upper Nanaimo Group (Upper Cretaceous), outer Gulf Islands of southwestern British Columbia; Canadian Journal of Earth Sciences, v. 29, no. 3, p. 574–595.
- Englert, R.G., Hubbard, S.M., Coutts, D.S. and Matthews, W.A. (2018): Tectonically controlled initiation of contemporaneous deep-water channel systems along a Late Cretaceous continental margin, western British Columbia, Canada; Sedimentology, v. 65, no. 7, p. 2404–2438.
- Ewald, J. (2013): CO<sub>2</sub> at NOAA's Mauna Loa Observatory reaches new milestone: tops 400 ppm; National Oceanic and Atmospheric Administration, U.S. Department of Commerce, NOAA Research News, May 10, 2013, URL <<https://gml.noaa.gov/news/pdfs/7074.pdf>> [September 2022].
- Flannigan, M. and Wagner, C.V. (1991): Climate change and wildfire in Canada; Canadian Journal of Forest Research, v. 21, no. 1, p. 66–72.
- Gabrielse, H. and Yorath, C.J., editors (1991): Geology of the Cordilleran Orogen in Canada; Geological Survey of Canada, Geology of Canada, no. 4, 844 p. (also Geological Society of America, Geology of North America, v. G-2).
- Gilley, B.H.T. (2003): Facies architecture and stratigraphy of the Paleogene Huntingdon Formation at Abbotsford, British Columbia; M.Sc. thesis, Simon Fraser University, 152 p.
- Giroto, K. (2022): Tectono-stratigraphic model for the early evolution of the Late Cretaceous Nanaimo Group: Georgia Basin, British Columbia, Canada; M.Sc. thesis, Simon Fraser University, 145 p.
- Gordy, P.L. (1988): Evaluation of the hydrocarbon potential of the Georgia depression; BC Ministry of Energy, Mines and Low Carbon Innovation, Geological Report 88–03.
- Groulx, B.J. and Mustard, P.S. (2004): Understanding the geological development of the Lower Mainland: the first step to informed land-use decisions; in Fraser River Delta, British Columbia: Issues of an Urban Estuary, B.J. Groulx, D.C. Mosher, J.L. Luternauer and D.E. Bilderback (ed.), Geological Survey of Canada, Bulletin 567, p. 1–22.
- Haggart, J.W. (1992): Progress in Jurassic and Cretaceous stratigraphy, Queen Charlotte Islands, British Columbia; in Current Research, Part A, Geological Survey of Canada, Paper 92-1A, p. 361–365.
- Haggart, J.W. (1993): Latest Jurassic and Cretaceous paleogeography of the northern Insular Belt, British Columbia; in Mesozoic Paleogeography of the Western United States, Proceedings of the American Association of Petroleum Geologists, Society of Economic Paleontologists and Mineralogists, Pacific Section, 1992 Meeting, Sacramento, California, G.C. Dunne and K.A. McDougall (ed.), Society of Economic Paleontologists and Mineralogists, Publication 71, p. 463–475.
- Haggart, J.W. and Graham, R. (2018): The crinoid *Marsupites* in the Upper Cretaceous Nanaimo Group, British Columbia: resolution of the Santonian–Campanian boundary in the North Pacific Province; Cretaceous Research, v. 87, p. 277–295.
- Haggart, J.W., Ward, P.D. and Orr, W. (2005): Turonian (Upper Cretaceous) lithostratigraphy and biochronology, southern Gulf Islands, British Columbia, and northern San Juan Islands, Washington State; Canadian Journal of Earth Sciences, v. 42, no. 11, p. 2001–2020.
- Hamblin, A. (2012): Upper Cretaceous Nanaimo Group of Vancouver Island as a potential bedrock aquifer zone: summary of previous literature and concepts; Geological Survey of Canada, Open File 7265, 20 p.
- Hannigan, P.K., Dietrich, J.R., Lee, P.J. and Osadetz, K.G. (2001): Petroleum resource potential of sedimentary basins on the Pacific margin of Canada; Geological Survey of Canada, Bulletin 564, 73 p., URL <<https://emrlibrary.gov.yk.ca/gsc/bulletins/564.pdf>> [September 2022].
- Hopkins, W.S. (1966): Palynology of Tertiary rocks of the Whatcom Basin, southwestern British Columbia and northwestern Washington; Ph.D. thesis, The University of British Columbia, 169 p.
- Hopkins, W.S. (1968): Subsurface Miocene rocks, British Columbia-Washington, a palynological investigation; Geological Society of America Bulletin, v. 79, no. 6, p. 763–768.
- Huang, C., Dashtgard, S.E., Haggart, J.W. and Giroto, K. (2022): Synthesis of chronostratigraphic data and methods in the Georgia Basin, Canada, with implications for convergent-margin basin chronology; Earth-Science Reviews, v. 231, art. 104076.
- Huang, C., Dashtgard, S.E., Kent, B.A., Gibson, H.D. and Matthews, W.A. (2019): Resolving the architecture and early evolution of a forearc basin (Georgia Basin, Canada) using detrital zircon; Scientific Reports, v. 9, no. 1, p. 1–12.
- Intergovernmental Panel on Climate Change (2014): Climate Change 2014: Synthesis Report, Contribution of Working Groups I, II and III to the Fifth Assessment Report of the Intergovernmental Panel on Climate Change; Intergovernmental Panel on Climate Change, Core Writing Team, R.K. Pachauri and L.A. Meyer (ed.), Geneva, Switzerland, 151 p.
- Johnson, S.Y. (1984): Stratigraphy, age, and paleogeography of the Eocene Chuckanut Formation, northwest Washington; Canadian Journal of Earth Sciences, v. 21, no. 1, p. 92–106.
- Johnson, S.Y. (1985): Eocene strike-slip faulting and nonmarine basin formation in Washington; Chapter 3 in Strike-Slip Deformation, Basin Formation, and Sedimentation, K.T. Biddle and N. Christie-Blick (ed.), Society for Sedimentary Geology, SEPM Special Publication No. 17, p. 78–90.

- Johnson, S. (1991): Sedimentation and tectonic setting of the Chuckanut Formation, northwest Washington; *Washington Geology*, v. 19, no. 4, p. 12–13.
- Johnston, W.A. (1923): *Geology of Fraser River Delta map area*; Geological Survey of Canada, Memoir 135, 87 p., 1 map.
- Johnstone, P., Mustard, P. and MacEachern, J. (2006): The basal unconformity of the Nanaimo Group, southwestern British Columbia: a Late Cretaceous storm-swept rocky shoreline; *Canadian Journal of Earth Sciences*, v. 43, no. 8, p. 1165–1181.
- Jones, M.T. (2016): Stratigraphy and architecture of shallow-marine strata on an active margin, lower Nanaimo Group, Vancouver Island, BC; M.Sc. thesis, Simon Fraser University, 85 p.
- Kaszuba, J.P., Janecky, D.R. and Snow, M.G. (2003): Carbon dioxide reaction processes in a model brine aquifer at 200 C and 200 bars: implications for geologic sequestration of carbon; *Applied Geochemistry*, v. 18, no. 7, p. 1065–1080.
- Katnick, D.C. and Mustard, P.S. (2003): Geology of Denman and Hornby islands, British Columbia: implications for Nanaimo Basin evolution and formal definition of the Geoffrey and Spray formations, Upper Cretaceous Nanaimo Group; *Canadian Journal of Earth Sciences*, v. 40, no. 3, p. 375–393.
- Keeling, C.D. (1960): The concentration and isotopic abundances of carbon dioxide in the atmosphere; *Tellus*, v. 12, no. 2, p. 200–203.
- Keighley, D. and Maher, C. (2015): A preliminary assessment of carbon storage suitability in deep underground geological formations of New Brunswick, Canada; *Atlantic Geology*, v. 51, p. 269–286.
- Kent, B.A., Dashtgard, S.E., Huang, C., MacEachern, J.A., Gibson, H.D. and Cathyl-Huhn, G. (2020): Initiation and early evolution of a forearc basin: Georgia Basin, Canada; *Basin Research*, v. 32, no. 1, p. 163–185.
- Kharaka, Y.K., Cole, D.R., Hovorka, S.D., Gunter, W., Knauss, K.G. and Freifeld, B. (2006): Gas-water-rock interactions in Frio Formation following CO<sub>2</sub> injection: implications for the storage of greenhouse gases in sedimentary basins; *Geology*, v. 34, no. 7, p. 577–580.
- Lane, J., Greig, C. and Garnett, A. (2021): Uncertain storage prospects create a conundrum for carbon capture and storage ambitions; *Nature Climate Change*, v. 11, no. 11, p. 925–936.
- Lynch, G. (1992): Deformation of Early Cretaceous volcanic-arc assemblages, southern Coast Belt, British Columbia; *Canadian Journal of Earth Sciences*, v. 29, no. 12, p. 2706–2721.
- Lynch, J.V.G. (1991): Georgia Basin Project: stratigraphy and structure of Gambier Group rocks in the Howe Sound-Mamquam River area, southwest Coast Belt, British Columbia; *in Current Research, Part A, Geological Survey of Canada, Paper 91-1A*, p. 49–58.
- McFarland, C.R. (1983): Oil and gas exploration in Washington, 1900–1982; State of Washington, Department of Natural Resources, Division of Geology and Earth Resources, Information Circular 75, 119 p.
- McGugan, A. (1979): Biostratigraphy and paleoecology of Upper Cretaceous (Campanian and Maestrichtian) foraminifera from the upper Lambert, Northumberland, and Spray formations, Gulf Islands, British Columbia, Canada; *Canadian Journal of Earth Sciences*, v. 16, no. 12, p. 2263–2274.
- Miall, A.D. (1984): Depositional systems; Chapter 2 *in Principles of Sedimentary Basin Analysis*, First Edition, Springer, New York, New York, p. 277–317.
- Miller, G.M. (1963): Early Eocene angular unconformity at western front of Northern Cascades, Whatcom County, Washington; Erratum; *AAPG Bulletin*, v. 47, no. 8, p. 1627–1627.
- Molnar, S., Cassidy, J.F., Dosso, S.E. and Olsen, K.B. (2010): 3D ground motion in the Georgia Basin region of SW British Columbia for Pacific Northwest scenario earthquakes; *in Proceedings of the 9<sup>th</sup> U.S. National and 10<sup>th</sup> Canadian Conference on Earthquake Engineering*, July 25–29, 2010, Toronto, Ontario, Paper No. 754.
- Monger, J. (1990): Georgia Basin: regional setting and adjacent Coast Mountains geology, British Columbia; *in Current Research, Part F, Geological Survey of Canada, Paper 90-1F*, p. 95–102.
- Monger, J. (1991a): Georgia Basin Project: structural evolution of parts of southern Insular and southwestern Coast belts; *in Current Research, Part A, Geological Survey of Canada, Paper 91-1A*, p. 219–228.
- Monger, J. (1991b): Late Mesozoic to Recent evolution of the Georgia Strait–Puget Sound region, British Columbia and Washington; *Washington Geology*, v. 19, no. 4, p. 3–9.
- Monger, J. and Journeay, J. (1994): Basement geology and tectonic evolution of the Vancouver region; *in Geology and Geological Hazards of the Vancouver Region, Southwestern British Columbia*, J.W.H. Monger (ed.), Geological Survey of Canada, Bulletin 481, p. 3–25.
- Monger, J. and Price, R. (2002): The Canadian Cordillera: geology and tectonic evolution; *CSEG Recorder*, v. 27, no. 2, p. 17–36.
- Monger, J., Van der Heyden, P., Journeay, J., Evenchick, C. and Mahoney, J. (1994): Jurassic-Cretaceous basins along the Canadian Coast Belt: their bearing on pre-mid-Cretaceous sinistral displacements; *Geology*, v. 22, no. 2, p. 175–178.
- Muller, J.E. and Jeletzky, J.A. (1970): Geology of the Upper Cretaceous Nanaimo Group, Vancouver Island and Gulf Islands, British Columbia; Geological Survey of Canada, Paper 69-25, 84 p.
- Mustard, P. (1991): Stratigraphy and sedimentology of the Georgia Basin, British Columbia and Washington State; *Washington Geology*, v. 19, p. 4.
- Mustard, P.S. and Monger, J. (1994): The Upper Cretaceous Nanaimo group, Georgia Basin; *in Geology and Geological Hazards of the Vancouver Region, Southwestern British Columbia*, J.W.H. Monger (ed.), Geological Survey of Canada, Bulletin 481, p. 27–95.
- Mustard, P.S. and Rouse, G.E. (1991): Sedimentary outliers of the eastern Georgia Basin margin, British Columbia; *in Current Research, Part A, Geological Survey of Canada, Paper 91-1A*, p. 229–240.
- Mustard, P.S., Rouse, G.E. and Monger, J. (1994): Stratigraphy and evolution of Tertiary Georgia Basin and subjacent Upper Cretaceous sedimentary rocks, southwestern British Columbia and northwestern Washington State; *in Geology and Geological Hazards of the Vancouver Region, Southwestern British Columbia*, Geological Survey of Canada, Bulletin 481, p. 97–169.
- Pacht, J. (1984): Petrologic evolution and paleogeography of the Late Cretaceous Nanaimo Basin, Washington and British Columbia: implications for Cretaceous tectonics; *Geological Society of America Bulletin*, v. 95, no. 7, p. 766–778.

- Pearce, J., La Croix, A., Brink, F., Hayes, P. and Underschultz, J. (2021): CO<sub>2</sub> mineral trapping comparison in different regions: predicted geochemical reactivity of the Precipice Sandstone reservoir and overlying Evergreen Formation; *Petroleum Geoscience*, v. 27, no. 3, URL <<https://www.earthdoc.org/content/journals/10.1144/petgeo2020-106>> [September 2022].
- Rouse, G.E., Lesack, K.A. and White, J.M. (1990): Palynology of Cretaceous and Tertiary strata of Georgia Basin, southwestern British Columbia; *in* Current Research, Part F, Geological Survey of Canada, Paper 90-1F, p. 109–113.
- Shukla, R., Ranjith, P., Haque, A. and Choi, X. (2010): A review of studies on CO<sub>2</sub> sequestration and caprock integrity; *Fuel*, v. 89, no. 10, p. 2651–2664.
- Sliter, W.V. (1973): Upper Cretaceous foraminifers from the Vancouver Island area, British Columbia, Canada; *The Journal of Foraminiferal Research*, v. 3, no. 4, p. 167–186.
- Stephenson, M.H., Ringrose, P., Geiger, S., Bridden, M. and Schofield, D. (2019): Geoscience and decarbonization: current status and future directions; *Petroleum Geoscience*, v. 25, no. 4, p. 501–508.
- Takano, O. and Tsuji, T. (2017): Fluvial to bay sequence stratigraphy and seismic facies of the Cretaceous to Paleogene successions in the MITI Sanriku-oki well and the vicinities, the Sanriku-oki forearc basin, northeast Japan; *Island Arc*, v. 26, no. 4, art. e12184.
- Takano, O., Itoh, Y. and Kusumoto, S. (2013): Variation in forearc basin configuration and basin-filling depositional systems as a function of trench slope break development and strike-slip movement: examples from the Cenozoic Ishikari–Sanriku-Oki and Tokai-Oki–Kumano-Nada forearc basins, Japan; Chapter 1 *in* Mechanism of Sedimentary Basin Formation - Multidisciplinary Approach on Active Plate Margins, Y. Itoh (ed.), *InTech*, p. 3–25.
- Taylor, A. and Goldring, R. (1993): Description and analysis of bioturbation and ichnofabric; *Journal of the Geological Society*, v. 150, no. 1, p. 141–148.
- Underschultz, J., Boreham, C., Dance, T., Stalker, L., Freifeld, B., Kirste, D. and Ennis-King, J. (2011): CO<sub>2</sub> storage in a depleted gas field: an overview of the CO<sub>2</sub>CRC Otway Project and initial results; *International Journal of Greenhouse Gas Control*, v. 5, no. 4, p. 922–932.
- U.S. Energy Information Administration (2021): International Energy Outlook 2021; U.S. Energy Information Administration, URL <<https://www.eia.gov/outlooks/ieo/>> [September 2022].
- Vance, J. (1975): Bedrock geology of San Juan County; *in* Geology and Water Resources of the San Juan Islands, San Juan County, Washington, R.H. Russell (ed.), Washington Department of Ecology, Office of Technical Services, Water-Supply Bulletin No. 46, p. 3–19.
- Ward, P.D., Haggart, J.W., Mitchell, R., Kirschvink, J.L. and Tobin, T. (2012): Integration of macrofossil biostratigraphy and magnetostratigraphy for the Pacific Coast Upper Cretaceous (Campanian–Maastrichtian) of North America and implications for correlation with the Western Interior and Tethys; *Geological Society of America Bulletin*, v. 124, no. 5–6, p. 957–974.
- Wheeler, J.O., Brookfield, A.J., Gabrielse, H., Monger, J.W.H., Tipper, H.W. and Woodsworth, G.J. (1991): Terrane map of the Canadian Cordillera; Geological Survey of Canada, ‘A’ Series Map 1713A, 2 sheets, URL <<https://doi.org/10.4095/133550>>.
- Zelt, B., Ellis, R., Zelt, C., Hyndman, R., Lowe, C., Spence, G. and Fisher, M. (2001): Three-dimensional crustal velocity structure beneath the Strait of Georgia, British Columbia; *Geophysical Journal International*, v. 144, no. 3, p. 695–712.



# Garibaldi Geothermal Volcanic Belt Assessment Project, Southwestern British Columbia (Part of NTS 092J), Phase 2: 2022 Field Report

**S.E. Grasby**, Natural Resources Canada, Geological Survey of Canada–Calgary, Calgary, Alberta, [steve.grasby@canada.ca](mailto:steve.grasby@canada.ca)

**A. Borch**, The University of British Columbia, Vancouver, British Columbia

**A. Calahorrano-Di Patre**, Simon Fraser University, Burnaby, British Columbia

**Z. Chen**, Natural Resources Canada, Geological Survey of Canada–Calgary, Calgary, Alberta

**J. Craven**, Natural Resources Canada, Geological Survey of Canada–Central, Ottawa, Ontario

**X. Liu**, Natural Resources Canada, Geological Survey of Canada–Calgary, Calgary, Alberta

**M. Muhammad**, Simon Fraser University, Burnaby, British Columbia

**J.K. Russell**, The University of British Columbia, Vancouver, British Columbia

**V. Tschirhart**, Natural Resources Canada, Geological Survey of Canada–Central, Ottawa, Ontario

**M.J. Unsworth**, University of Alberta, Edmonton, Alberta

**G. Williams-Jones**, Simon Fraser University, Burnaby, British Columbia

**W. Yuan**, Natural Resources Canada, Geological Survey of Canada–Calgary, Calgary, Alberta

---

Grasby, S.E., Borch, A., Calahorrano-Di Patre, A., Chen, Z., Craven, J., Liu, X., Muhammad, M., Russell, J.K., Tschirhart, V., Unsworth, M.J., Williams-Jones, G. and Yuan, W. (2023): Garibaldi Geothermal Volcanic Belt Assessment Project, southwestern British Columbia (part of NTS 092J), phase 2: 2022 field report; in Geoscience BC Summary of Activities 2022: Energy and Water, Geoscience BC, Report 2023-02, p. 47–54.

## Introduction

Renewable energy demand is increasing greatly to meet Canada’s goal of reaching net-zero emissions by 2050. This has led to renewed interest in geothermal energy as a source of both green heat and power. A particular focus has been placed on high-temperature resources of the Garibaldi volcanic belt (Figure 1), first defined by research wells drilled in the early 1980s near Mount Meager and Mount Cayley, two volcanic systems within the larger Garibaldi belt (Jessop, 2008; Grasby et al., 2011). A new research project, funded by Natural Resources Canada’s Emerging Renewable Power Program and Geoscience BC, was initiated, with the first phase focused on the Mount Meager area in the summers of 2019 and 2020 (Grasby et al., 2021). A second phase moved the focus to the Mount Cayley area, an area with limited previous exploration. This paper reports on the nature of the 2022 field program and data collected in the final year of phase 2 of the Garibaldi Geothermal Volcanic Belt Assessment Project.

---

*This publication is also available, free of charge, as colour digital files in Adobe Acrobat® PDF format from the Geoscience BC website: <http://geosciencebc.com/updates/summary-of-activities/>.*

## Garibaldi Volcanic Belt

The Garibaldi volcanic belt represents a chain of young (less than 11 000 years old) volcanoes in southwestern British Columbia (BC), in a region also known to have abundant thermal springs. Natural Resources Canada (NRCan), along with BC Hydro, conducted initial exploration drilling in the 1980s at the Mount Meager volcano that defined high-temperature geothermal resources, exceeding 250°C (Jessop, 2008; Witter, 2019). Results of this work defined a world-class thermal resource, although the permeability was insufficient to allow economic development. A lack of geoscience information regarding the regional controls on permeability posed a significant drilling risk for subsequent industry exploration in the region (Witter, 2019).

A project to reduce exploration risk was initiated in 2019 by the Geological Survey of Canada (GSC) of NRCan, in partnership with The University of British Columbia (UBC), Simon Fraser University (SFU), Douglas College (DC), University of Calgary (UofC) and University of Alberta (UofA), to develop a multidisciplinary approach to reducing exploration risk through an integrated geological and geophysical field campaign. The project incorporates a range of geoscience tools, including remote sensing, bedrock mapping,

fracture measurements, geochemistry, and magnetotelluric (MT), gravity and passive-seismic surveys. The ultimate project goal is to develop new predictive tools for finding permeable aquifers at depth. Results will also aid development of new geothermal-resource models, creating greater certainty in national geothermal-resource assessments and supporting development of effective regulatory environments.

### Mount Cayley Field Program

Field teams from UBC, SFU, UofA and the GSC participated in the 2022 field program. Fieldwork was focused on logging roads along the flanks of Mount Cayley, as well as areas around the massif accessible by helicopter. Field planning began with engagement with Squamish First Nation and co-development of a modified field plan that limited impacts in areas of special concern. The local knowledge provided through the engagement process was of significant benefit to field operations. As well, Environmental Monitors from the Squamish First Nation were engaged to ensure that helicopter work to reach higher levels of Mount Cayley did not cause any wildlife disturbance. The field program focused on

- 1) establishing an array of MT stations to image the volcanic plumbing (UofA);
- 2) establishing audio-magnetotelluric (AMT) stations to study the shallow structure that included the hydrothermal systems (GSC);
- 3) a gravity survey that will provide insight into potential magma chambers (SFU);
- 4) bedrock mapping and paleomagnetic studies to provide information on the rock types that form the geothermal reservoir, and eruption history (UBC);
- 5) ground-temperature survey, and fracture, rock-property and thermal-anomaly studies (GSC) that will provide information on permeable networks, heat conduction and heat production; and
- 6) structural geology studies (SFU) to elucidate the regional stress fields and associated fault and fracture systems.

### Work Conducted During the 2022 Field Program

#### Broadband Magnetotelluric

Previous MT studies in the Garibaldi belt have shown the presence of a low-resistivity layer in the crust in the depth range 5–10 km. These have included previous MT studies around Mount Meager and Mount Cayley in which the low-resistivity

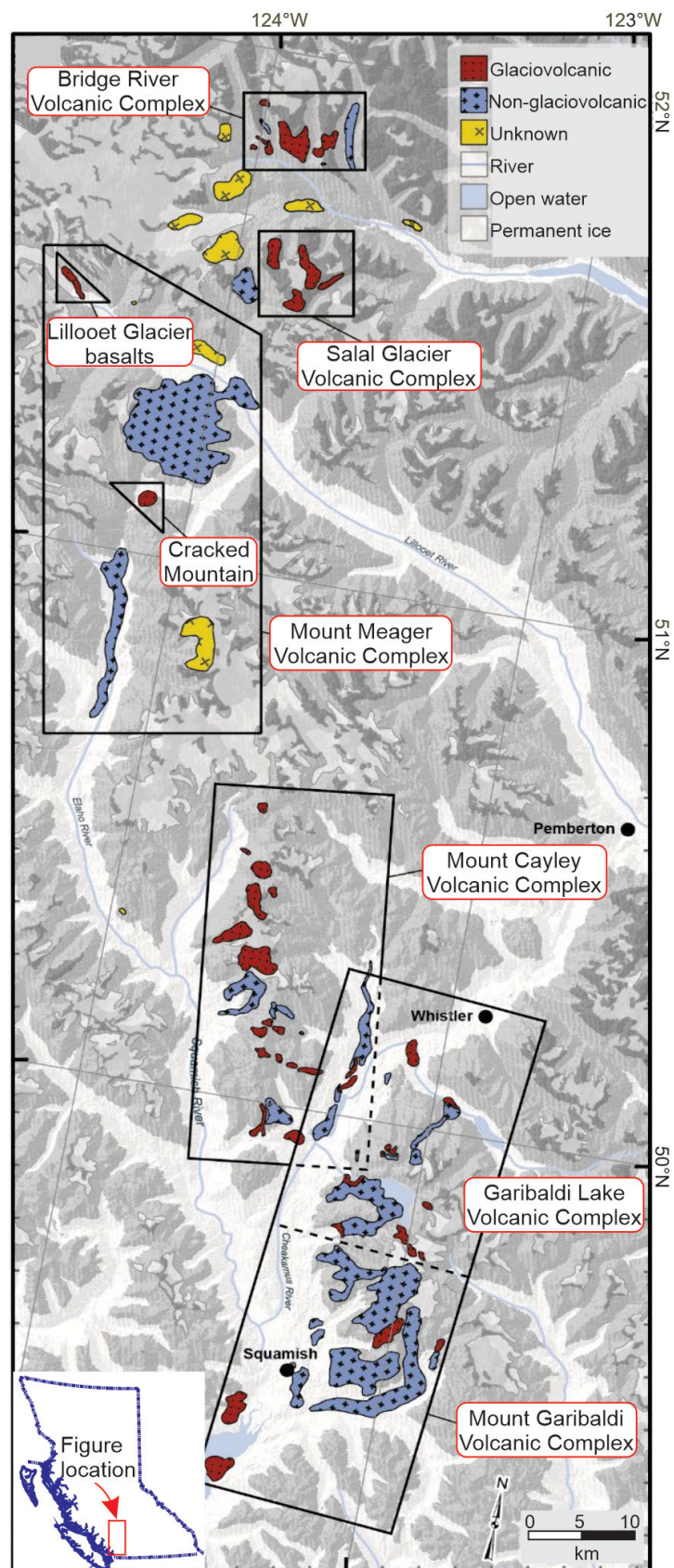


**Figure 1.** Volcanic complexes of the Garibaldi belt, showing the location of Mount Meager, the focus of phase 1, and the Mount Cayley area, the focus of phase 2 (after Wilson and Russell, 2018).

layer was interpreted as being due to a region of aqueous fluids or partial melt. Understanding the spatial extent and composition of this layer is important in both geothermal research and investigations of volcano hazards.

Magnetotelluric data collection by this project since 2019 has greatly improved knowledge of this low resistivity layer. The station distribution after the 2021 field season is shown in Figure 2a. In the winter of 2022, the UofA undertook 3-D inversions of the MT data that were used to produce 3-D resistivity models of the crust within the Garibaldi belt. This type of subsurface imaging is analogous to procedures used in medical imaging to look inside the human body. These 3-D resistivity models gave new insights into the geometry of the low-resistivity layer beneath Mount Cayley and Mount Meager. However, the 3-D inversions also showed that the nonuniform MT station coverage limits the ability to effectively map the low-resistivity layer and, by implication, the distribution of geothermal fluids. The MT data collection in 2022 (Figure 2b) was planned to address the following shortcomings in the existing MT dataset (Figure 2a):

- 1) Existing coverage is limited around Mount Cayley. Additional MT stations are needed to better understand the spatial distribution of subsurface aqueous fluids and partial melt beneath surface geothermal manifestations.
- 2) Existing coverage is sparse in areas between the major volcanic centres in the Garibaldi belt. Additional MT stations are needed to understand if partial melt is localized beneath the most recently active volcanic centres or more uniformly distributed along the entire Garibaldi belt.

In the summer of 2022, the UofA continued the regional magnetotelluric (MT) exploration to address these points. This research used Phoenix MTU-5C instruments, owned by the university, to collect broadband MT data that could image electrical resistivity from the surface to a depth of 20–30 km. Measurements of electrical resistivity are sensitive to the presence of aqueous fluids and partial melt, and provide important information about the supply of fluids and heat to shallow geothermal reservoirs.

In 2022, broadband MT data were collected at 15 locations in the Mount Cayley area, with each recording lasting 1–2 days.

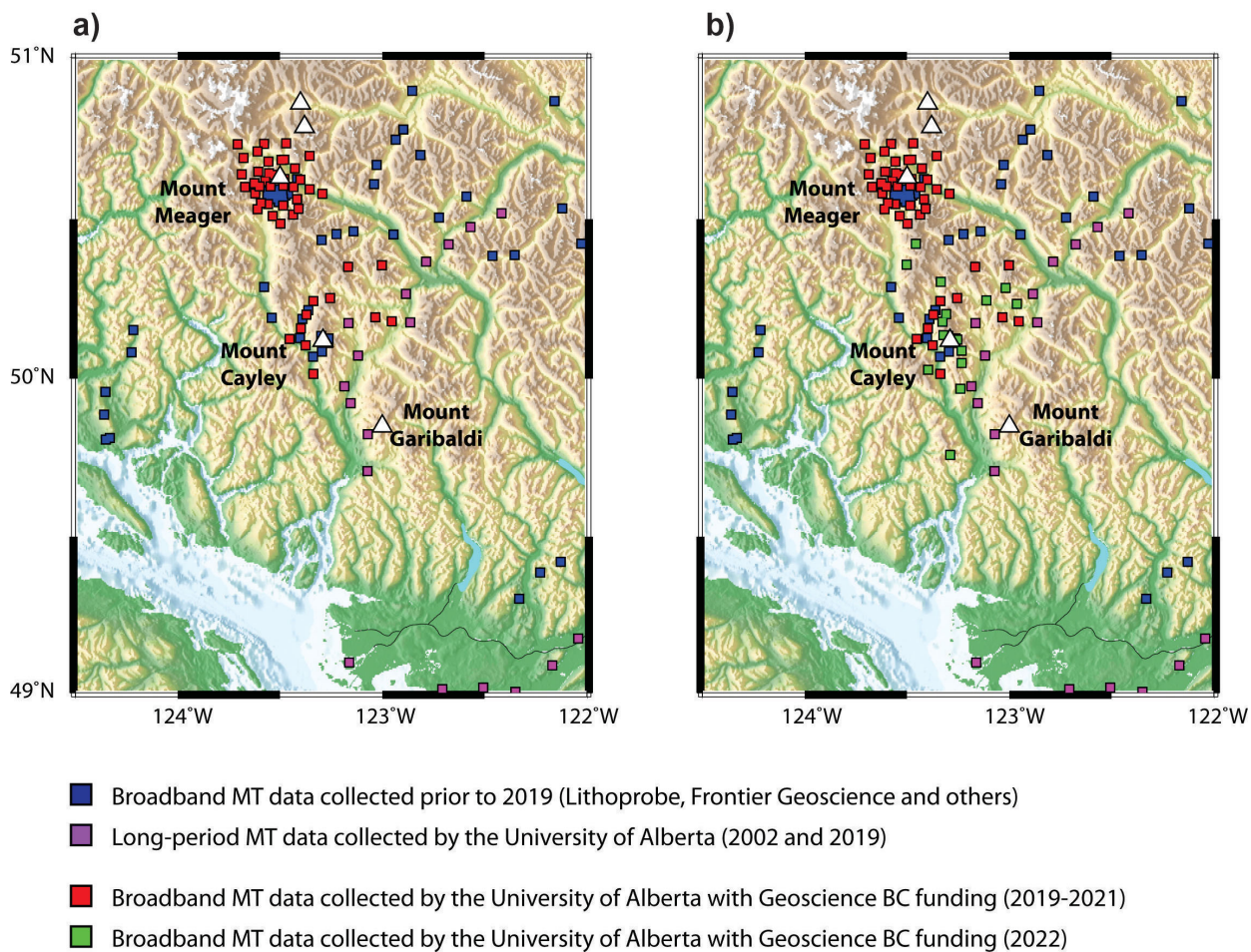


**Figure 2.** Distribution of magnetotelluric stations in the Garibaldi belt, showing a) MT data coverage after the 2021 field season, and b) the grid with the addition of the new MT data collected in the 2022 field season.

The MT data collection began on Saturday, August 20 and concluded on Monday, August 29. Strong geomagnetic signals and careful installation of sensors resulted in high-quality MT data. The station locations are listed in Table 1. The time-series data were recorded with sample rates of 150 Hz and 24 000 Hz, and the total volume of data from the 15 stations was 60.7 GB.

The new MT data are currently being processed to obtain the best possible estimates of impedances and vertical–magnetic-field transfer functions. The processed MT data will be used to update the 3-D inversions later in 2022.

### Audio-Magnetotelluric

Magnetotelluric (MT) is a passive geophysical technique that measures Earth’s electric and magnetic fields, from which one can calculate a subsurface resistivity model. Resistivity is sensitive to lithology, porosity and permeability of the rock; composition and temperature of associated fluids; and host-rock metallic content (including sulphides and graphite). As a result, MT data are useful in geothermal studies because they can generate images of the relationships between fluid pathways and hydrothermal alteration. Previous regional broadband MT surveys (Jones and Dumas, 1993) identified potential alteration zones below Mount Cayley; however, the nature and geometry of the systems was poorly resolved due to the limited aperture, bandwidth and inversion resources at the time (e.g., only 2-D modelling was available). As well, the region is incredibly difficult to access, with limited helicopter-landing sites and steep topography making acquisition of ground geophysical datasets tenuous and costly. Imaging parts of the geothermal system that are in the upper 1–2 km only requires high-frequency MT measurements in the band 10 000–1 Hz, referred to as audio-magnetotelluric (AMT) measurements, or airborne techniques that can also image the near-surface resistivity. Rather than doing extensive ground geophysical surveys, this study will acquire airborne passive electromagnetic (EM) data augmented with ground AMT data to provide the extensive coverage and systematic sampling for this inaccessible terrain.

Data from 10 AMT stations were collected at Mount Cayley during August 2022 and a request for procurement of a passive EM survey is currently in development. This study will integrate the two geophysical methods (AMT and passive EM) to test the ability of joint AMT-EM inversions to image and detect geothermal-system parameters at shallow depths (hundreds of metres), and ultimately test whether the fluid conduits imaged in the models can be related to the locations of known warm and hot springs. If the technique is indeed sensitive to hostrock lithology, alteration and porosity, there is also potential to infer rock shear

**Table 1.** Location of broadband MT stations in the Mount Cayley area in August 2022.

Station name	Data folder name	Latitude (°)	Longitude (°)	Access
CAY200	10352_2022-08-20-202459	50.246	-123.112	Road
CAY201	10379_2022-08-21-000133	50.235	-122.963	Road
CAY202	10351_2022-08-21-194753	50.285	-123.018	Road
CAY203	10379_2022-08-22-201854	50.423	-123.457	Helicopter
CAY204	10351_2022-08-23-181219	50.088	-123.233	Helicopter
CAY205	10430_2022-08-23-205628	50.203	-123.309	Helicopter
CAY206	10351_2022-08-24-180540	50.304	-123.335	Helicopter
CAY207	10379_2022-08-24-212027	50.358	-123.502	Helicopter
CAY208	10430_2022-08-25-184417	50.137	-123.322	Helicopter
CAY209	10351_2022-08-25-222546	50.123	-123.254	Helicopter
CAY210	10430_2022-08-26-172126	50.028	-123.397	Helicopter
CAY211	10379_2022-08-26-212410	50.049	-123.233	Helicopter
CAY212	10430_2022-08-27-231634	49.968	-123.239	Helicopter
CAY213	10379_2022-08-28-181550	49.759	-123.289	Helicopter
CAY214	10351_2022-08-28-210413	50.179	-123.327	Helicopter

strength and detect zones of weakness that are more susceptible to mechanical failure, which would contribute to reducing the risk of landslides when developing geothermal resources. Analysis of the new resistivity 3-D models from Mount Cayley will be supported by other geological and geophysical datasets collected in the 2022 field campaign and during previous exploration.

### Gravity Survey

During the summer 2022 field season, the Simon Fraser University (SFU) team continued with the gravity exploration of the Mount Cayley Volcanic Complex. In the 2021 field season, 75 gravity sites had been surveyed around Mount Cayley and surrounding peaks (e.g., Mount Callaghan, Mount Brew, Brandywine Mountain) through several days of surveys conducted by helicopter, truck and foot. In a similar way, three gravity surveys were conducted during the summer of 2022 around the Mount Cayley Volcanic Complex to increase the density of gravity measurement sites on the already-established grid. Two of these surveys were conducted with an SFU truck (July 4–8 and August 15–17, 2022) and one employed a helicopter (September 2–3, 2022).

The main focus of these three surveys was to a) infill the gravity grid on the western flank of the Mount Cayley Volcanic Complex, particularly alongside the Squamish River Forest Service Road (SRFSR) and perpendicular logging roads; b) partially cover the area inside the Callaghan Conservancy, east of Mount Callaghan; and c) resolve any other lingering voids between measured sites (e.g., on the east flank of Mount Brew). Infilling the western flank of Mount Cayley had proven difficult in the past because the SRFSR tends to flood when the river level increases above 4 m, so surveys need to be carefully planned and, even then, an ex-

cursion might not be possible. The Callaghan Conservancy area posed other accessibility challenges, as the team had no permission to land a helicopter in this area of very few roads. Therefore, all the measurements in this large area would have to be done on foot, making it difficult to cover.

Despite these challenges, all three surveys were successfully completed during the summer field season, with 67 additional gravity sites being measured using two LaCoste & Romberg relative gravity meters around the Mount Cayley Volcanic Complex. All measurements were related to a survey reference station in Squamish (SFU 1), which was measured at the beginning and end of the survey loop, and secondary reference sites for instrumental drift control were chosen based on the locations of sites measured that day. Since SFU 1 had been previously tied to the absolute gravity grid established by the GSC, the absolute values for all survey points around Mt Cayley can be calculated based on the relative gravity measurements. The position of each gravity site was measured using a Juniper Geode GNSS receiver. The total number of gravity sites for the Mount Cayley Volcanic Complex grid is now 142 (Figure 3); data from these sites will be used to produce a Bouguer anomaly map of the volcanic complex.

### Bedrock Mapping and Paleomagnetic Sampling

The UBC team conducted work in three distinct areas (Figure 4) to constrain the recent eruption history of the area: the Elaho basalts and Free Will peak in the Mount Meager volcanic field, and the Ember Ridge domes in the Mount Cayley volcanic field.

### Elaho Basalt Mapping and Paleomagnetic Sampling

The team from UBC completed two days of vehicle-supported mapping and paleomagnetic sampling of the southern portion of the Elaho basalts, and two days of helicopter-supported mapping and sampling in the northern portion of the Elaho and Meager valleys. They collected seven paleomagnetic samples from minimum and maximum stratigraphic locations at the Elaho waterfall (local name) and at the Clendinning Creek–Elaho River confluence. Corresponding hand samples were collected for geochemistry and Ar/Ar dating. Analysis of these samples will determine the duration of this eruption; coupled with new and previous Ar/Ar dates, these analyses will clarify the timing of the Elaho eruption in relation to the Mount Meager volcanic field. Elucidation of the most recent eruptions will assist in understanding the activity of potential magma chambers in the subsurface. New mapping has increased the aerial extent of volcanics ~4 km east of the Elaho waterfall. Paleovalley reconstruction, coupled with thickness measurements, will provide an approx-

imate erupted volume. Geochemical analysis will clarify stratigraphic units and possibly provide information on magma-chamber depth and dynamics.

### Free Will Mapping and Paleomagnetic Sampling

The UBC team also completed three days of mapping and paleomagnetic sampling on Free Will peak, as well as helicopter-supported photogrammetry. Initial results indicate that Free Will peak is a pre- to syn-Fraser-age subglacial eruption of interbedded lapilli to ash tuff, and hyaloclastite and autobrecciated pillow basalt. Superficially, the Free Will volcanic edifice resembles the nearby Crack Mountain volcanic edifice. It is highly glaciated and has crystalline glacial erratics both atop the volcanic edifice and included as accidental clasts within the ash and lapilli tuff, indicating that the eruption may have preserved evidence of the ice-melting process during the initial stages of the subglacial eruption. Analysis of high-resolution photogrammetry of the steep, inaccessible edifice slopes will provide insight into volcanoclastic and crosscutting dike structures, as well as total erupted volume. Argon/argon radiometric, geochemical and paleomagnetic analysis will clarify the timing and duration of the eruption.

### Mount Cayley Volcanic Field Paleomagnetic Sampling

The UBC team further completed two days of paleomagnetic sampling of the glaciovolcanic edifices of the Mount Cayley volcanic field. Some locations were resampled to improve the accuracy of 2021 paleomagnetic datasets. New

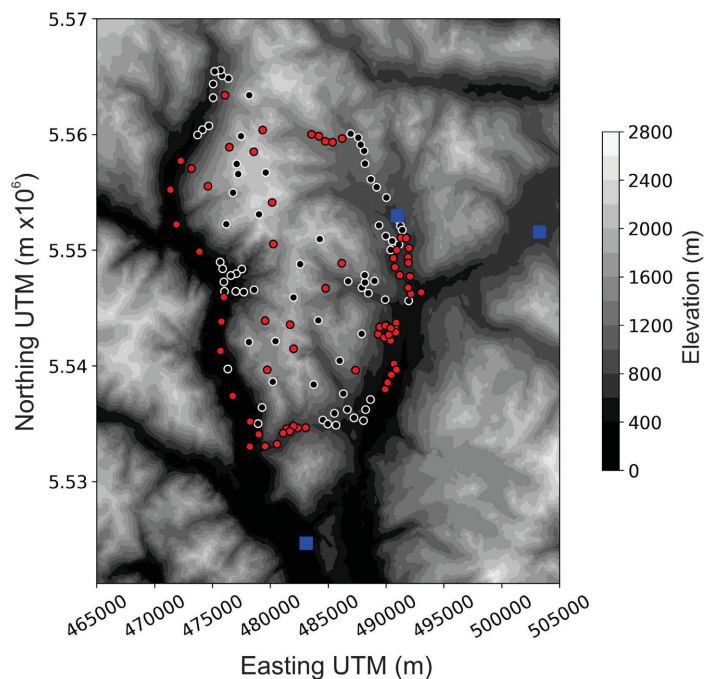


**Figure 3.** Shaded-relief map of the Mount Cayley area, showing locations of gravity survey stations. Red dots are new stations measured in 2022, black dots are stations collected in 2021, and blue squares are base stations.

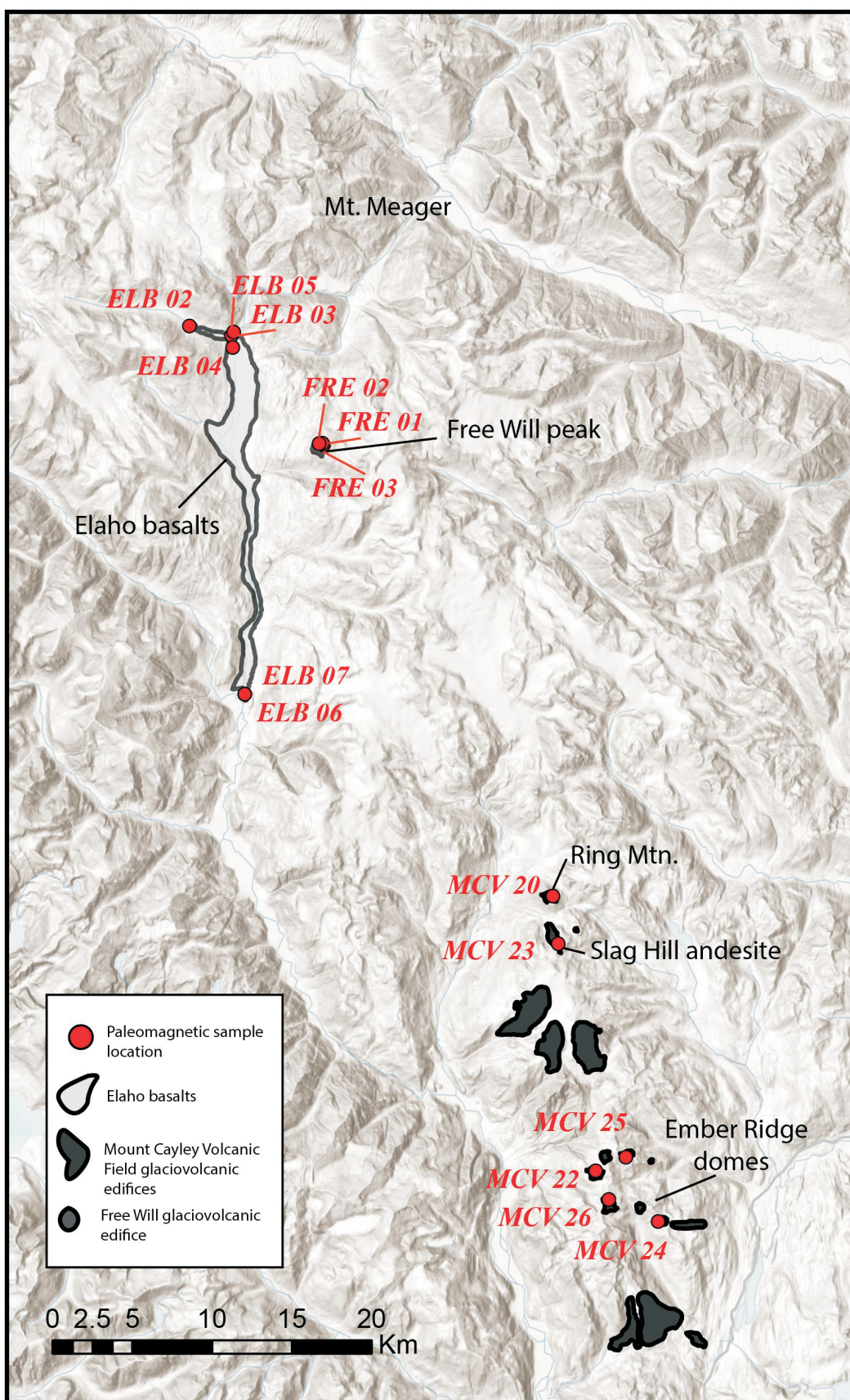


**Figure 4.** Location of 2022 paleomagnetic-sampling programs targeting the Elaho basalts and Free Will volcano in the Mount Meager volcanic field and the Ember Ridge domes in the Mount Cayley volcanic field.

locations, including multiple individual Ember Ridge glaciovolcanic edifices, were also sampled. Coupled with Ar/Ar data, this suite of paleomagnetic samples will form a local paleosecular variation curve for the Mount Cayley, Mount Garibaldi and Mount Meager volcanic fields.

### Temperature Survey

Twenty-six temperature loggers were used in 13 sites at Mount Cayley by the GSC to record variations in ground-surface temperature. Ground temperatures were measured using miniature temperature-data loggers (HOBO® Water Temp Pro v2). The temperature-data logger has a resolution of 0.2°C and temperature range of -40 to 70°C in air and up to 50°C in water. At each site, two HOBO temperature loggers were buried in soil and set to record the environmental temperature every 30 minutes. One was deployed on the surface to account for the solar radiance and the other was buried at a depth of 30–50 cm, depending on the ground condition. Figure 5 shows the temperature recorded for the last winter and spring seasons at the Mount Cayley ground-temperature monitoring sites. At each site, thermal and the associated visual photos were taken to evaluate the environmental factors, such as shadiness and vegetation covering.

A total of 155 thermal images were taken at the key field sites. These include 48 images from 13 logger sites in the

Squamish Valley, 15 images from the Shovelnose warm spring, 12 images and 1 video from the Pebble Creek hot spring and 3 images from the No Good warm spring. Comparative analysis of these data is ongoing.

### Fracture Measurements

Fracture measurements were taken at seven outcrop stations on the ridges around Mount Cayley. In total, 87 fractures were measured for strike, dip direction and dip angle (Figure 6). These data will be analyzed further for study of the stress regime and drilling design.

### Structural Geology

Previous exploration of the Mount Meager area defined faulting as being related to 1) tectonic stress during the onset of mountain building (e.g., Owl Creek fault), 2) volcanism, and 3) mass creep and gravitational failure (Fairbank et al., 1980, 1981). In the summer of 2022, a new type of tectonic-stress-related fault was identified that is synchronous with and/or postdates the latest volcanic activity at Mount Meager. This work is ongoing and will include analyzing paleomagnetic samples and conducting radiometric dating. This work helps to date the latest tectonic fault activity and potentially define the trigger mechanism for the latest volcanic eruption 2400 years ago on Mount Meager.

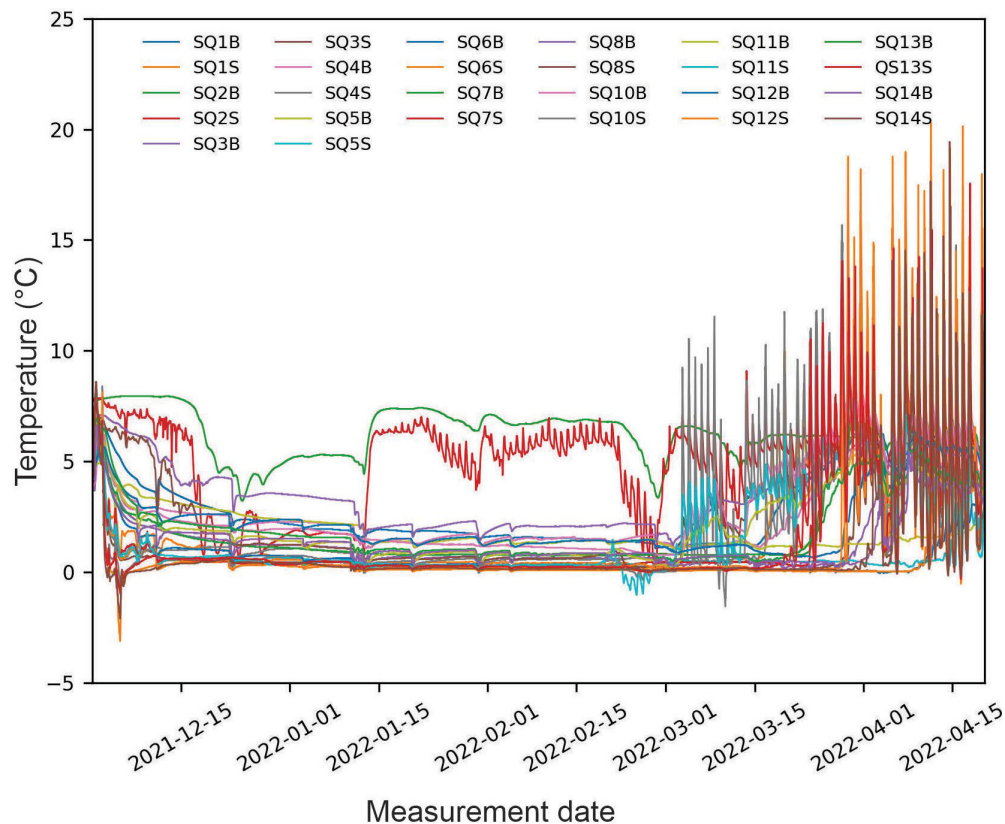


Figure 5. Temperatures recorded at 13 ground-temperature monitoring sites at Mount Cayley.



**Figure 6.** Collection of fracture measurements from outcrops along the ridges of Mount Cayley.

In addition, it will help improve understanding of the tectonic history of the Mount Cayley area.

### Summary

Summer 2022 was a successful field season, with large volumes of new data collected as part of geophysical and geological surveys in the Mount Cayley area. Data collected are currently being processed and interpreted. All raw data will be released in 2023 and interpreted results will be presented in a series of reports, peer-reviewed scientific papers and presentations by various members of the project. The Garibaldi Geothermal Volcanic Belt Assessment Project will also wrap up in 2023.

### Acknowledgments

The authors gratefully acknowledge the funding from Natural Resources Canada and Geoscience BC that supported the 2022 fieldwork. The University of Alberta (UofA) recognizes funding for all travels costs that was provided by Future Energy Systems—a UofA research program funded by the Natural Sciences and Engineering Research Council of Canada (NSERC) through the Canada First Research Excellence Fund (CFREF). Squamish Nation is thanked for allowing this research to proceed on their traditional territory. Environmental monitors L. Rivers and K. Thompson provided excellent field support. The authors also thank

K. Beausoleil, B. Chase and E. Slobodian for their assistance in the field in 2022. The excellent pilots at No Limits Helicopters made this work possible. M. Hedhli provided a helpful review.

### References

- Fairbank, B., Reader, J. and Sadlier-Brown, T. (1980): NSBG Ltd 1980 Mar – 1979 drilling and exploration program, Meager Creek geothermal area, Upper Lillooet River, BC; private report for BC Hydro.
- Fairbank, B., Reader, J., Openshaw, R.E. and Sadlier-Brown, T. (1981): 1981 Jun. 1980 drilling and exploration program – Meager Creek geothermal area, Upper Lillooet River, BC; private report for BC Hydro.
- Grasby, S.E., Allen, D.M., Bell, S., Chen, Z., Ferguson, G., Jessop, A., Kelman, M., Ko, M., Majorowicz, J., Moore, M., Raymond, J. and Therrien, R. (2011): Geothermal energy resource potential of Canada; Geological Survey of Canada, Open File 6914, 322 p., URL <<https://doi.org/10.4095/288745>>.
- Grasby, S.E., Ansari, S.M., Barendregt, R.W., Borch, A., Calahorrano-DiPatre, A., Chen, Z., Craven, J.A., Dettmer, J., Gilbert, H., Haneson, C., Harris, M., Hormozzade, F., Leiter, S., Liu, J., Muhammad, M., Quane, S.L., Russell, J.K., Salvage, R.O., Savard, G., Tschirhart, V. et al. (2021): Garibaldi Geothermal Energy Project – Phase 1 – Final Report. Geoscience BC Report 2021-08, 276 p., URL <[http://www.geosciencebc.com/i/project\\_data/GBCReport2021-08/GBCR%202021-08%20Garibaldi%20Geothermal%20Energy%20Project%20-%20Phase%201.pdf](http://www.geosciencebc.com/i/project_data/GBCReport2021-08/GBCR%202021-08%20Garibaldi%20Geothermal%20Energy%20Project%20-%20Phase%201.pdf)> [October 2022].
- Jessop, A. (2008): Review of National Geothermal Energy Program, Phase 2 – geothermal potential of the Cordillera; Geological Survey of Canada, Open File 5906, 86 p., URL <<https://doi.org/10.4095/225917>>.
- Jones, A.G. and Dumas, I. (1993) Electromagnetic images of a volcanic zone; *Physics of the Earth and Planetary Interiors*, v. 81, no. 1–4, p. 289–314.
- Wilson, A.M. and Russell, J.K. (2018): Quaternary glacio-volcanism in the Canadian Cascade volcanic arc – paleoenvironmental implications; *in* Field Volcanology: A Tribute to the Distinguished Career of Don Swanson, M. Poland, M. Garcia, V. Camp and A. Grunder (ed.), Geological Society of America, Special Papers, v. 538, URL <[https://doi.org/10.1130/2018.2538\(06\)](https://doi.org/10.1130/2018.2538(06))>.
- Witter, J. (2019): South Meager geothermal project – new perspectives from recently unearthed data; Geoscience BC, Report 2019-07, 5 p., URL <<http://www.geosciencebc.com/i/pdf/Report-2019-07-Innovate-Geothermal.pdf>> [October 2022].

# Investigation of Geothermal Systems in the Mount Meager Volcanic Complex, Southwestern British Columbia (Part of NTS 092J), Using 3-D Inversion of Audio-Magnetotelluric Data

F. Hormozzade Ghalati<sup>1</sup>, Department of Earth Sciences, Carleton University, Ottawa, Ontario, fatemehormozzadeghal@cmail.carleton.ca

J.A. Craven, Natural Resources Canada, Geological Survey of Canada–Central, Ottawa, Ontario

D. Motazedian, Department of Earth Sciences, Carleton University, Ottawa, Ontario

S.E. Grasby, Natural Resources Canada, Geological Survey of Canada–Calgary, Calgary, Alberta

---

Hormozzade Ghalati, F., Craven, J.A., Motazedian, D. and Grasby, S.E. (2023): Investigation of geothermal systems in the Mount Meager Volcanic Complex, southwestern British Columbia (part of NTS 092J), using 3-D inversion of audio-magnetotelluric data; *in* Geoscience BC Summary of Activities 2022: Energy and Water, Geoscience BC, Report 2023-02, p. 55–62.

## Introduction

Geothermal energy can provide reliable electricity and heat generation sources. Geothermal systems are geological settings defined by temperature, and geological and hydrological characteristics. In addition to heat and fluid source characteristics, reservoir properties such as porosity and permeability play an important role in determining whether a reservoir can be economically exploited for geothermal energy (Williams et al., 2011; Moeck, 2014).

Different geological, geochemical and geophysical techniques have been used to evaluate geothermal systems around the world. Geophysical exploration methods are required to image the fluid and temperature regimes of a geothermal system, as they provide a means of resolving reservoir physical parameters such as porosity and permeability (van Leeuwen et al., 2016). The fluid flow pathways in these reservoirs are often controlled by permeable and porous material created by geological features such as fractures, joints and faults. The objectives of these geophysical surveys are to define the boundary of a geothermal reservoir and its physical properties in order to evaluate its commercial viability (Didana et al., 2017; Thiel, 2017).

The magnetotelluric (MT) method is an electromagnetic exploration technique that measures the magnetic and electric fields on the Earth's surface (Chave and Jones, 2012). Natural electromagnetic waves span a broad frequency range of 0.001 to 40 000 Hz. The audio-magnetotelluric (AMT) method measures the natural electromagnetic fields at the higher frequencies (1 to 40 000 Hz), which permits mapping of shallow subsurface structures.

This project investigates the geothermal systems in the Mount Meager Volcanic Complex (MMVC) of southwestern British Columbia (BC) using 3-D inversion of AMT data. This project was initiated in 2019 in support of the geothermal research at the MMVC as part of the Garibaldi Geothermal Volcanic Belt Assessment Project (Grasby et al., 2020, 2021, 2023). This paper reviews the background of the AMT research and summarizes the results and the progress of ongoing research.

## Study Area and Geological Setting

The MMVC, with elevations rising to >2600 m, is an active volcanic complex within the Garibaldi volcanic belt, situated approximately 150 km north of Vancouver, BC (Figure 1; Ghomshei and Clark, 1993; Jessop, 2008). The Garibaldi volcanic belt is a glaciovolcanic arc of young (<11 000 years old) volcanoes (e.g., Mount Garibaldi, Mount Cayley, Mount Meager [Wilson and Russell, 2018; Venugopal et al., 2020]), extending from the northern part of the State of Washington through southwestern BC (Figure 1; Jessop, 2008).

The geological units underlying the MMVC (including Mount Meager, Plinth Peak and Pylon Peak) are Mesozoic, fractured, crystalline and metamorphic rocks (Read, 1977). The volcanic rocks in the MMVC include basalt, andesite and rhyodacite flows, rhyodacite domes and pyroclastics (Read, 1977). The hydraulic conductivity of these basement rocks and volcanic rocks is mainly controlled by fracture porosity (Jamieson, 1981). In the MMVC, springs and vents trend northward and occur where rocks are fractured and dissected by faults (Bernard, 2020). Among these springs are the Meager Creek (30–59°C) and Placid (45°C) hot springs, and No Good warm spring (30–40°C), all of which lie along Meager Creek (Ghomshei and Clark, 1993; Proenza, 2012; Huang, 2019). Significant faults include the Meager Creek, No Good and Camp faults (Figure 2).

---

<sup>1</sup>The lead author is a 2022 Geoscience BC Scholarship recipient.

This publication is also available, free of charge, as colour digital files in Adobe Acrobat® PDF format from the Geoscience BC website: <http://geosciencebc.com/updates/summary-of-activities/>.

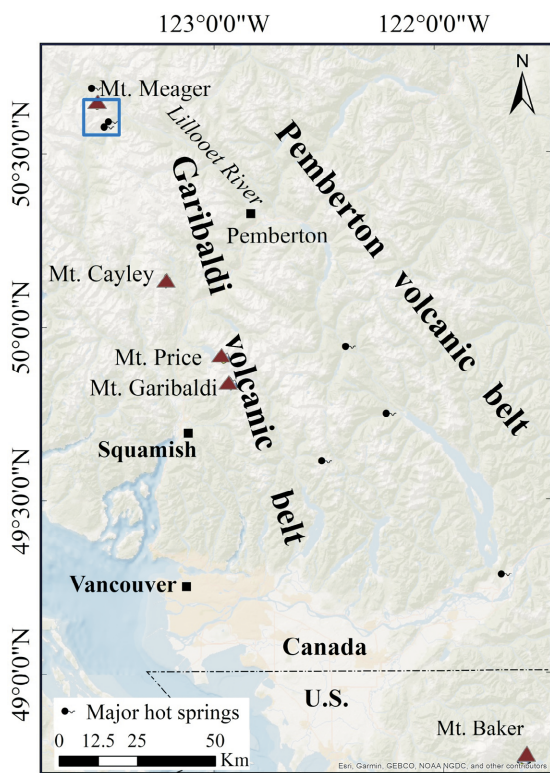


**Figure 1.** Location of the Garibaldi volcanic belt, southwestern British Columbia. Study area outlined in blue in northwestern corner (after Lewis et al., 1978; Hormozzade Ghalati et al., 2022).

## Project Background

Research and exploration of geothermal resources at the MMVC, which has one of the highest geothermal potentials in Canada, have been conducted since the 1970s (Grasby et al., 2012). Previous MT surveys of the area used few stations and (now) outdated techniques (Jones and Dumas, 1993; Candy, 2001). By employing new techniques and equipment, a comprehensive AMT dataset (from 84 stations) was collected in 2019, and for the first time focused on the surface-to-reservoir depths to address the gaps of earlier studies (Figure 2; Craven et al., 2020; Hormozzade Ghalati et al., 2021a, b).

## Data and Methodology

The MT method is a passive electromagnetic method that uses the Earth’s natural electric ( $E$ ) and magnetic ( $H$ ) fields to identify subsurface electrical resistivity structures (Simpson and Bahr, 2005; Chave and Jones, 2012). In the MT method, an impedance tensor ( $Z$ ) relates the  $E$  and  $H$  components in  $x$  and  $y$  directions (geographic coordinates), defining north and east, respectively, as

$$\begin{bmatrix} E_x \\ E_y \end{bmatrix} = \begin{bmatrix} Z_{xx} & Z_{xy} \\ Z_{yx} & Z_{yy} \end{bmatrix} \begin{bmatrix} H_x \\ H_y \end{bmatrix} \quad (1)$$

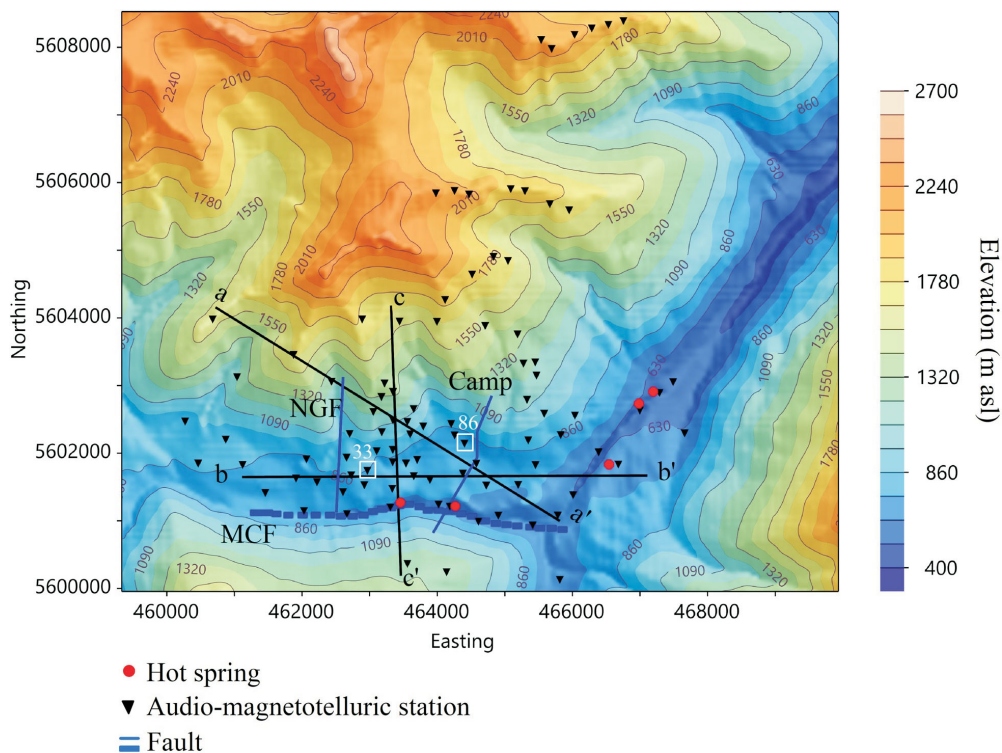


**Figure 2.** Overview of the study area, Mount Meager Volcanic Complex. Locations of stations in Figure 3 and cross-sections in Figure 5 are shown. All co-ordinates are in UTM Zone 10N, NAD 83. Abbreviations: Camp, Camp fault; MCF, Meager Creek fault; NGF, No Good fault.

Using inversion techniques, apparent resistivity ( $\rho_a$ ) and the phase ( $\Phi$ ) are calculated (in  $i$  and  $j$  directions) from the impedance tensor's components, in imaginary (Im) and real (Re) parts, as functions of frequency (Equations 2, 3), depending on the angular frequency ( $\omega$ ) and the magnetic permeability of free space ( $\mu_0$ ; Simpson and Bahr, 2005).

$$\rho_{a,ij}(\omega) = \frac{1}{\omega\mu_0} [Z_{ij}(\omega)]^2 \quad (2)$$

$$\Phi_{ij}(\omega) = \tan^{-1} \left( \frac{\text{Im}(Z_{ij}(\omega))}{\text{Re}(Z_{ij}(\omega))} \right) \quad (3)$$

Producing an electrical resistivity model from inversion of MT data provides a tool for estimating the physical properties of rocks. The electrical resistivity of rocks is influenced by factors such as lithology, porosity, temperature and salinity of the fluid filling the pores (Chave and Jones, 2012). Also, fault and fracture zones that contribute to fluid circulation may exhibit electrical resistivity differences (Muñoz, 2014). Rocks have different mineral contents with variable pore shapes and interconnectivity, all of which can influence the electrical resistivity ( $\rho=1/\sigma$  where  $\sigma$  is electrical conductivity), defined by Archie's law (Archie, 1942):

$$\sigma_f = \sigma_b \phi^{-m}, \quad (4)$$

where  $\phi$  is porosity,  $m$  is the cementation factor,  $\sigma_b$  is the bulk electrical conductivity and  $\sigma_f$  is the fluid electrical conductivity (Siemens/metre [S/m]). A modified Archie's law defines the relationship between electrical conductivity and porosity considering two-phased electrical conductivity ( $\sigma_s$  is the solid phase conductivity of the material [S/m]; Glover et al., 2000):

$$\sigma_b = \sigma_f \phi^m + \sigma_s (1-\phi)^p \quad (5)$$

$$p = \frac{\log(1-\phi^m)}{\log(1-\phi)}$$

## Results

This paper presents an overview of the project's preliminary results and the ongoing research direction. Detailed results of the 3-D inversion of the AMT data can be found in Hormozzade Ghalati et al. (2022).

The preferred electrical resistivity model is based on CCG's RLM3D MT inversion code, used to invert the impedance tensors (Soyer et al., 2020). The model was discretized into 153 by 116 by 89 cells in three dimensions, northwest-southeast, northeast-southwest and depth, respectively. The central core of the model mesh was divided into 75 by 75 m cells for lateral discretization. Padding was added around the core area for boundary condition calculations. The dimensions of these paddings were calculated

using a multiplicative factor of 1.5 in all lateral directions. Layers in the MT model were discretized into 40 m thicknesses at elevations of 475–2350 m above sea level (asl), to give high accuracy responses for the data on the mountainsides. Subsequent layers were increased by a factor of 1.12 to a depth of 3500 m below sea level (bsl), and a factor of 1.25 to the bottom of the model. The overall root mean square (RMS) of the inversion was 1.30 after 75 iterations. The apparent resistivity and phase responses of the 3-D inversion model fit well to the observed data. Comparison between the observed data and the calculated responses for two stations (33 and 86) were plotted to assess the data misfit at the final iteration (Figure 3a, b).

The resistivity model normally identifies values above 200 ohm·m ( $\Omega\cdot\text{m}$ ) that are immediately under the surface, which can be interpreted as a region (R) where hot geothermal fluids do not alter the rocks and the temperature is less than 70°C. The section beneath this layer is a conductive zone. At MMVC, two conductive zones (C1, C2) were correlated with the location of faults, distribution of alteration minerals, as reported in borehole geological logs, and measured temperatures (Figures 4, 5a–c). Conductive zone C1 reaches the surface where hot and warm springs seep into Meager Creek and is well correlated with the location of springs (Figure 5b, c). In boreholes, these shallower zones (C1, C2) can be correlated to argillic alteration minerals, characterized by the presence of smectite, illite and rare kaolinite, and measured temperatures of 70–160°C (Proenza, 2012, and references contained therein). The C1 and C2 conductive zones observed in the model are interpreted to map the low permeability clay-rich layers that act as caprocks and enable the accumulation of deeper hot fluids. The caprock is located on top of a zone with higher resistivity values (15–150  $\Omega\cdot\text{m}$ ), corresponding to borehole temperatures of 160–270°C (Figure 5a; Proenza, 2012, and references contained therein).

The results show the potential of using 3-D inversion of AMT data to map the fluid pathways at MMVC. These pathways are moderately conductive zones that show high porosity using Archie's law and modified Archie's law (Equations 4, 5). Moreover, these pathways correlate with lost-circulation zones in borehole logs (Proenza, 2012, and references contained therein).

## Summary and Future Work

This project provides a detailed near-surface electrical resistivity model of the Mount Meager Volcanic Complex (MMVC) study area, using data from a dense grid of audiomagnetotelluric (AMT) stations, and a modern algorithm, which allowed 3-D mapping of the reservoir zones that accounted for the steep mountain topography. The resistivity model demonstrates the pattern of caprock and fluid flow zones in the area. Geological log and temperature data were

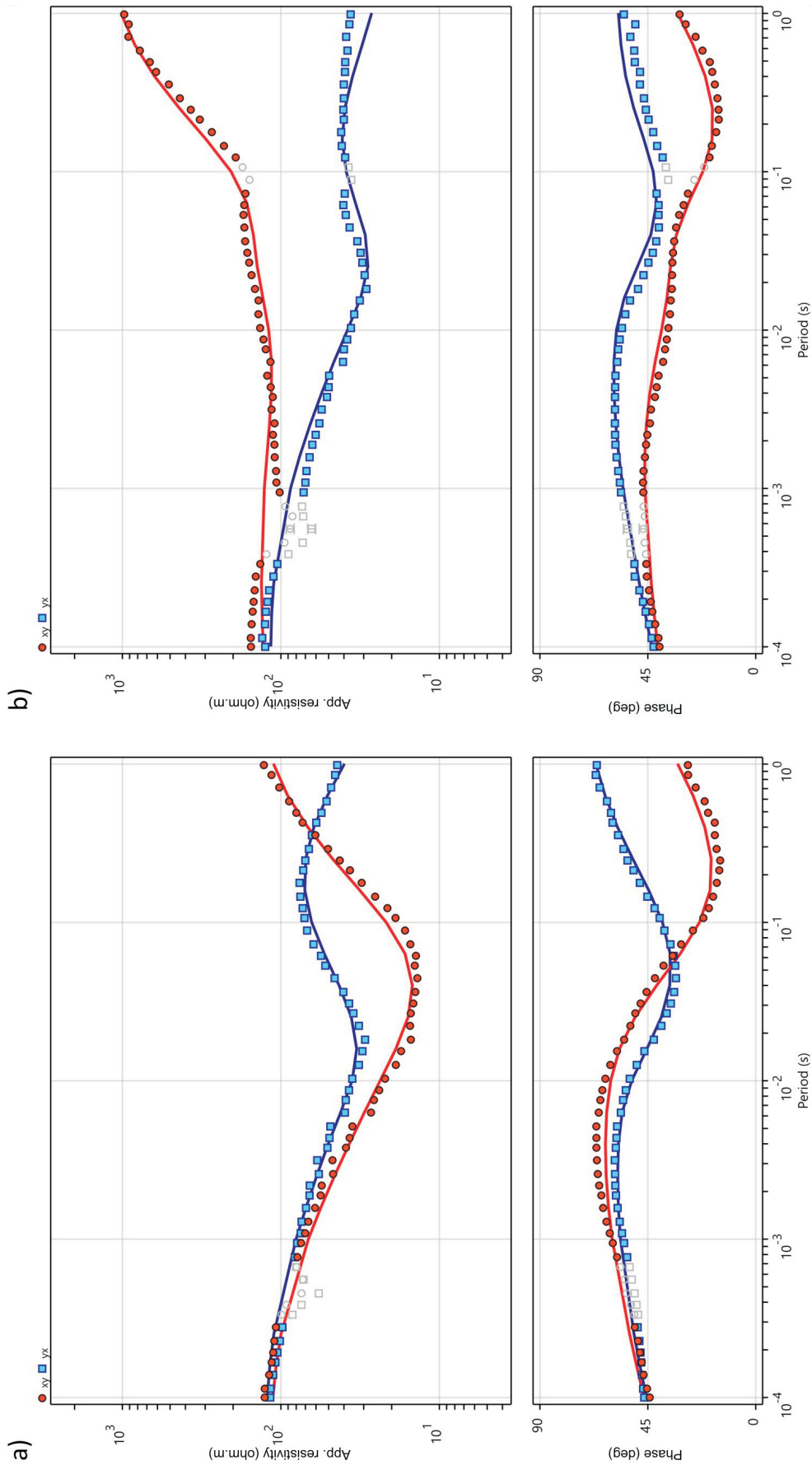


**Figure 3.** Fit of the observed and estimated apparent (App.) resistivity and phase of the preferred 3-D inversion model for **a)** station 33 and **b)** station 86, Mount Meager Volcanic Complex study area (see Figure 2 for station locations). The observed values of xy and yx components are represented by red circles and blue squares and the estimated xy and yx components are shown by red and blue lines, respectively. Masked data are shown in grey. Abbreviation: deg, degrees.

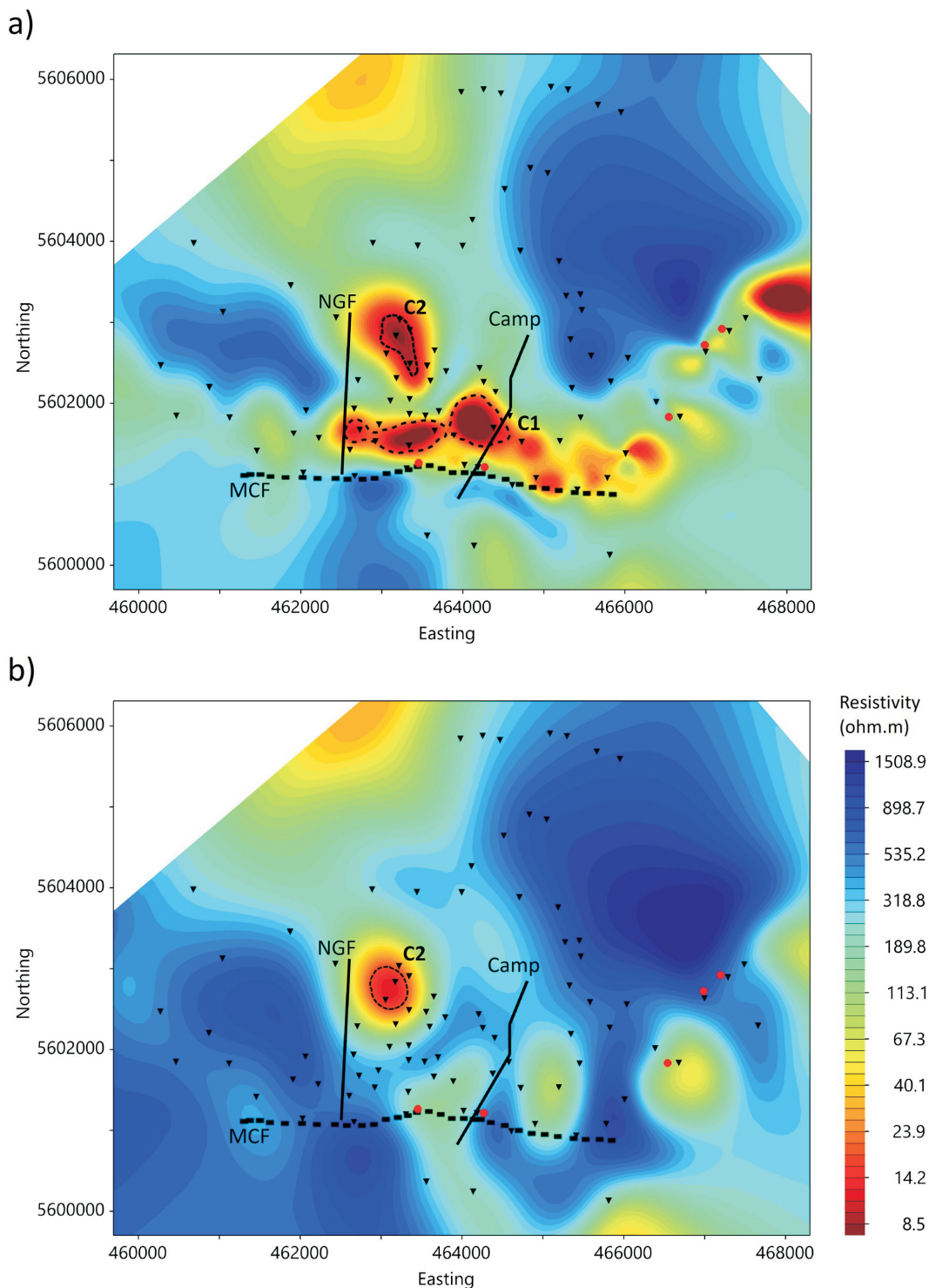
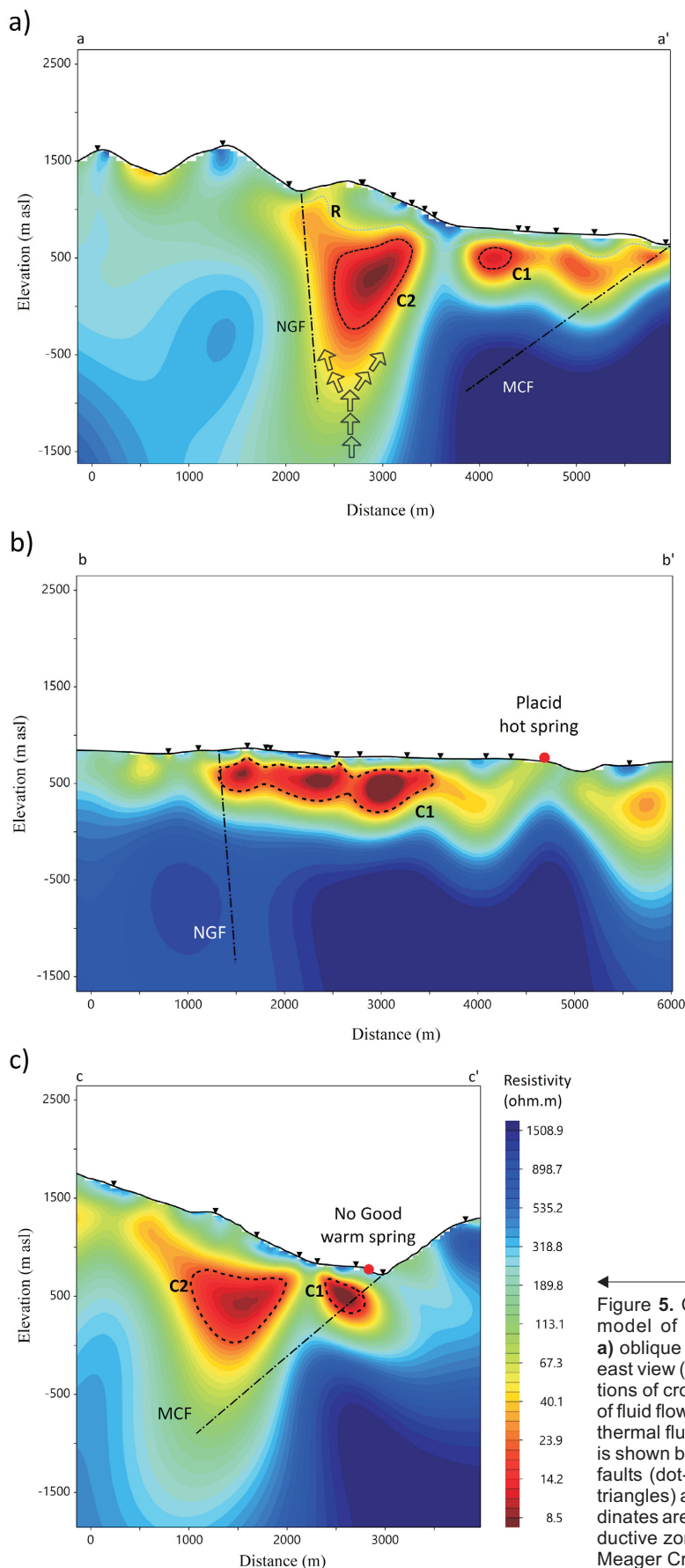


**Figure 4.** Horizontal plan views from the final audio-magnetotelluric model at elevations of **a)** 500 m above sea level (m asl), and **b)** 0 m asl, at the Mount Meager Volcanic Complex study area. Location of hot springs (red dots), faults (solid and dashed lines) and audio-magnetotelluric stations (black triangles) are shown. Colour bar is the same for both plots. All co-ordinates are in UTM Zone 10N, NAD 83. Abbreviations: C1, C1 conductive zone; C2, C2 conductive zone; Camp, Camp fault; MCF, Meager Creek fault; NGF, No Good fault.



integrated into the resistivity model. A possible interpretation for the conductive zones is that they are impermeable caprocks that act as the seal for underlying geothermal reservoirs. The caprock is interpreted to be deeper in the northern part of the study area, which can be considered for exploitation purposes. Since clay minerals do not have sufficient effective porosity and permeability to permit fluid flow to the production wells, considering such models reduces the risk of future development of geothermal resources.

As this is an ongoing project, further studies are needed to evaluate the petrophysical properties of the geothermal reservoirs. Future work is planned to 1) include laboratory measurements and rock physical properties to estimate reservoir characteristics based on the AMT electrical resistivity model of the MMVC study area and 2) incorporate a previously published deep MT model to find the relationship between shallow conductors, magma source and possible fluid pathways at the MMVC study area.

The MMVC was selected for the current study due to a wealth of legacy data, a result of its role as the first target for geothermal exploration in Canada. This area has potential due to the existence of warm and hot springs, extensive borehole coverage and nearby communities supportive of alternative energy development. Results of this project will improve the understanding of the geology and hydrothermal alteration caused by circulating hot water and provide insight into ideal locations for further production and reinjection boreholes. The results and the continuation of this research will support the broader goals of reducing the technical and economic risks of geothermal exploration in the Garibaldi volcanic belt.

Figure 5. Cross-sectional views through the final 3-D resistivity model of the Mount Meager Volcanic Complex study area: **a)** oblique view in northwest-southeast direction (a–a<sup>1</sup>), **b)** west-east view (b–b<sup>1</sup>), **c)** north-south view (c–c<sup>1</sup>). See Figure 2 for locations of cross-sections. Black arrows show the potential direction of fluid flow. The limit of the near surface region (R) where hot geothermal fluids do not alter the rocks and the temperature is <70°C is shown by a dashed blue line. Location of hot springs (red dots), faults (dot-dash lines) and audio-magnetotelluric stations (black triangles) are shown. Colour bar is the same for all plots. All co-ordinates are in UTM Zone 10N, NAD 83. Abbreviations: C1, C1 conductive zone; C2, C2 conductive zone; Camp, Camp fault; MCF, Meager Creek fault; NGF, No Good fault.

## Acknowledgments

This project was funded by Natural Resources Canada and Geoscience BC and benefited from support of the Natural Sciences and Engineering Research Council of Canada through Carleton University. The authors would like to thank W. Yuan for reviewing this manuscript. The authors would like to thank E. Roots for providing his pyMT program, V. Tschirhart, R. Bryant, S.M. Ansari and J. Liu for helping during the field survey, T. Jenkins from the Lil'wat First Nation for ensuring wildlife were undisturbed, M. Accurso, D. Vincent and R. Slinger for piloting (No Limits Helicopters), and Innergex Renewable Energy Inc. for providing significant access to their field bunkhouse.

## References

- Archie, G.E. (1942): The electrical resistivity log as an aid in determining some reservoir characteristics; *Transactions of the AIME*, v. 146, no. 1, p. 54–62, URL <<https://doi.org/10.2118/942054-G>>.
- Bernard, K. (2020): Epithermal clast coating inside the rock avalanche-debris flow deposits from Mount Meager Volcanic Complex, British Columbia (Canada); *Journal of Volcanology and Geothermal Research*, v. 402, art. 1069994, URL <<https://doi.org/10.1016/j.jvolgeores.2020.106994>>.
- Candy, C. (2001): Crew development corporation report on a magnetotelluric survey, South Meager geothermal project, Pemberton, British Columbia; Frontier Geosciences Inc., unpublished report for Frontier Geosciences project FG1-581.
- Chave, A.D. and Jones, A.G. (2012): *The Magnetotelluric Method: Theory and Practice*; Cambridge University Press, New York, New York, 552 p.
- Craven, J.A., Hormozzade, F., Tschirhart, V., Ansari, M., Bryant, R. and Montezadian, D. (2020): Overview of the 2019 audiomagnetotelluric survey of the Mount Meager geothermal reservoir; Chapter 6 in *Garibaldi Geothermal Energy Project, Mount Meager 2019 - Field Report*, Geoscience BC, Report 2020-09, p. 126–147, URL <[https://www.geosciencebc.com/i/project\\_data/GBCReport2020-09/GeoscienceBCReport%202020-09.pdf](https://www.geosciencebc.com/i/project_data/GBCReport2020-09/GeoscienceBCReport%202020-09.pdf)> [March 2021].
- Didana, Y.L., Heinson, G., Thiel, S. and Krieger, L. (2017): Magnetotelluric monitoring of permeability enhancement at enhanced geothermal system project; *Geothermics*, v. 66, p. 23–38, <<https://doi.org/10.1016/j.geothermics.2016.11.005>>.
- Ghomshei, M.M. and Clark, I.D. (1993): Oxygen and hydrogen isotopes in deep thermal waters from the south Meager Creek geothermal area, British Columbia, Canada; *Geothermics*, v. 22, no. 2, p. 79–89, URL <[https://doi.org/10.1016/0375-6505\(93\)90048-R](https://doi.org/10.1016/0375-6505(93)90048-R)>.
- Glover, P.W.J., Hole, M.J. and Pous, J. (2000): A modified Archie's law for two conducting phases; *Earth and Planetary Science Letters*, v. 180, no. 3–4, p. 369–383, URL <<https://www.sciencedirect.com/science/article/pii/S0012821X00001680>> [May 2022].
- Grasby, S.E., Allen, D.M., Bell, S., Chen, Z., Ferguson, G., Jessop, A., Kelman, M., Ko, M., Majorowicz, J., Moore, M., Raymond, J. and Therrien, R. (2012): Geothermal energy resource potential of Canada; Geological Survey of Canada, Open File 6914, 322 p., URL <<https://doi.org/10.4095/291488>>.
- Grasby, S.E., Ansari, S.M., Barendregt, R.W., Borch, A., Calahorrano-DiPatre, A., Chen, Z., Craven, J.A., Dettmer, J., Gilbert, H., Hannenson, C., Harris, M., Hormozzade, F., Leiter, S., Liu, J., Muhammad, M., Quane, S.L., Russell, J.K., Salvage, R.O., Savard, G., Tschirhart, V. et al. (2021): Garibaldi Geothermal Energy Project – phase 1 – final report; Geoscience BC, Report 2021–08, 276 p., URL <[https://www.geosciencebc.com/i/project\\_data/GBCReport2021-08/GBCR%202021-08%20Garibaldi%20Geothermal%20Energy%20Project%20-%20Phase%201.pdf](https://www.geosciencebc.com/i/project_data/GBCReport2021-08/GBCR%202021-08%20Garibaldi%20Geothermal%20Energy%20Project%20-%20Phase%201.pdf)> [February 2022].
- Grasby, S.E., Ansari, S.M., Calahorrano-DiPatre, A., Chen, Z., Craven, J.A., Dettmer, J., Gilbert, H., Hannenson, C., Harris, M., Liu, J., Muhammad, M., Russell, K., Salvage, R.O., Savard, G., Tschirhart, V., Unsworth, M.J., Vigouroux-Caillibot, N. and Williams-Jones, G. (2020): Geothermal resource potential of the Garibaldi volcanic belt, southwestern British Columbia (part of NTS 092J); in *Geoscience BC Summary of Activities 2019: Energy and Water*, Geoscience BC, Report 2020-02, p. 103–108, URL <[https://www.geosciencebc.com/i/pdf/SummaryofActivities2019/EW/Project%202018-004\\_EW\\_SOA2019.pdf](https://www.geosciencebc.com/i/pdf/SummaryofActivities2019/EW/Project%202018-004_EW_SOA2019.pdf)> [February 2022].
- Grasby, S.E., Borch, A., Calahorrano-DiPatre, A., Chen, Z., Craven, J., Liu, X., Muhammad, M., Russell, J.K., Tschirhart, V., Unsworth, M.J., Williams-Jones, G. and Yuan, W. (2023): Garibaldi Geothermal Volcanic Belt Assessment Project, southwestern British Columbia (part of NTS 092J) phase 2: 2022 field report; in *Geoscience BC Summary of Activities 2022: Energy and Water*, Geoscience BC, Report 2023-02, p. 47–54, URL <<https://geosciencebc.com/updates/summary-of-activities>>.
- Hormozzade Ghalati, F., Craven, J.A., Motazedian, D., Grasby, S.E. and Roots, E. (2021a): Shallow geothermal reservoir exploration in Mt. Meager, British Columbia, Canada; American Geophysical Union, AGU Fall Meeting, December 13–17, 2021, New Orleans, Louisiana, abstract, URL <<https://ui.adsabs.harvard.edu/abs/2021AGUFMGP21A..10H/abstract>> [December 2021].
- Hormozzade Ghalati, F., Craven, J.A., Motazedian, D., Grasby, S.E., Roots, E., Tschirhart, V., Ansari, S.M. and Liu, J. (2021b): Exploring the near surface geothermal structure at Mt. Meager, British Columbia, Canada; European Geosciences Union, EGU General Assembly Conference, April 19–30, 2021, virtual, abstract EGU21-12542, URL <<https://doi.org/10.5194/egusphere-egu21-12542>>.
- Hormozzade Ghalati, F., Craven, J.A., Motazedian, D., Grasby, S.E. and Tschirhart, V. (2022): Modeling a fractured geothermal reservoir using 3-D AMT data inversion: insights from Garibaldi volcanic belt, British Columbia, Canada; *Geothermics*, v. 105, art. 102528, URL <<https://doi.org/10.1016/j.geothermics.2022.102528>>.
- Huang, K. (2019): Geochemical analysis of thermal fluids from southern Mount Meager, British Columbia, Canada; M.Sc. thesis, University of Iceland, 92 p., URL <<https://skemman.is/bitstream/1946/33384/1/Katherine%20Huang%20MS%20Thesis.pdf>> [September 2021].
- Jamieson, G.R. (1981): A preliminary study of the regional groundwater flow in the Meager Mountain geothermal area, British Columbia; M.Sc. thesis, The University of British Columbia, 163 p., URL <<http://hdl.handle.net/2429/22494>> [May 2020].

- Jessop, A. (2008): Review of National Geothermal Energy Program, Phase 2 – geothermal potential of the Cordillera; Geological Survey of Canada, Open File 5906, 86 p., URL <<https://doi.org/10.4095/225917>>.
- Jones, A.G. and Dumas, I. (1993): Electromagnetic images of a volcanic zone; *Physics of the Earth and Planetary Interiors*, v. 81, p. 289–314, URL <[https://doi.org/10.1016/0031-9201\(93\)90137-X](https://doi.org/10.1016/0031-9201(93)90137-X)>.
- Lewis, T.J., Judge, A.S. and Souther, J.G. (1978): Possible geothermal resources in the Coast Plutonic Complex of southern British Columbia, Canada; *Pure and Applied Geophysics*, v. 117, no. 1, p. 172–179, URL <<https://doi.org/10.1007/BF00879744>>.
- Moeck, I.S. (2014): Catalog of geothermal play types based on geologic controls; *Renewable and Sustainable Energy Reviews*, v. 37, p. 867–882, URL <<https://doi.org/10.1016/j.rser.2014.05.032>>.
- Muñoz, G. (2014): Exploring for geothermal resources with electromagnetic methods; *Surveys in Geophysics*, v. 35, p. 101–122, URL <<https://doi.org/10.1007/s10712-013-9236-0>>.
- Proenza, Y. (2012): Geothermal data compilation and analysis of Alterra Power's upper Lillooet property; M.Eng. thesis, The University of British Columbia, 47 p., URL <[https://www.geosciencebc.com/i/project\\_data/GBC2017-006/Yuliana%20Proenza%20MEng%20Project.zip](https://www.geosciencebc.com/i/project_data/GBC2017-006/Yuliana%20Proenza%20MEng%20Project.zip)> [September 2019].
- Read, P.B. (1977): Meager Creek volcanic complex, southwestern British Columbia; *in* Report of Activities, Part A, Geological Survey of Canada, Paper no. 77-1A, p. 277–281.
- Simpson, F. and Bahr, K. (2005): *Practical Magnetotellurics*; Cambridge University Press, Cambridge, United Kingdom, 270 p., URL <<https://doi.org/10.1017/CBO9780511614095>>.
- Soyer, W., Mackie, R., Miorelli, F., Schifano, V. and Hallinan, S. (2020): 3D inversion modeling of natural and controlled source EM in complex terrain; European Association of Geoscientists & Engineers, NSG2020 3rd Conference on Geophysics for Mineral Exploration and Mining, December 7, 2020, virtual, v. 2020, p. 1–4, URL <<https://doi.org/10.3997/2214-4609.202020208>>.
- Thiel, S. (2017): Electromagnetic monitoring of hydraulic fracturing: relationship to permeability, seismicity, and stress; *Surveys in Geophysics*, v. 38, no. 5, p. 1133–1169, URL <<https://doi.org/10.1007/s10712-017-9426-2>>.
- van Leeuwen, W.A. (2016): Geothermal exploration using the magnetotelluric method; Ph.D. thesis, Utrecht University, 277 p., URL <<https://dspace.library.uu.nl/bitstream/handle/1874/340000/vLeeuwen.pdf?sequence=1&isAllowed=y>> [November 2022].
- Venugopal, S., Moune, S., Williams-Jones, G., Druitt, T., Vigouroux, N., Wilson, A. and Russell, J.K. (2020): Two distinct mantle sources beneath the Garibaldi volcanic belt: insight from olivine-hosted melt inclusions; *Chemical Geology*, v. 532, art. 119346, URL <<https://doi.org/10.1016/j.chemgeo.2019.119346>>.
- Williams, C.F., Reed, M.J. and Anderson, A.F. (2011): Updating the classification of geothermal resources; *in* Proceedings, 36th Workshop on Geothermal Reservoir Engineering, Stanford University, January 31–February 2, 2011, Stanford, California, URL <<http://pangea.stanford.edu/ERE/pdf/IGAstandard/SGW/2011/williams.pdf>> [February 2022].
- Wilson, A.M. and Russell, J.K. (2018): Quaternary glaciovolcanism in the Canadian Cascade volcanic arc – paleoenvironmental implications; *in* Field Volcanology: A Tribute to the Distinguished Career of Don Swanson, M.P. Poland, M.O. Garcia, V.E. Camp and A. Grunder (ed.), Geological Society of America, Special Paper 538, p. 133–157, URL <[https://doi.org/10.1130/2018.2538\(06\)](https://doi.org/10.1130/2018.2538(06))>.

## Pilot Collaborative Water Monitoring Program, Northeastern British Columbia (NTS 094A and Parts of 093O, P, 094B, G, H): Year Two Update

**R.L. Rolick, British Columbia Oil and Gas Commission, Fort St. John, British Columbia, ryan.rolick@bcogc.ca**

**S.L. Lapp, Climatederra Consulting Ltd., Fort St. John, British Columbia**

**E.G. Johnson, British Columbia Ministry of Energy, Mines and Low Carbon Innovation, Victoria, British Columbia**

**D.L. Cottrell, Shell Canada Ltd., Calgary, Alberta**

**W.T. Van Dijk, Matrix Solutions Inc., Edmonton, Alberta**

**B. Shepherd, Matrix Solutions Inc., Grande Prairie, Alberta**

---

Rolick, R.L., Lapp, S.L., Johnson, E.G., Cottrell, D.L., Van Dijk, W.T. and Shepherd, B. (2023): Pilot Collaborative Water Monitoring Program, northeastern British Columbia (NTS 094A and parts of 093O, P, 094B, G, H): year two update; *in* Geoscience BC Summary of Activities 2022: Energy and Water, Geoscience BC, Report 2023-02, p. 63–72.

### Program Background

The Pilot Collaborative Water Monitoring Program was initiated in 2020 to address needs identified during projects such as British Columbia's (BC) Provincial Regional Strategic Environmental Assessment and Northeast Water Strategy, and findings in the *Scientific Review of Hydraulic Fracturing in British Columbia* (Scientific Hydraulic Fracturing Review Panel, 2019). The collaboration involves three Geoscience BC water projects aimed at further understanding the hydrological, hydrogeological and climatic interactions in northeastern BC, and incorporating Traditional Knowledge into this understanding.

- 1) Northeast B.C. Hydrometric Monitoring Project (Project 2019-016): installation of five hydrometric stations to measure surface water quantity.
- 2) Co-ordinated Groundwater, Surface Water and Climate Monitoring Program, Northeast B.C. (Project 2019-023): co-location of supplemental monitoring to greatly expand collected knowledge at the monitoring sites, increase the opportunity for research and understanding into watershed processes, and increase the capacity and participation of local First Nations as a partner in water monitoring. Supplemental monitoring includes the installation of groundwater monitoring wells for water quantity and quality where it is anticipated there will be groundwater–surface water interaction; surface water quality monitoring, including benthic invertebrate sampling; installation or improvement of local climate stations to monitor factors that affect surface and groundwater, such as rainfall, snowfall, humidity, wind and

solar radiation; and training of local First Nations to capture data and maintain equipment.

- 3) Traditional Knowledge Project (Project 2019-018): an innovative venture to bridge communication barriers and gain understanding through the gathering of Traditional Knowledge at each monitoring site at specific seasonal times, with the goal to braid Traditional Knowledge with Western-style scientific observations.

By co-locating groundwater monitoring stations near hydrometric stations, particularly at sites identified as regional data gaps, not only are project costs reduced, but the research will hopefully answer several key questions with the datasets produced (groundwater quantity and quality, surface water quantity and quality, and climate data). This approach will maximize the return on 'foundational science' through a more complete baseline monitoring program, which will augment the existing approved Surface Water Quantity Monitoring and Traditional Knowledge programs. The baseline data will allow for advanced analysis to support assessment of groundwater–surface water interaction, watershed water balance calculations and meteorological data, to support a variety of assessments.

### Project Updates

This program was initiated with a virtual kick-off workshop on December 2, 2020, with the six Treaty 8 First Nations (FN) located within the study area boundary in attendance, along with program partners from the BC Oil and Gas Commission, the BC Ministry of Energy, Mines and Low Carbon Innovation, Shell Canada Ltd., Matrix Solutions Inc. (Matrix) and Geoscience BC. The six First Nation communities included Blueberry River First Nations (BRFN), Doig River First Nation (DRFN), Halfway River First Nation (HRFN), McLeod Lake Indian Band (MLIB),

---

*This publication is also available, free of charge, as colour digital files in Adobe Acrobat® PDF format from the Geoscience BC website: <http://geosciencebc.com/updates/summary-of-activities/>.*

Saulteau First Nations (SFN) and West Moberly First Nations (WMFN). All First Nations expressed interest in participating in the research and monitoring partnership, and in joining program staff during field site visits. Participation in field site visits decreased in 2022 to five First Nations, with WMFN not participating.

With most of the monitoring infrastructure installed by the fall of 2021, a fair amount of data were collected in 2022, with site visits to each station scheduled and co-ordinated directly with each respective First Nation. Hydrometric monitoring was conducted monthly between April and October. Four groundwater monitoring wells were drilled and installed in March 2022, and groundwater monitoring was conducted in the spring and fall of 2022. Surface water quality samples were collected in June of 2022 to add summer sampling data to the fall and early winter samples collected in 2021. A spring sample will be collected in early 2023 to ensure sampling is carried out during all four seasons at each monitoring location.

Climate data were collected from two new stations installed in late 2021, at Stewart Creek and Alexander Creek, and two additional stations were partially installed at the Blueberry River and Doig River (upgrades to the BC Wildfire Service’s [BCWS] Osborn wildfire climate station) sites in late 2022. Due to supply-chain manufacturing delays for some of the sensors, the Blueberry River and Doig River station installations will not be completed until 2023.

### Site Criteria

Sites identified and with all necessary instrumentation installed in 2021 were monitored throughout the 2022 open-water season. No additional sites are anticipated to be added to the network at this time. Please refer to Lapp et al. (2022) for an explanation of the criteria for site selection. Table 1 summarizes details of the hydrometric monitoring stations and Figure 1 shows their location.

## Ongoing Monitoring

### Hydrometric Stations

A total of five hydrometric stations were installed in the late summer and early fall of 2021. In April 2022, the stations were set to record the spring freshet and were then visited

monthly to collect manual discharge measurements. First Nation community members were invited to participate in the equipment installation and ongoing monitoring of the station associated with their community. Water Officers from BC’s Ministry of Forests (MOF), based in Fort St. John, also participated in the installation of the stations and monitoring of water quantity at these locations. At each hydrometric station, the equipment consists of OTT HydroMet GmbH’s OTT PLS sensors with Sutron XLink 100 loggers. A final field visit to each of the stations was conducted in October 2022, to winterize them. The photos in Figure 2 show a variety of the hydrometric monitoring activities at each station.

### Groundwater Wells

Groundwater monitoring wells were installed at four locations (Blueberry River, Alexander Creek, Stewart Creek and Hulcross Creek) in March 2022, immediately following the issuance of permits from MOF. The wells were drilled and installed using an air rotary drilling rig supplied by Anderson Water Services Ltd. of Fort St John, under the supervision of Matrix field staff (Figure 3). Each well was constructed to meet the requirements of the Provincial Groundwater Observation Well Network, including 3-inch-diameter PVC well casing. A dedicated pressure transducer was deployed in each monitoring well to collect continuous groundwater level data. The transducer data were calibrated to a reference point by measuring the depth of the water level during groundwater monitoring events.

Groundwater quality samples were collected from the wells twice in 2022 (June and October). Prior to sample collection, each well was purged of stagnant water using a submersible pump or bailer to allow the inflow of formation water, a process referred to as ‘well development’ in the sections below.

The hydraulic conductivity of the screened formation was assessed in 2022 by conducting a slug test or pumping test at each well.

The purpose of water wells is to monitor the groundwater level in the shallow subsurface (unconfined aquifer), monitor water quality in shallow groundwater, and ultimately, in co-ordination with the surface water and climate monitoring, provide information about surface water–groundwater

**Table 1.** Summary of the site locations and associated First Nation communities. All co-ordinates are in UTM Zone 10N, NAD83. Abbreviations: BRFN, Blueberry River First Nations; DRFN, Doig River First Nation; HRFN, Halfway River First Nation; MLIB, McLeod Lake Indian Band; SFN, Saulteau First Nations; WMFN, West Moberly First Nations.

Location	First Nation	Easting	Northing
Blueberry River on Mile 98 Road	BRFN	578627	6290276
Doig River at Doig River First Nation	DRFN	653587	6273135
Alexander Creek on Mile 95 Road	HRFN	574248	6271384
Stewart Creek at Stewart Lake Road	MLIB	620969	6201392
Hulcross Creek on Moberly Forest Service Road	SFN/WMFN	563289	6181243

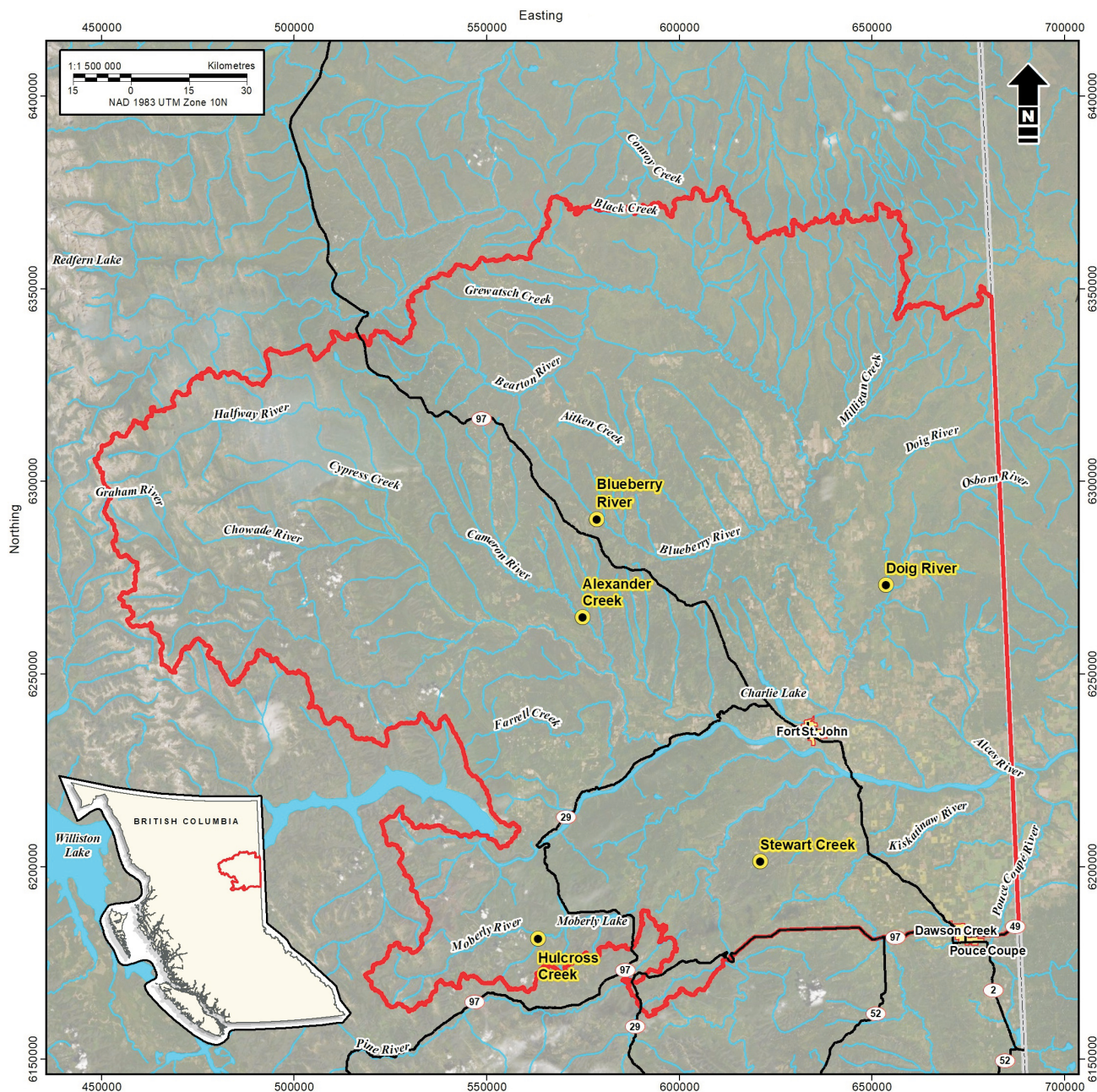


Figure 1. Location of the study area (outlined in red) and water monitoring sites (highlighted in yellow).

interaction. As such, wells were sited proximal to hydro-metric stations. Some locations provided the added opportunity for testing the possible existence of a paleovalley at a slightly deeper horizon. Paleovalley research in this region has been supported by Geoscience BC with mapping, airborne geophysics, ground-based geophysics and drilling. Where possible, water wells were drilled to sufficient depths to confirm the presence of predicted paleovalleys.

### Water Quality

There is general consensus that insufficient water quality monitoring data exist in northeastern BC (Northeast Water

Strategy, 2017, 2018). Sampling water quality in conjunction with stream volume helps identify any linked parameters, such as dissolved solids and dissolved oxygen. The original program proposed water quality sampling at monitoring sites through four time frames during the open-water season (one in spring, two in summer, and one in fall). Surface water quality monitoring in 2021 was planned for all five monitoring locations during the four time frames; however, due to the time required to select and establish the monitoring sites and receive program consensus earlier in the year, sampling was only completed twice (August and October) at all but the Stewart Creek location (October only). For that reason, further sampling was required in

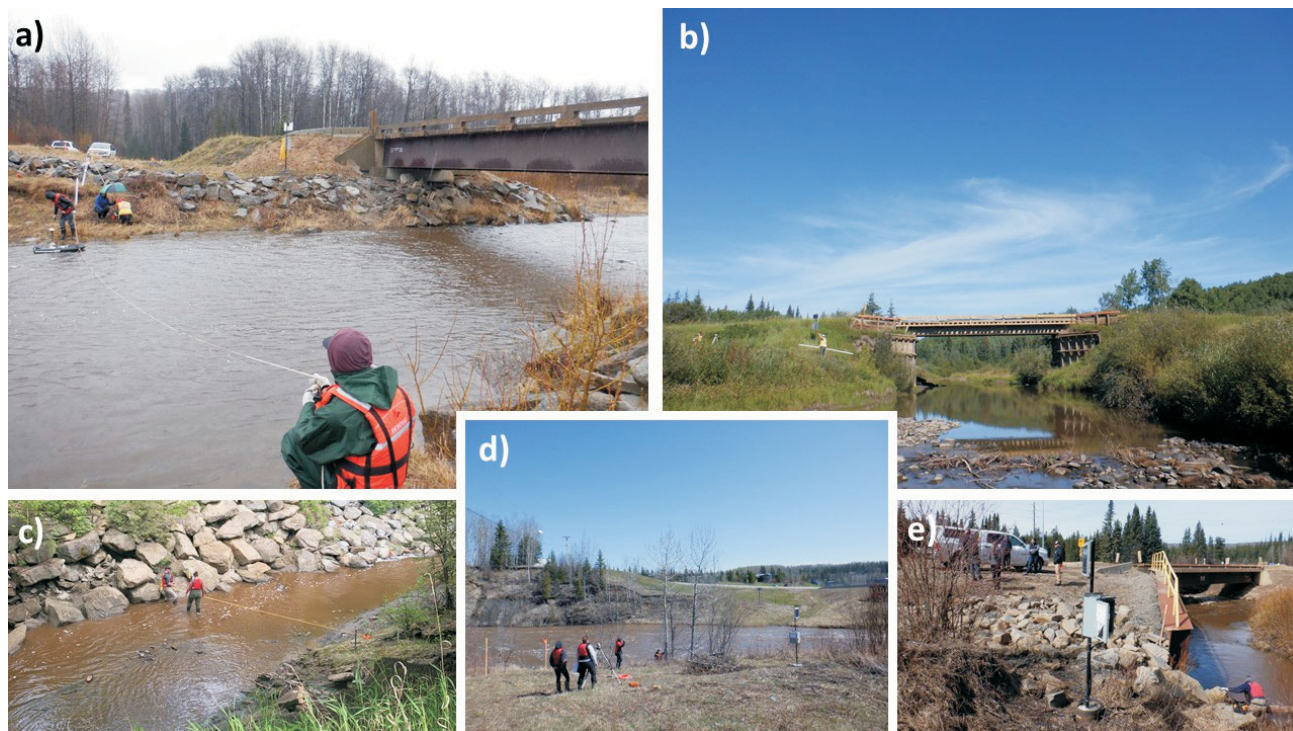


**Figure 2.** Hydrometric station equipment and monitoring activity at **a)** Hulcross Creek, **b)** Blueberry River, **c)** Alexander Creek, **d)** Doig River and **e)** Stewart Creek.

2022; however, it was decided that collecting a sample during each of the four major seasons (spring, summer, fall and winter) would provide a better understanding of seasonality in surface water chemistry at each monitoring location. Information about the sampling completed is detailed in the sections below. Surface water quality monitoring for the program includes sampling both field and laboratory parameters. Routine field parameters sampled include dissolved oxygen, temperature, pH and electrical conductivity; laboratory parameters sampled include the same routine field parameters in addition to turbidity, major ions, total and dissolved metals, total organic carbon, coliforms and total plate count, biochemical and chemical oxygen demand, and hydrocarbons.

In order to collect further information on aquatic ecosystem health at each monitoring location, in addition to water quality sampling, benthic invertebrate sampling was proposed at the start of the program for two monitoring sites, following the Canadian Aquatic Biomonitoring Network (CABIN) protocol. It was determined in 2021 that Matrix would investigate site suitability and benthic community diversity at all monitoring locations using CABIN methods. Information on benthic invertebrates was collected in 2021 at or near four of the monitoring sites. The results will be entered into the national CABIN database, and compared to other sites and models (including provincial datasets) to determine their overall suitability for further monitoring and evaluation of relative stream health. The

CABIN program assesses the aquatic health of streams through the collection of benthic invertebrate samples. Benthic invertebrate sampling at the selected sites was completed by a CABIN-certified Matrix staff member.

Due to program delays and associated cost implications, and considering the sampling already completed in 2021, it was determined that no further CABIN sampling would be completed in 2022. Determination of future assessments will be made based on results of the 2021 assessments.

### Climate Stations

Climate data will be used to support assessment of the water balance at each of the monitoring sites. Climate data parameters include precipitation and snow, air temperature, wind speed and direction, barometric pressure, and relative humidity. Climate stations do not need to be situated at the exact location as the hydrometric sites and monitoring wells because of the regional nature of weather systems; climate measurements in the vicinity of a monitoring site are sufficient for research needs. Additionally, climate monitoring results are superior when the station is located away from road activity, in a sheltered spot where it is not unduly influenced by wind; the hydrometric and groundwater sites are located near active roadways. Equipment to allow remote data collection at the stations has not been installed at this time, so data are manually collected, at minimum every three months, or more often as time/budget permits. Climate stations were installed using a combination of

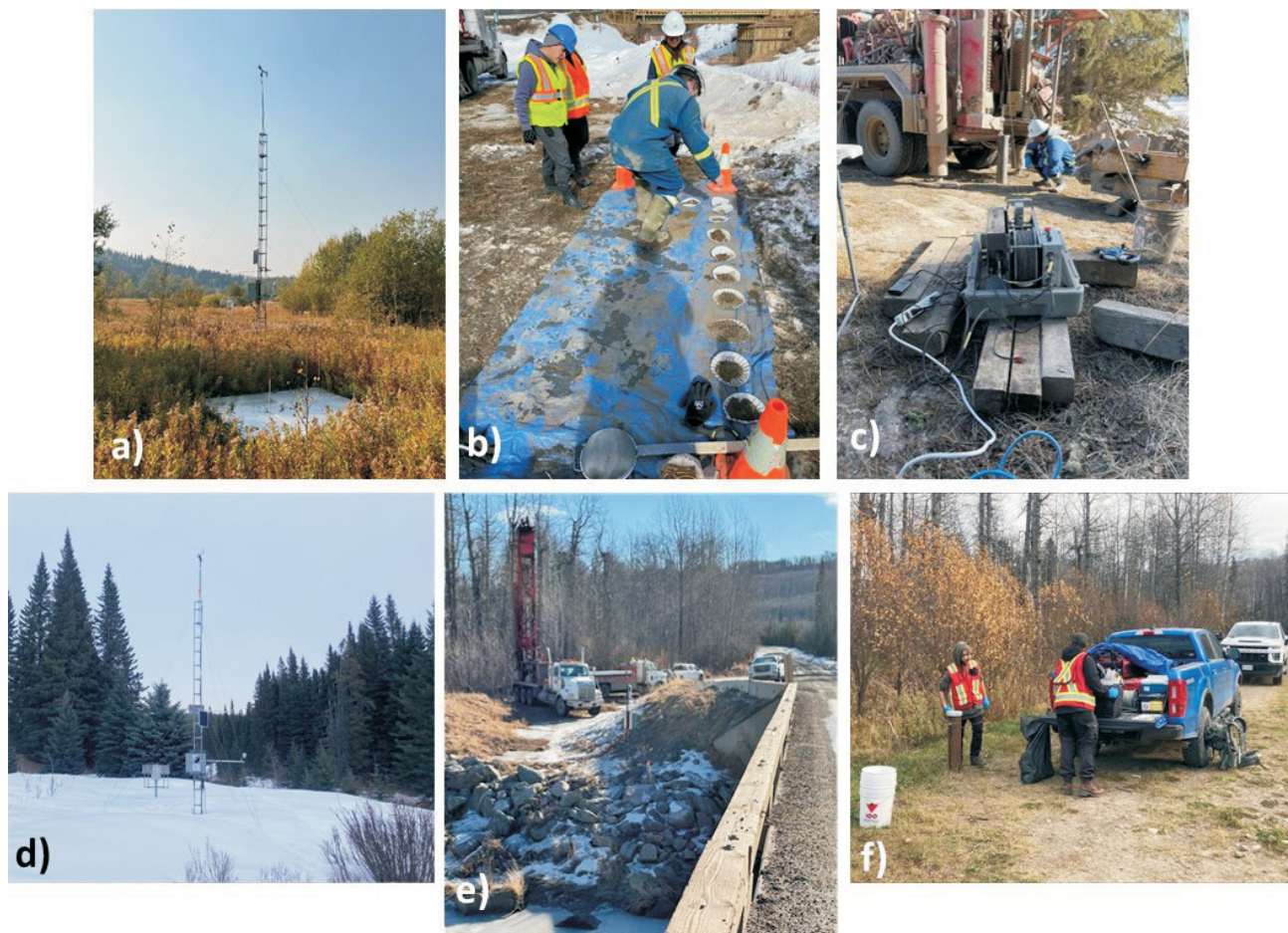


**Figure 3.** Examples of monitoring sites and Matrix Solutions Inc.'s well installation and monitoring: **a)** Alexander Creek climate station; September 15, 2022; **b)** examining drill cuttings during installation of the Blueberry River groundwater well; March 15, 2022; **c)** Stewart Creek groundwater well installation; March 18, 2022; **d)** Stewart Creek climate station; March 11, 2022; **e)** Hulcross Creek groundwater well installation; March 20, 2022; **f)** Hulcross Creek groundwater sampling; October 18, 2022.

provincial and federal government criteria for siting sensors.

Table 2 shows a summary of the monitoring completed in 2022 at each site, as discussed above.

### Site Status

#### Blueberry River at Mile 98 Road

This site is within 10 km of the community of Wonowon, which marks the site of Mile 101 on the historic Alaska Highway (Highway 97 on Figure 1). The contributing watershed area is 312 km<sup>2</sup>. The hydrometric station was set to start recording on April 6, 2022, and subsequent stream-flow measurements were conducted on May 18, June 22, August 4 and 17, September 22 and October 6, 2022. The station was decommissioned for winter during the October 6 visit and will be restarted in April 2023 to capture spring freshet.

Matrix completed surface water quality and CABIN sampling on August 17, 2021 with two members from BRFN.

At that time, Matrix learned BRFN had already established a CABIN monitoring site at this same location in 2019, and members of the BRFN intend to continue their CABIN sampling program at this site with staff who have been trained by CABIN. For the purpose of the co-ordinated program, Matrix also collected CABIN samples at this site, and have shared the initial results with BRFN.

Surface water quality was sampled a second time on October 20, 2021, and again on June 22, 2022. Water quality sampling will be completed a final time in spring of 2023.

Climate data for the Blueberry River site were sourced from regional climate monitoring stations for the years 2020, 2021 and 2022. Matrix began installation of a new climate station at the Blueberry River monitoring site in fall 2022, but will not be able to complete the installation of all monitoring equipment until early 2023 due to manufacturer supply-chain delays.

A groundwater monitoring well was installed at the Blueberry River location on March 15–16, 2022. The well

**Table 2.** Summary of monitoring being carried out at each location. An 'X' in a cell indicates that type of monitoring is being carried out at that site. Abbreviations: BRFN, Blueberry River First Nations; CABIN, Canadian Aquatic Biomonitoring Network; DRFN, Doig River First Nation; HRFN, Halfway River First Nation; MLIB, McLeod Lake Indian Band; SFN, Saulteau First Nations; WMFN, West Moberly First Nations.

Location	First Nation	Hydrometric station	Groundwater well	Water quality	CABIN <sup>1</sup>	Climate station
Blueberry River on Mile 98 Road	BRFN	X	X	X	X	Regional <sup>2</sup>
Doig River at Doig River First Nation	DRFN	X		X	X	Regional <sup>3</sup>
Alexander Creek on Mile 95 Road	HRFN	X	X	X	X	X
Stewart Creek at Stewart Lake Road	MLIB	X	X	X	X	X
Hulcross Creek on Moberly Forest Service Road	SFN/WMFN	X	X	X	X	Regional

<sup>1</sup>Each site is being assessed for CABIN suitability.

<sup>2</sup>Climate station installation began in late 2022 and will be finished in spring 2023.

<sup>3</sup>Matrix Solutions Inc. will add additional sensors to the BC Ministry of Forests' Osborn wildfire station for this program. Upgrades began in late 2022 and will be finished in spring 2023.

screen was installed at a depth of 33.5 to 36.5 m below ground level (BGL), within bedrock of the Dunvegan Formation. Well development was conducted by airlifting with Anderson Water Services on April 11, 2022. A pressure-logging instrument (Solinst Levelogger) was deployed to collect continuous water level data. Groundwater was monitored twice in 2022: 1) on June 22 an electrical submersible pump was used to collect groundwater samples, and a pumping test was conducted to estimate the hydraulic conductivity of the aquifer; 2) collection of water level data and groundwater sampling using a submersible pump were carried out on October 17.

### Doig River at Doig River First Nation

The site is located within the Doig River First Nation community, approximately 200 m from the band office. The contributing watershed area is 416 km<sup>2</sup>. The station was set to start recording on April 8, 2022, and subsequent streamflow measurements were conducted on May 20, June 23, July 20, August 11, September 23 and October 7, 2022. The station was decommissioned for winter during the October 7 visit and will be restarted in April 2023 to capture spring freshet.

Matrix completed surface water quality and CABIN sampling at Doig River on August 18, 2021, which coincided with the hydrometric station installation. Water quality was sampled a second time on October 20, 2021, and again on June 23, 2022. Surface water quality will be sampled a final time in spring of 2023.

Climate data for the Doig River site were sourced from regional climate monitoring stations for the years 2020, 2021 and 2022. When this report was being written, Matrix had a tentative agreement with the managers of BCWS climate monitoring division to add sensors to their Osborn climate station, located approximately 7.5 km southeast of this program's monitoring site. Providing the agreement is fully executed, Matrix will begin installing additional sensors at the Osborn station in the fall of 2022 and complete the up-

grades in early 2023, once all sensors are received from the manufacturer.

### Alexander Creek at Mile 95 Road

The site is within 15 km of the Halfway River First Nation. The contributing watershed area is 134 km<sup>2</sup>. The station was set to start recording on April 13, 2022, with subsequent streamflow measurements conducted on May 16, June 16, July 25, August 18 and September 15, 2022, with the last visit and winter decommission planned for October 19, 2022. The station will be restarted in April 2023 to capture spring freshet.

Matrix completed surface water quality and CABIN sampling on August 17, 2021, which coincided with the hydrometric station installation. Three representatives from HRFN were present at the time of the site visit. Surface water quality was sampled a second time on October 20, 2021, and again on June 16, 2022. Water quality will be sampled a final time in spring of 2023.

A new climate station was installed in early November 2021, approximately 1.5 km west of the Alexander Creek monitoring site. The climate station is equipped with sensors to record air temperature, year-round precipitation, snow-water equivalent, wind, relative humidity and barometric pressure. Regional climate data will be used to supplement and compare to data collected at the program's climate station.

A groundwater monitoring well was installed at the Alexander Creek location on March 17, 2022. The well screen was installed at a depth of 3.0 to 6.1 m BGL, within a unit of sand and gravel. Well development was conducted by bailing the well, and a pressure-logging instrument (Solinst Levelogger) was deployed in the well on March 23, 2022. Groundwater monitoring was conducted on June 16, 2022; the well was purged and sampled using a bailer, and a slug test was conducted to estimate the hydraulic conductivity of the aquifer. Groundwater was monitored a second time

on October 17, 2022, and included collection of water level data and groundwater sampling using a bailer.

### Stewart Creek at Stewart Lake Road

The station is located within the MLIB summer area and south of Stewart Lake. The contributing watershed area is 24 km<sup>2</sup>. The hydrometric station was set to start recording on April 14, 2022, with subsequent streamflow measurements conducted on May 17, June 17, July 26, August 19 and September 16, 2022, with the last visit and winter decommission planned for October 20, 2022. The station will be restarted in April 2023 to capture spring freshet.

Water quality was sampled on October 21, 2021 and June 17, 2022. Water quality at this site will be sampled again in late fall 2022 and spring 2023.

A new climate station was installed approximately 0.5 km west of the Stewart Creek monitoring site in early November 2021. The climate station is equipped with sensors to record air temperature, year-round precipitation, snow-water equivalent, wind, relative humidity and barometric pressure.

A groundwater monitoring well was installed at the Stewart Creek location on March 18, 2022. The well screen was installed at a depth of 18.3 to 19.8 m BGL, within glacial till. Well development was conducted by purging with a submersible pump on April 5, 2022. A pressure-logging instrument (Solinst Levelogger) was deployed to collect continuous water level data. Groundwater was monitored twice in 2022: 1) on June 17 the well was purged and sampled using an electric submersible pump, and a slug test was conducted to estimate the hydraulic conductivity of the aquifer; 2) water level data were collected and groundwater sampling using a purge pump and bailer was carried out on October 18.

### Hulcross Creek at Moberly Forest Service Road

The Hulcross Creek site is located west of the West Moberly and Sauteau First Nations, within the Moberly Lake watershed. The contributing watershed area is 132 km<sup>2</sup>. The hydrometric station was set to start recording on April 5, 2022, with subsequent streamflow measurements conducted on May 19, June 27, July 27, August 29, September 20 and October 5, 2022. As the stream was open and flowing during the April 5 visit, an additional flow measurement was conducted at that time. The station was decommissioned for winter during the October 5 visit and will be restarted in April 2023 to capture spring freshet.

Matrix completed surface water quality sampling at Hulcross Creek on August 25 and October 21, 2021, and July 18, 2022. Final sampling will be completed in spring of 2023.

Benthic invertebrate sampling to collect CABIN data was conducted by Matrix on August 17, 2021; however, due to a location error, the work was completed at Dixie Creek, located east of Hulcross Creek. Despite the location error, the CABIN results will be shared with SFN and WMFN, as it may be of value for other watershed studies.

Regional climate data for the Hulcross Creek monitoring site for 2020, 2021 and 2022 will be sourced from Environment and Climate Change Canada's climate monitoring station at the Chetwynd airport, approximately 25 km to the southeast.

A groundwater monitoring well was installed at the Hulcross Creek location on March 18–19, 2022. A borehole was drilled to a depth of 47.8 m without encountering bedrock. After encountering borehole stability issues, the first borehole was plugged and an adjacent borehole was drilled for the installation of a monitoring well. The well was screened at a depth of 3.0 to 4.5 m BGL, within a unit of sand and gravel. Well development was conducted by bailing the well, and a pressure-logging instrument (Solinst Levelogger) was deployed in the well on April 8, 2022. Groundwater was monitored twice in 2022: 1) on July 18 the well was sampled using a bailer, and a slug test was conducted to estimate the hydraulic conductivity of the aquifer; 2) water level data were collected and the groundwater was sampled using a bailer on October 17.

### Traditional Knowledge

This project seeks to include a holistic understanding of First Nation values, and their relationship with water. The McLeod Lake Indian Band and the Halfway River First Nations agreed to participate in the Traditional Knowledge-gathering project. On May 17, 2022, a field visit to the Stewart Creek hydrometric station was conducted with two members of the MLIB. The discussions included the historical use and importance of the area to the MLIB, and the traditional practices conducted in the area. A lot of conversation focused on the impact to water quality and quantity from development and land-use changes. Due to travel restrictions related to COVID-19, MLIB members who live on reserve were unable to attend the field visit, so a follow-up community meeting was held later that same day, with the project team brought in virtually, to hear the community's stories and view of water.

A separate meeting was also held with the HRFN, on May 16, 2022. The morning session included First Nation staff and a couple of elders sharing stories about and uses of water. There was also a discussion around environmental indicators of drought and changes in water quality. The afternoon was spent at the Alexander Creek hydrometric station, which included additional elders, with the focus on historical uses of water and changes to water associated with development.

At both the Stewart Creek and Alexander Creek field days, the First Nation members were able to watch and learn how streamflow measurements are taken. Follow-up meetings will be planned during the winter of 2022–23, with an optional field trip in the summer of 2023 to collect additional Traditional Knowledge with both communities. A final report will be prepared as part of the end of the project, scheduled for December 2023.

## Summary and Next Steps

The program moved successfully forward in 2022, with a full season of monitoring for hydrometrics, and partial data collection for water quality and groundwater. Climate stations were installed and data were collected at the Alexander Creek and Stewart Creek sites, while installation of climate stations at the Blueberry River monitoring site and southeast of the Doig River monitoring site will commence in late fall 2022. The project team was able to successfully engage with five of the six First Nation communities within the study area for participation in monitoring activities at the five locations.

### Hydrometric

Hydrometric data for the open-water season of 2022 (April to October) were collected at all five stations. During the winter of 2022–23 the data will be processed in accordance with the standards of BC's Resources Information Standards Committee (Resources Information Standards Committee, 2018), and posted for the public to access through the BC Water Portal ([www.waterportal.geoweb.bcogc.ca](http://www.waterportal.geoweb.bcogc.ca)) and the provincial database Aquarius (<https://aqrt.nrs.gov.bc.ca>). With funding expected to be extended to December 2023, the hydrometric stations will be reinstated in the spring to capture a full open-water season of data, including freshet.

### Water Quality

Over the winter of 2022–23, Matrix will begin to tabulate and compare sampling results at all five monitoring locations. With funding extended to December 2023, additional sampling will be completed in the spring and summer of 2023. Full results will be tabulated, analyzed for trends, and summarized in the final report at the end of 2023.

### Climate

As mentioned above, installation of the two remaining climate stations—at Blueberry River and Doig River—will begin in late 2022 and continue into 2023. Over the winter of 2022–23, Matrix will begin to summarize and compare climate data from all five monitoring locations, supplemented with regional climate data. Full results will be analyzed for trends and summarized or compared in the final report at the end of 2023.

## Groundwater

In spring 2023, groundwater sampling will be completed at each site a final time. The groundwater data, including borehole logs, groundwater quality, hydraulic conductivity testing and groundwater levels, will be compiled and compared against climate and hydrometric data.

## First Nations Training

Training of First Nations community members was delivered in 2022 to develop skills and facilitate ongoing participation in the program. Matrix conducted a training webinar covering climate, groundwater and water quality sampling on April 7, 2022. A training day for hydrometric monitoring was delivered on September 21, 2022, with assistance from staff from the BC Ministry of Environment and Climate Change Strategy. This consisted of a classroom-based training session, followed by field-based training, and covered all aspects of hydrometric monitoring.

The program team has requested and received an extension to the project completion date from Geoscience BC to December 2023, to ensure another full season of monitoring can be completed in 2023. The team is also exploring future funding options, to ensure the monitoring continues past the expiration of the Geoscience BC funding.

All project findings will be published in a final report, scheduled for December 2023.

## Acknowledgments

Special thanks to C. van Geloven with the BC Ministry of Forests for conducting the peer review, and Geoscience BC for providing the project funding.

## References

- Lapp, S.L., Johnson, E.G., Cottrell, D.L., Van Dijk, W.T., Shepherd, B.P. and Rolick, R.L. (2022): Pilot Collaborative Water Monitoring Program, northeastern British Columbia (NTS 094A, parts of 0930, P, 094B, G, H): year one update; in Geoscience BC Summary of Activities 2021: Energy and Water, Geoscience BC, Report 2022-02, p. 95–102, URL <[https://cdn.geosciencebc.com/pdf/SummaryofActivities2021/EW/Project%202019-016,018,023\\_EWSOA2021.pdf](https://cdn.geosciencebc.com/pdf/SummaryofActivities2021/EW/Project%202019-016,018,023_EWSOA2021.pdf)> [October 2022].
- Northeast Water Strategy (2017): A disturbance-sensitivity based approach to prioritizing water monitoring in northeast B.C., part 1: report; BC Ministry of Environment and Climate Change Strategy, 119 p., URL <[https://www2.gov.bc.ca/assets/gov/environment/air-land-water/northeast-water-strategy/disturbance\\_sensitivity\\_based\\_approach.pdf](https://www2.gov.bc.ca/assets/gov/environment/air-land-water/northeast-water-strategy/disturbance_sensitivity_based_approach.pdf)> [September 2022].
- Northeast Water Strategy (2018): Surface water quality data summary for northeast British Columbia; BC Ministry of Environment and Climate Change Strategy, 59 p., URL <[https://www2.gov.bc.ca/assets/gov/environment/air-land-water/northeast-water-strategy/news\\_ne\\_wq\\_summary\\_2018.pdf](https://www2.gov.bc.ca/assets/gov/environment/air-land-water/northeast-water-strategy/news_ne_wq_summary_2018.pdf)> [September 2022].

Resources Information Standards Committee (2018): Manual of British Columbia hydrometric standards, version 2.0, December 2018; BC Ministry of Environment and Climate Change Strategy, Knowledge Management Branch, 160 p., URL <[https://www2.gov.bc.ca/assets/gov/environment/natural-resource-stewardship/nr-laws-policy/risc/man\\_bc\\_hydrometric\\_stand\\_v2.pdf](https://www2.gov.bc.ca/assets/gov/environment/natural-resource-stewardship/nr-laws-policy/risc/man_bc_hydrometric_stand_v2.pdf)> [September 2022].

Scientific Hydraulic Fracturing Review Panel (2019): Scientific review of hydraulic fracturing in British Columbia; BC Ministry of Energy, Mines and Low Carbon Innovation, 220 p., URL <[https://www2.gov.bc.ca/assets/gov/farming-natural-resources-and-industry/natural-gas-oil/responsible-oil-gas-development/scientific\\_hydraulic\\_fracturing\\_review\\_panel\\_final\\_report.pdf](https://www2.gov.bc.ca/assets/gov/farming-natural-resources-and-industry/natural-gas-oil/responsible-oil-gas-development/scientific_hydraulic_fracturing_review_panel_final_report.pdf)> [September 2022].







SUITE 1101-750 WEST PENDER ST  
VANCOUVER, BC V6C 2T7 CANADA  
604 662 4147

info@geosciencebc.com  
**geosciencebc.com**

